# KINETICS AND MECHANISM OF THE CO-OXIDATION OF ALDEHYDES AND MODEL ORGANIC SULFUR COMPOUNDS IN STUDIES RELATED TO THE OXO-DESULFURIZATION OF FUEL OIL AND COAL

Thesis by

Russell Leslie Bone

In Partial Fulfillment of the Requirements

for the Degree of

Doctor of Philosophy

California Institute of Technology

Pasadena, California 91125

1981

(Submitted January 22, 1981)

To my parents, who knew I was headed
for graduate school since kindergarten
and supported me in that goal.

ACKNOWLEDGEMENTS

I would like to take this opportunity to express my admiration and appreciation to my advisor, William H. Corcoran. His guidance, in addition to the freedom in research which he allowed, was an inspiration to me.

I gratefully acknowledge the support of the National Science Foundation, Jet Propulsion Laboratory, the Bechtel Corporation and the Beaumont Foundation during my tenure as a graduate student.

I would also like to thank the staff at Caltech for their cheerful helpfulness. In particular, I am grateful to George Griffith, Hollis Reamer, Donna Johnson, and Lenore Kerner for their ability to seemingly drop everything to help solve a problem.

My interaction with the other members of the Corcoran group was especially enjoyable. Jim Kralik, Nick Vasilakos, Gary Whatley and Samir Barudi deserve mention specifically for not only putting up with me as office-mates and lab partners but also acting as sounding boards for ideas and as friends. I am also deeply indebted to Amir Attar for introducing me to the laboratory equipment and oxo-desulfurization in general. In addition, I would like to thank all my fellow graduate students, too numerous to list, who contributed to my education, philosophically as well as technically.

These acknowledgements would not be complete without mentioning Yolande Johnson and Pamela Brazile who typed this thesis and helped to keep me sane during the process.

# ABSTRACT

Reaction rates and mechanisms in the oxidation of organic sulfur compounds by perbenzoic acid generated in situ from benzaldehyde autoxidation were investigated. Dibenzothiophene and diphenyl sulfide were utilized as model sulfur compounds typical of those present in residual oil and coal. The aromatic nature of a fuel medium was simulated by bromobenzene solvent. Reaction samples were quantitatively analyzed primarily by means of high-pressure liquid chromatography. Diffusion of oxygen, peracid decomposition, and direct oxidation of aldehyde by peracid were found to limit the formation of peracid. Activation energies for decomposition of the peracid and for direct oxidation of the aldehyde by peracid were obtained and used to explain the maximum in oxidation efficiency with respect to temperature observed for dibenzothiophene. Perbenzoic acid was found to be selective in oxidizing diphenyl sulfide and dibenzothiophene to the corresponding sulfoxides and sulfones. At 75$^{o}$C, diphenyl sulfide was only oxidized approximately twice as rapidly as dibenzothiophene, in contrast with the higher rates reported by other investigators. Both sulfur compounds were found to inhibit the rate of benzaldehyde autoxidation.

# TABLE OF CONTENTS

# LIST OF FIGURES

# LIST OF TABLES

# NOMENCLATURE

| | |
|---|---|
| a | ratio of interfacial area to volume |
| a,b,c | grouped constants in autoxidation rate expression |
| A | pre-exponential factor |
| $C_A$ | concentration of oxygen in the liquid phase |
| $C_B$ | concentration of aldehyde in the liquid phase |
| D | dielectric constant |
| $\mathcal{D}$ | diffusivity of $O_2$ in the liquid phase |
| DBT | dibenzothiophene |
| DBTO | dibenzothiophene sulfoxide |
| $DBTO_2$ | dibenzothiophene sulfone |
| DPS | diphenyl sulfide |
| E | activation energy |
| GC | gas chromatography |
| HPLC | high pressure liquid chromatography |
| $\Delta H^o$ | standard state enthalpy of solution |
| H,K | Henry's Law constant, distribution constant |
| i | value at gas-liquid interface |
| I | photochemical initiation |
| IR | infrared |
| ID | inside diameter |
| k | rate constant, capacity factor |
| $k_{Ag}$ | oxygen mass transfer coefficient, gas phase |
| $k_{Al}$ | oxygen mass transfer coefficient, liquid phase |
| $K_o$ | overall mass transfer coefficient for oxygen, based on gas phase |

| | |
|---|---|
| M | flow conversion parameter |
| n | reaction order, oxidation state |
| N | Normal |
| NMR | Nuclear Magnetic Resonance |
| OD | outside diameter |
| P | partial pressure |
| POB | perbenzoic acid |
| POA | peracetic acid |
| R | gas constant |
| R· | organic radical |
| $R_i$ | initiation rate |
| RCHO | aldehyde |
| RCO· | alkoxy radical |
| $RCO_3$· | acyl peroxy radical |
| ROOH | organic peroxide |
| $RO_2$· | peroxy radical |
| $RCO_2H$ | organic acid |
| $RCO_3H$ | peracid |
| R´ | rate of peracid decomposition |
| $\Delta S$ | entropy |
| SSF | Saybolt seconds, $^oF$ |
| t | time |
| T | temperature, K |
| UV | ultraviolet |
| $\alpha,\beta,\gamma$ | grouped constants in rate expression |
| $\phi OH$ | phenol |
| * | activated specie |

[ ] concentration of

# CHAPTER 1 INTRODUCTION

One conclusion is obvious from the national focus on energy policy in the last decade: there is no single source of energy available with current technology which will satisfy U.S. needs. Energy self-sufficiency will require a variety of approaches, and the nation must work to keep a maximum of options available. As the lighter hydrocarbons become scarce, the short-range burden of supplying energy will very likely rest to a large extent on the heavy fossil fuels: residual oil, coal, shale oil and coal liquids. Viable alternatives must be compatible with environmental considerations, in particular, the emissions of sulfur oxides need to be restricted to avoid extensive damage to air quality. With this motivation, some preliminary mechanistic studies were undertaken with possible ultimate application to an oxo-desulfurization process for residual oil and coal.

## Characterization of the Problem

Presently, residual fuel oil provides approximately 8% of the total energy consumed in the United States (101). Coal supplies 20% of the nation's needs, with the remaining demand being met primarily by natural gas and other crude fractions. Much of the fuel oil and coal burned today is utilized by the electric utility industry which uses 13% oil and 48% coal as its fundamental energy sources.

The sulfur content of these two fuels varies widely and can be as high as 5 wt% in some production areas (102).

Sulfur in crude tends to accumulate in the residual fractions, resulting in an average between 1 and 2 wt% in fuel oil. Current crude charges tend to be heavier and contain more sulfur than those in the past as the more desirable light, sweet crudes are being depleted. The sulfur found in the heavier crude cuts is characteristically in the form of condensed thiophenic rings such as benzothiophene, dibenzothiophene and their derivatives, but also includes a large amount of sulfides (103,104,105). These sulfur forms are listed in Table 1.1 along with some additional sulfur compounds found in lesser amounts. Coal usually averages around 3 wt% sulfur, approximately half of which is contained in inorganic $FeS_2$ crystals interspersed within the coal matrix. The remaining organic sulfur is dominated by thiophenic and sulfidic compounds analogous to those found in residual oil.

Current federal standards as set by the U.S. Environmental Protection Agency (106) for coal-fired electric utility steam generating units allow only 1.2 lb. of $SO_2$ per million BTU of fuel and require a 90% reduction in emissions. When emissions are less than 0.6 lb of $SO_2$ per million BTU only a 70% reduction is required. The standards for oil-fired utility boilers are more strict: 0.8 lb $SO_2$ per million BTU and 90% reduction or 0.2 lb $SO_2$ per million BTU with no reduction requirement. The recent addition of the reduction regulation to the emission standards necessitates that a desulfurization process be associated with all

TABLE 1.1 COMMON SULFUR FORMS IN FUEL OIL

CONDENSED THIOPHENES

BENZOTHIOPHENES 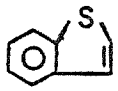

DIBENZOTHIOPHENES 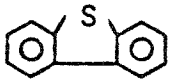

BENZONAPHTHALENIC THIOPHENES 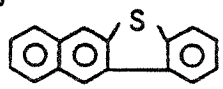

SULFIDES

CYCLOSULFIDES 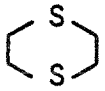

ALIPHATIC R-S-R

AROMATIC 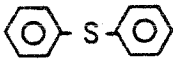

MERCAPTANS

THIOPHENOLS 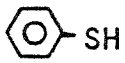

ALKYL R-SH

THIAZOLE DERIVATIVES 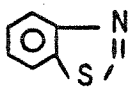

newly installed fossil-fuel power plants except those burning extremely low sulfur oil.

There are two basic approaches to meet air quality standards for sulfur oxide emissions: 1) desulfurization of gaseous combustion products, and 2) desulfurization of the fuel prior to combustion. Stack-gas-scrubbing processes have only been recently commercialized (107,108,109). The low concentration of $SO_2$ in the flue gas results in mass-transfer problems which exact large economic penalties in the form of huge processing units and large operating costs. The current processes under development for the pretreatment of coal in general only remove the pyritic sulfur. In most cases, removal of pyritic sulfur alone is not enough to meet emission standards. These methods include mechanical separation of the pyritic crystals after grinding, leaching after mild oxidation (Meyers' process and JPL's low-temperature chlorinolysis), centrifugal separation, electrostatic separation, magnetization and flotation techniques (110,111). In the case of oil pretreatment, hydrodesulfurization technology is well established (112,113,114,115). The basic reaction is the reduction of sulfur to $H_2S$ as follows:

$$\begin{matrix} R' \\ \diagdown \\ \quad S \\ \diagup \\ R \end{matrix} \; + \; 2H_2 \xrightleftharpoons{cat} H_2S + RH + R'H$$

The Claus process is commonly used to convert the $H_2S$ to elemental sulfur.

$$3H_2S + 3O_2 \longrightarrow 2H_2O + 2SO_2$$

$$SO_2 + 2H_2S \longrightarrow 2H_2O + 3S$$

Hydrodesulfurization requires a catalyst, high temperatures and pressures (500-800°F; 150-3000 psig) and is rather unreliable for heavier crude cuts because of increased coking of catalyst encountered under the more severe operating conditions, however. A source of hydrogen is also necessary (300-1300 SCF/BBL) which ultimately must come from crude hydrocarbons or natural gas, the reserves of both of which are rapidly dwindling. In addition, the selectivity of hydrodesulfurization is poor for residual oil where thiophenes are a major sulfur form. A considerable amount of hydrogen is used to saturate the thiophenic ring before sulfur extrusion takes place.

Oxo-desulfurization

In the past, oxo-desulfurization has not been used commercially because most of the common inexpensive oxidants are unselective, resulting in large losses in heating value. The high cost and scarcity of feed stock necessary, severe conditions required, and lack of effectiveness on thiophenic sulfur for current processes has stimulated renewed interest in selective oxidation under mild conditions as a method for removing sulfur from both coal and residual oil. The basic scheme consists of selectively oxidizing the organic sulfur compounds to the corresponding sulfones, destabilizing

the carbon-sulfur bond (116). The sulfones are then pyrolized, releasing $SO_2$, as shown below.

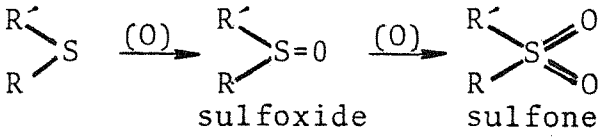



The pyrolysis step has been investigated by other workers (117,118) and will not be discussed further. Among other alternatives, the $SO_2$ can be oxidized to $SO_3$ and absorbed in water to form sulfuric acid; this technology is available from the development of stack-gas treaters.

In the first step of the sequence, i.e. the oxidation of sulfur compounds to sulfones, numerous oxidants have been found which can effect this conversion (119,120,121, 122,123,124,125), including $KMnO_4$, $HNO_3$, $CrO_3$, $H_2O_2$/acetic acid, $Cl_2/H_2O$, and hydroperoxides. Hydroperoxides, in particular, are an economically attractive means for oxidizing sulfur compounds since they may be generated in situ by air oxidation of the hydrocarbons already present in residual oil (118,126). Although adequate for the oxidation of sulfides, hydroperoxides were found to be ineffective in oxidizing thiophenes under mild conditions (140°C, 1 atm). A large proportion of sulfur in coal and residual oil is thiophenic. This fact provides the motivation for develop-

ment of a selective oxidation process for thiophenes which would encompass the advantages of in situ oxidation with air.

Rationale

Organic peracids have been shown to selectively oxidize thiophenic as well as sulfidic sulfur compounds yielding sulfoxides, sulfones and the corresponding organic acid (see Chapter 3 for a detailed literature review). They may be formed in situ by the autoxidation of aldehydes via a mechanism analogous to the formation of peroxides from hydrocarbons (see Chapter 2 for a detailed literature review). The following oxo-desulfurization scheme emerges from the combination of these two facts: 1) oxidize a mixture of aldehyde and fuel with air to form peracid in situ, 2) the peracid generated will selectively oxidize the sulfur compounds to sulfoxides and sulfones which may be decomposed by pyrolysis. While these two oxidation processes have been studied separately, no kinetic information is available with which to evaluate the feasibility of the co-oxidation of aldehydes and sulfur compounds.

Research Goals

Thus, the primary goals of this study were: 1) verify experimentally if selective oxidation of model sulfur compounds can be accomplished at low temperatures by peracids generated from in situ oxidation of aldehydes, 2) determine the conditions required for maximum formation of peracid, 3) derive kinetic data for selected model systems containing sulfur compounds, 4) determine the conditions of most efficient use of aldehyde feedstock, and 5) investigate the

kinetics in a residual fuel environment. A secondary goal was to demonstrate the versatility of liquid chromatography in the analysis of these types of reacting systems.

Organization

Chapter 2 consists of a review of the literature on the autoxidation of aldehydes to form peracids. Chapter 3 is a corresponding review of the oxidation of sulfur compounds by peracids. The equipment and procedures used to study the combination of these two processes is described in Chapter 4. Chapter 5 contains the experimental results and discussion; these results are summarized and conclusions drawn in Chapter 6. Appendix A details analogous work done in decane solvent in the presence of ultraviolet light. Appendix B discusses the development of the procedures used in the analysis of reactor samples by liquid chromatography. These methods were also used in the analysis of a $Cl_2/H_2O$ system for oxidation of sulfur compounds described in Appendix C.

# CHAPTER 2 AUTOXIDATION OF ALDEHYDES BY MOLECULAR OXYGEN

The low temperature (<200°C), low pressure (≤1 atm.) autoxidation of aldehydes by molecular oxygen proceeds via a mechanism very similar to that for the autoxidation of hydrocarbons (201,202,203,204,205,206). The original proposition and evidence for the radical-chain mechanism now generally accepted was advanced by Backstrom in 1934 (207). This mechanism consists of three distinct types of reaction steps: 1) initiation reactions, where more free radicals are produced as products than are consumed as reactants; 2) propagation reactions, where the same number of free radicals is produced as is consumed; and 3) termination reactions, where more free radicals are consumed than are produced.

## Initiation Reactions

The free radicals required to initiate the chain mechanism can be produced by a variety of methods: thermal decomposition of unstable compounds (208,209), metal ion catalysts (210, 211,212,213,214), ultraviolet light (215,216), ozone (217), or hydrogen abstraction by oxygen (218,219,220,221). Typical unstable initiators are azo and peroxy compounds, which decompose by the mechanisms shown below (203,222):

Hydroperoxides $ROOH \longrightarrow RO\cdot + \cdot OH$

$2ROOH \longrightarrow RO\cdot + RO_2\cdot + H_2O$

Dialkyl peroxides $ROOR' \longrightarrow RO\cdot + \cdot OR'$

Peracids $RCOOOH \longrightarrow RCO_2\cdot + \cdot OH$

Peresters $RCOOOR' \longrightarrow RCO_2\cdot + \cdot OR'$

Diacyl peroxides $RCOOOCOR \longrightarrow 2RCO_2\cdot$

Di-t-butylhyponitrite $(CH_3)_3CO\text{-}N = N\text{-}OC(CH_3)_3 \longrightarrow 2(CH_3)_3CO\cdot + N_2$

Azo isopropane $(CH_3)_2CHN = NCH(CH_3)_2 \longrightarrow 2(CH_3)_2CH\cdot + N_2$

Azo isobutyronitrile $(CH_3)_2\underset{\underset{CN}{|}}{C}\text{-}N = N\text{-}\underset{\underset{CN}{|}}{C}(CH_3)_2 \longrightarrow 2(CH_3)_2\underset{\underset{CN}{|}}{C}\cdot + N_2$

Table 2.1 gives the bond energies and half-life data for some common initiators. Salts of manganese, copper, iron, cobalt, and other heavy metals have also been shown to be effective initiators of aldehyde autoxidations (206). Bawn and coworkers (210,214) postulated that reactions of the type

$$M^{n+} + RCHO \longrightarrow M^{(n-1)+} + RCO\cdot + H^+$$

were responsible. Later studies (212,213) at higher metal ion catalyst concentrations indicated that the following initiation reactions may also be important:

$$M^{(n-1)+} + RCO_3H \longrightarrow M^{n+} + RCO_2\cdot + OH^-$$

$$M^n + RCO_3H \longrightarrow M^{(n-1)+} + RCO_3\cdot + H^+$$

The catalytic effect by metals can be eliminated by complexing them with ethylenediaminetetraacetic acid (EDTA) (223). Acceleration of the autoxidation of aldehydes by light was first observed as early as 1832 by Wohler and Liebig (204). Ultraviolet light was later shown to be more effective than sunlight (224), and quantum yields in the thousands lent strong support to the concept of chain reactions. Melville and coworkers (215,216) attributed this rate enhancement to photo-initiation by the reaction

$$RCHO \xrightarrow{h\nu} RCO\cdot + H\cdot$$

Table 2.1 Dissociation Parameters for Some Common Initiators (203)

| Name | Structure | Activation Energy (kcal/mole) | $^{o}C$ for 1 hr. half-life |
|---|---|---|---|
| Hydrogen peroxide | HO-OH | 48 | |
| t-Butyl hydroperoxide | t-BuO-OH | 42 | |
| t-Butyl peroxide | t-BuO-OBu-t | 37 | 150 |
| t-Butyl perbenzoate | t-BuO-OCPh (O) | 34 | 125 |
| Benzoyl peroxide | PhCO-OCPh (O, O) | 30 | 95 |
| Acetyl peroxide | $CH_3CO$-OC$CH_3$ (O, O) | 30-32 | 85 |
| t-Butyl peroxalate | t-BuO-OCCO-OBu-t (OO) | 25.5 | 40 |
| t-Butyl hyponitrite | t-BuO-N=N-OBu-t | 28 | 60 |
| Azoisobutyronitrile | $(CH_3)_2C$(CN)-N=N-C(CN)$(CH_3)_2$ | 30 | 85 |

Attempts to trap H· during acetaldehyde photolysis have failed and the actual photo-initiation process probably involves the following mechanism, which is kinetically equivalent to the previous reaction for a long chain reaction.

$$RCHO \longrightarrow R\cdot + \cdot CHO$$

$$R\cdot + O_2 \longrightarrow RO_2\cdot$$

$$RO_2\cdot + RCHO \longrightarrow RO_2H + RCO\cdot$$

The large increases in the rate of benzaldehyde oxidation in the presence of ultraviolet light have been confirmed during the course of this work (see Appendix A). Ozone has been successfully used to initiate the autoxidation of aldehydes (217,225), although a mechanism has only recently been proposed (226). Initiation via hydrogen abstraction by oxygen, viz.

$$RH + O_2 \longrightarrow R\cdot + HO_2\cdot$$

is thermodynamically and kinetically unfavorable for most hydrocarbons. However, the above reaction is generally feasible for compounds with weak C-H bonds and capable of forming resonance-stabilized radicals, such as aldehydes

$$RCHO + O_2 \longrightarrow RCO\cdot + HO_2\cdot$$

The rate of initiation with molecular oxygen is strongly dependent on the bond energy of the hydrogen, larger rates being associated with smaller bond energies. Some pertinent bond-dissociation energies for different classes of hydrogens are given in Table 2.2. Hydrogen abstraction by oxygen as an initiation step was used to explain the purely thermal oxi-

Table 2.2 R-H Bond Dissociation Energies (202,203,205)

| Structure | Bond Energy (kcal/mole) | Structure | Bond energy (kcal/mole) |
|---|---|---|---|
| $CH_3$-H | 103 | $RC(=O)$-H | 86 |
| n-$C_3H_7$-H | 99 | $CH_3S$-H | 88 |
| iso-$C_3H_7$-H | 94 | $CH_3PH$-H | 85 |
| t-$C_4H_9$-H | 90 | PhO-H | 88 |
| $CH_2$=CH-H | 105 | PhNH-H | 80 |
| $C_6H_5$-H | 103 | ROO-H | 90 |
| $CH_2$=CH-$CH_2$-H | 85 | RO-H | 102 |
| $PhCH_2$-H | 85 | $RC(=O)O$-H | 103 |

dation of n-decanal and benzaldehyde in the absence of ultraviolet light observed by Melville and coworkers (215,216). Mulcahy and Watt (227) were unable to reconcile their thermal oxidation data for benzaldehyde with this initiation reaction, however.

Propagation Reactions

In the autoxidation of aldehydes, two reactions form the backbone of the chain (207). First, oxygen adds to the acyl radical formed in the initiation reactions

$$RCO\cdot + O_2 \xrightarrow{k_1} RCO_3\cdot$$

This addition is extremely rapid with practically zero activation energy and is diffusion-controlled in most cases ($k_1 > 10^9 \frac{\ell}{\text{mole} \cdot \text{sec}}$). At an oxygen partial pressure greater than 100 torr, the rate controlling step is invariably hydrogen abstraction by the acyl peroxy radical (203)

$$RCHO + RCO_3\cdot \xrightarrow{k_2} RCO\cdot + RCO_3H$$

These two reactions complete the chain, the result being the production of a peracid molecule from oxygen and an aldehyde. Chain lengths (i.e., cycles through propagation per initiation step) as high as fifty thousand have been observed experimentally (206). The rate constant for hydrogen abstraction in the second propagation step ($k_2$) can be roughly related to the exothermicity of this reaction. Thus, high rates of oxidation are expected where the bond which is formed ($RO_2$-H) is stronger than that which is broken (R-H). The peroxide hydrogen bond strength has been estimated

at approximately 90 kcal/mole which is larger than that for benzylic, allylic, or aldehydic C-H bonds, and about the same as a tertiary C-H bond in a saturated hydrocarbon (see Table 2.2). Peroxy radicals are relatively stable and are quite selective, preferentially abstracting the most weakly bound hydrogen. For comparison, the relative rates of hydrogen abstraction of primary, secondary, and tertiary hydrocarbons is 1:30:300 (228). Some additional rate constants for hydrogen transfer by peroxy radicals are given in Table 2.3. The ease of hydrogen abstraction of hydrogens on carbon bonded to oxygen can be attributed to resonance of the free radical electron with the electrons of oxygen in the product. It is interesting to note that the activation energy and pre-exponential factor for the second propagation step ($k_2$) are well correlated by

$$\log A = 4 + 0.5\ E$$

where A is in $\frac{\ell}{\text{mole} \cdot \text{sec}}$ and E is in $\frac{\text{kcal}}{\text{mole}}$ (202). Depending on the type of initiation, other radicals may contribute to chain propagation. For example, in the case of thermal initiation, the reaction

$$RCHO + HO_2\cdot \longrightarrow RCO\cdot + H_2O_2$$

may also be significant.

Termination Reactions

Termination can occur by the combination of two free radicals or reaction of a radical with an inert substance to give a product so unreactive as to effectively

Table 2.3 Rate Constants for Hydrogen Abstraction Reactions (202,203).

| Substrate | Radical | Temp (°C) | $k_p$ (ℓ/mole/sec) | $E_a$ (kcal/mole) |
|---|---|---|---|---|
| Benzaldehyde | Benzoyl | 5 | 1900 | |
| Decanal | Hydroxy-decyl | 5 | 720 | |
| Cyclohexene | Cyclohexenyl | 40 | 3.7 | 7.0 |
| 1-Methylcyclohexene | 1-Methylcyclohexenyl | 40 | 5.5 | 6.0 |
| 4-Methylcyclohexene | 4-Methylcyclohexenyl | 40 | 7.0 | 9.5 |
| 4,5-Dimethylcyclohexene | 4,5- Dimethylcyclohexenyl | 40 | 18.2 | 8.3 |
| Tetralin | Cumyl | 30 | 1.65 | |
| Tetralin | Tetralyl | 30 | 6.4 | |
| Ethyl benzene | 1-Phenethyl | 70 | 0.9 | 8.5 |
| Isopropyl benzene | α-Cumyl | 50 | 0.31 | 6.7 |

Table 2.3 (contd.)

| Substrate | Radical | Temp ($^{o}$C) | $k_p$ (ℓ/mole/sec) | $E_a$ (kcal/mole) |
|---|---|---|---|---|
| 1-Octene | Octenyl | 40 | 0.05 | 7.0 |
| Phenol | Polyperoxystyryl | 65 | $5*10^3$ | |
| Diphenylamine | Polyperoxystyryl | 65 | $20*10^3$ | |

end the chain. In autoxidation of aldehydes, termination is assumed to be by combination of the chain carriers

$$\left.\begin{array}{l} 2\ RCO\cdot \longrightarrow \\ RCO\cdot + RCO_3\cdot \longrightarrow \\ 2RCO_3\cdot \longrightarrow \end{array}\right\} \text{Products}$$

The reactions take place with an activation energy on the order of 1-2 $\frac{kcal}{mole}$. The unstable oxides formed rapidly decompose to products which depend upon the structure of the organic R group (229). The most important termination reactions are those between the radicals in the highest concentration. The kinetics of the reaction are quite sensitive to the chain-ending step. At low partial pressures of oxygen, the first termination reaction is the most important. It results in an overall rate that is first order in oxygen, if photo-initiation is assumed (206). At oxygen pressures greater than 100 torr, where $RCO_3\cdot$ is the most abundant radical, the third termination reaction will dominate, resulting in an oxidation rate that is independent of oxygen concentration (230). This effect has been observed experimentally (227). Table 2.4 shows some selected rate constants for termination.

Kinetics

Thus, the low temperature, uninhibited autoxidation of aldehydes can be generally described by the following reaction mechanism where the partial pressure of oxygen is greater than 100 torr:

Table 2.4 Rate Constants for Peroxy Radical Terminations (203,216)

| Radical | $2k_t$ at 30°C (ℓ/mole/sec) | |
|---|---|---|
| Primary, $RCH_2O_2\cdot$ | $2\text{-}4 * 10^8$ | |
| Secondary, $R_2CHO_2\cdot$ | $2\text{-}4 * 10^7$ | (benzylic) |
| | $1\text{-}10 * 10^6$ | (allylic) |
| | $6\text{-}8 * 10^6$ | (cyclic) |
| Tertiary $R_3CO_2\cdot$ | $0.1\text{-}60 * 10^4$ | |
| $HO_2\cdot$ | $1.2 * 10^9$ | |
| Cumyl peroxy | $9 * 10^6$ | |
| Benzoyl peroxy | $4.5 * 10^8$ | |
| Tetralyl peroxy | $4.4 * 10^7$ | |
| Hydroxy-decyl peroxy | $1.6 * 10^7$ | |
| Cyclohexenyl peroxy | $2.2 * 10^6$ | |

$$\text{Initiation} \quad \xrightarrow{R_i} RCO\cdot$$

$$\text{Propagation} \quad RCO\cdot + O_2 \xrightarrow{k_1} RCO_3\cdot$$

$$RCO_3\cdot + RCHO \xrightarrow{k_2} RCO\cdot + RCO_3H$$

$$\text{Termination} \quad 2\ RCO_3\cdot \xrightarrow{k_3} \text{non-radical products}$$

Application of the steady-state approximation to the radicals RCO· and $RCO_3$· yields the rate expression

$$\frac{d[RCHO]}{dt} = -k_2 \left(\frac{R_i}{2k_3}\right)^{1/2} [RCHO]$$

when the autoxidation is initiated by a process which is independent of aldehyde concentration (e.g., light or benzoyl peroxide), the general body of experimental evidence supports the first order dependence on aldehyde in the overall rate predicted above. There is no general consensus on the order in aldehyde for the thermally initiated autoxidation, however. The disagreement between Mulcahy and Watt, and Cooper and Melville over the mechanism of thermal initiation illustrates the confusion. Cooper and Melville (215) found a dependence on $(\text{aldehyde})^{3/2}$ during their studies of the thermal autoxidation of decanal, leading them to postulate the initiation step

$$RCHO + O_2 \longrightarrow RCO\cdot + HO_2\cdot$$

On the other hand, Mulcahy and Watt (227) observed a second-order dependence and were led to include an activated species to maintain a consistent mechanism:

$$RCHO \longrightarrow RCHO^*$$

The complex expression below for the oxidation order in aldehyde has also been proposed and can be made consistent with all

the observed data by proper adjustment of the constants.

$$\text{Rate} \propto \frac{a[\text{RCHO}]^2}{b[\text{RCHO}]+c}$$

A similar situation exists for the dependence of the overall rate on oxygen. Aldehyde autoxidation rates have been observed with oxygen orders varying from zero to one (206). All of the reported work is in harmony with the equation

$$\text{Rate} \propto \frac{a[O_2]}{b + c[O_2]}$$

Some typical values of overall rates of autoxidation which have been observed experimentally are summarized in Table 2.5.

Activation Energies

The determination of the overall activation energy for reactions between dissolved gas and liquid involves both a chemical-rate term and a physical equilibrium term, unless the reaction rate is not a function of dissolved gas. This is because a change in rate with temperature will reflect not only the activation energy but also the effect of temperature on gas solubility. If the oxidation rate is of order n in dissolved gas,

$$R = \text{reaction rate} = k[O_2]^n f(c) = Ae^{-E/RT}[O_2]^n f(c)$$

where f(c) represents the rate dependence on the concentration of liquid reactants. If Henry's Law is obeyed,

$$K = \frac{[O_2]}{P_{O_2}} \Rightarrow \ln K = \ln[O_2] - \ln(P_{O_2})$$

At constant pressure, the Gibbs-Helmhotz equation implies

$$\frac{d\ln K}{d(1/T)} = \frac{d\ln[O_2]}{d(1/T)} = \frac{-\Delta H^o}{R}$$

Table 2.5 Reaction Rates for the Autoxidation of Aldehydes (206)

| Aldehyde | Initiation | $O_2$ Partial Pressure | Temp ($^oC$) | Solvent | Mole Fraction Aldehyde | Rate*$10^5$ (moles $O_2$/ sec/mole Aldehyde |
|---|---|---|---|---|---|---|
| Decanal | Photo | 650 mm. | 5 | None | 1 | 7.71 |
| Decanal | Thermal | 650 mm. | 5 | None | 1 | 1.87 |
| Heptanal | Photo | 650 mm. | 29 | None | 1 | 19. |
| Heptanal | Thermal | 650 mm. | 29 | None | 1 | 0.75 |
| Benzaldehyde | Photo | 1 atm. | Room | None | 1 | 36. |
| Benzaldehyde | Thermal | 1 atm. | Room | None | 1 | 0.24 |
| Benzaldehyde | Photo | 1 atm. | Room | None | 1 | 2.9 |
| Benzaldehyde | Thermal | 1 atm. | Room | None | 1 | 2.8 |
| Heptanal | Photo | 1 atm. | Room | None | 1 | 3.1 |
| Heptanal | Thermal | 1 atm. | Room | None | 1 | 2.4 |
| Benzaldehyde | Photo | 650 mm. | 5 | Decane | 0.251 | 21.5 |
| Benzaldehyde | Thermal | 650 mm. | 5 | Decane | 0.251 | 2.15 |
| Benzaldehyde | Benzoyl peroxide | 523 mm. | 24 | Benzene | 0.224 | 4.1 |
| Benzaldehyde | Thermal | 600 mm. | 24 | Benzene | 0.179 | 1.2 |
| Butanal | No ozone | 130 mm. | 0 | $CCl_4$ | 0.25 | 0.027 |

Table 2.5 (contd.)

| Aldehyde | Initiation | $O_2$ Partial Pressure | Temp ($^{\circ}C$) | Solvent | Mole Fraction Aldehyde | Rate*$10^5$ (moles $O_2$ sec/mole Aldehyde |
|---|---|---|---|---|---|---|
| Butanal | $10^{-7} O_3/O_2$ | 130 mm. | 0 | $CCl_4$ | 0.25 | 0.55 |

where $\Delta H^{o}$ is the standard state enthalpy of solution of oxygen in aldehyde. The heat of solution of most gases in most liquids varies from 0.5-5 $\frac{kcal}{mole}$. From the expression for the reaction rate

$$\ell nR = \ell n(f(c)) + n\ell n[O_2] + \ell nk$$

Therefore

$$\frac{d\ell nR}{d(1/T)} = \frac{-n\Delta H^{o}}{R} - \frac{E}{R} = \frac{-(E+n\Delta H^{o})}{R} = \frac{-E(observed)}{R}$$

Table 2.6 gives some experimental values for the activation energy of the overall rate of autoxidation. The constants in the Arrhenius equations for the elementary radical processes involved in the autoxidation are just now being evaluated. Approximate values are listed in Table 2.7.

Decomposition

The peracids formed by the free-radical chain undergo rapid decomposition upon heating, in some cases explosively (224,231,232). Peracetic acid, for example, explodes violently when heated to 110°C while perbenzoic acid decomposes smoothly to primarily benzoic acid at 80-100°C. Two different mechanisms have been proposed to explain the two principal modes of decomposition observed (205). In dilute solution in the absence of oxygen and radical inhibitors, the following pseudo-first order chain mechanism is assumed to predominate:

$$RCO_2H \xrightarrow{\Delta} RC(=O)-O\cdot + \cdot OH$$

$$RC(=O)-O\cdot \longrightarrow R\cdot + CO_2 \uparrow$$

Table 2.6 Experimental Activation Energies (206)

| Aldehyde | Initiation | Oxygen Order | $E_a$, experimental (kcal/mole) |
|---|---|---|---|
| Decanal | Photo | 0 | 3.7 |
| Decanal | Thermal | 0.5 | 11.5 |
| Heptanal | Photo | 1 | 3.9 |
| Benzaldehyde | Photo | 0 | 1.8 |
| Benzaldehyde | Thermal | 0 | 7.6 |
| Benzaldehyde | Thermal | 0-1 | 17.7 |
| Acetaldehyde | Photochemical | 0-1 | 3.5 |
| Benzaldehyde | Photochemical | | 5. |

Table 2.7 Experimental Activation Energies of Reactions Involved in Autoxidation of Aldehydes (206)

| Reaction | $E_a$(kcal/mole) |
|---|---|
| $X \longrightarrow 2RCO_2H$ | 15-16 |
| $RCHO \xrightarrow{h\nu} R\cdot + CHO\cdot$ | 0 |
| $R\cdot + O_2 \longrightarrow RO_2\cdot$ | 0 |
| $RO_2\cdot + RCHO \longrightarrow RO_2H + RCO\cdot$ | 4 |
| $RCO\cdot + O_2 \longrightarrow RCO_3\cdot$ | 0 |
| $RCO_3\cdot + RCHO \longrightarrow RCO_3H + RCO\cdot$ | 4 |
| $2RCO_3\cdot \longrightarrow (RCO_3)_2$ | 1 |
| $RCO_3\cdot \longrightarrow RCO\cdot + \dot{O}_2$ | - |
| $M^{+3} + RCHO \longrightarrow M^{+2} + RCO\cdot + H^+$ | - |
| $RCO_4CR \longrightarrow RCO\cdot + RCO_3\cdot$ | - |
| $RCHO + O_2 \longrightarrow RCO\cdot + HO_2\cdot$ | 15.6 |
| $RCHO \longrightarrow RCHO^*$ | 13.5 |
| $2RCO\cdot \longrightarrow (RCO)_2$ | 1 |
| $RCO\cdot + RCO_3\cdot \longrightarrow$ products | 1 |
| $RCO\cdot + I \longrightarrow RCOI\cdot$ | - |
| $RCO_3\cdot + I \longrightarrow RCOI\cdot$ | - |

Table 2.7 (contd.)

| Reaction | $E_a$(kcal/mole) |
|---|---|
| $R'\cdot + R''\cdot \longrightarrow R'R''$ | 0 |
| $RCO_3H + RCHO + RCO_2H \longrightarrow X + RCO_2H$ | 7 |
| $RCHO^* + O_2 \longrightarrow RCHO_3^*$ | 3.5 |
| $RCHO_3^* + RCHO \longrightarrow RCO_3H + RCHO^*$ | 7 |
| $O_2 + RCHO \longrightarrow RCO\cdot + HO_2\cdot$ | 4 |
| $O\cdot + RCHO \longrightarrow OH\cdot + RCO\cdot$ | 4 |
| $2RO_2\cdot \longrightarrow$ products | 0 |
| $R\cdot + RO_2\cdot \longrightarrow$ products | 0 |
| $RCHO^* + RCHO \longrightarrow$ inactive products | |
| $RCHO_3^* \longrightarrow$ inactive products | |

I = Inhibitor

* = activated specie

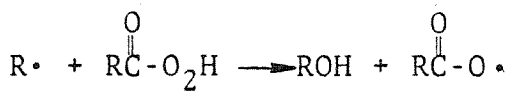

Thus, the production of free radicals during peracid decomposition can result in auto-acceleration of aldehyde oxidation by producing additional initiators. The radical R• can participate in other free radical reactions and can form three classes of hydrocarbons, as shown:

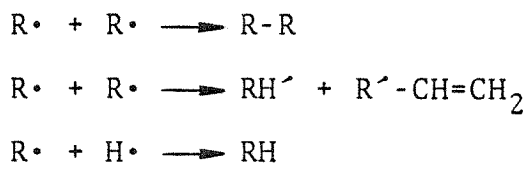

The second mode of decomposition is described by

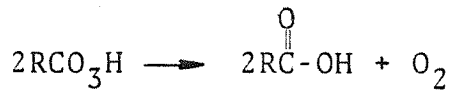

It does not involve radicals and generally occurs at a faster rate than the radical decomposition previously mentioned. The proposed mechanism (223,233) consists of attack of the peracid anion on the unionized peracid to form an intermediate which decomposes rapidly to give the carboxylic acid and oxygen as the main reaction products.

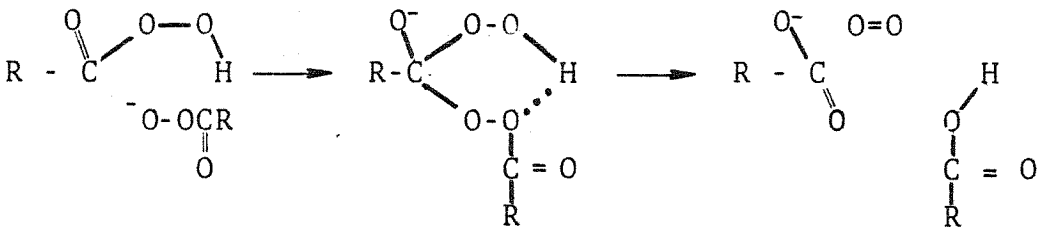

In practice, products from both mechanisms are usually found unless special precautions are taken to exclude one of the decomposition modes, resulting in an overall reaction order

of decomposition between 1 and 2 in peracid.

Inhibition and Retardation

In his early investigations of the autoxidation of aldehydes, Backstrom (207) noted that the order of benzaldehyde oxidation with respect to initiator depended upon the nature of the inhibitor employed. To explain this observation, Waters and Wickham-Jones (208) proposed the existence of two distinct mechanisms: chain-ending inhibition and chain-transfer retardation. The effect of each on the course of the oxidation is distinctly different. Inhibitors cause an induction period of nearly zero rate, during which they are destroyed and after which the reaction proceeds at its uninhibited rate. Retarders have much more persistence, acting as negative catalysts by allowing the oxidation to proceed at a steady, yet slower rate for a long time. Figure 2.1 illustrates this difference. Examples of inhibitors include unsaturated hydrocarbons, whereas the phenols act as retarders. Experimentally, it has been shown that inhibitor efficiency is independent of oxygen pressure (at oxygen pressures >100 torr) which is consistent with interruption of the radical chain by the reaction given below (204):

$$RCO_3\cdot + \text{Inhibitor} \longrightarrow \text{inactive products}$$

This type of inhibition appears to be a general situation and is certainly plausible because the acyl peroxy radicals are in highest concentration under most circumstances. Of course, once the inhibitor has been completely oxidized, the chain is free to propagate as though no inhibitor were

Figure 2.1 TYPICAL EFFECTS OF INHIBITORS AND RETARDERS ON AUTOXIDATION SYSTEMS

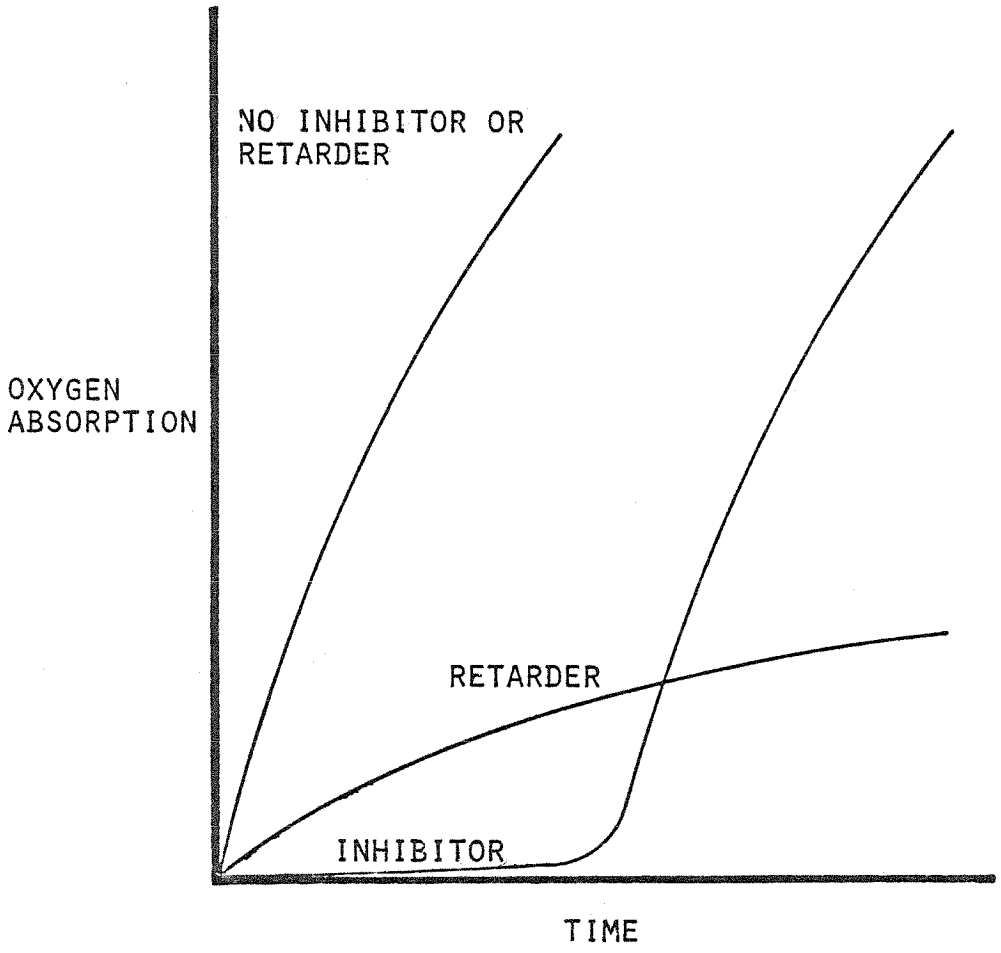

present. On the other hand, the much longer time scale of retarder action can only be explained by a series of chemical reactions where it is reformed. Thus, retarders are assumed to act as chain transfer agents, where a series of slow radical reactions are substituted for a sequence of normally rapid ones. For example,

$$\left.\begin{aligned} RCO\cdot + \text{ØOH} &\longrightarrow RCHO + \text{ØO}\cdot \\ RCO_3\cdot + \text{ØOH} &\longrightarrow RCO_3H + \text{ØO}\cdot \\ \text{ØO}\cdot + RCHO &\longrightarrow \text{ØOH} + RCO\cdot \end{aligned}\right\} \text{Chain transfer}$$

$$2\text{ØO}\cdot \longrightarrow \text{phenol dimer} \qquad \text{Chain termination}$$

The inclusion of the above reactions in the chain mechanism for autoxidation of benzaldehyde has been used successfully to explain the experimental results obtained in the presence of p-cresol (208).

Peracid-Aldehyde Reaction

During autoxidation of aldehydes, the peracid formed can react directly with the aldehyde by a non-radical mechanism. In the case of acetaldehyde, a stable peracetic acid-acetaldehyde adduct has been isolated with the structure (234)

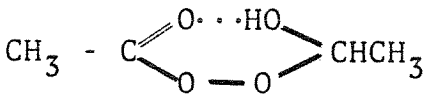

acetaldehyde monoperacetate (AMP)

Depending upon reaction conditions, this addition product will decompose to the reactants or two molecules of acetic acid (235). The combination is apparently more rapid than the decomposition. The corresponding activation energies are 7 and 15 kcals, respectively (236). No such interme-

diate has been isolated for the benzaldehyde-perbenzoic acid system. Instead, a Baeyer-Villiger reaction mechanism is assumed to produce two molecules of benzoic acid directly. With proper choice of solvent and electron-donating substituents, the rearrangement can be shifted to also give phenol (237).

Hydrolysis of Peracids

In the presence of water, peracids participate in the following equilibrium:

$$RCO_3H + H_2O \rightleftharpoons RCO_2H + H_2O$$

Under the proper set of conditions, this equilibrium can be driven to the left to produce peracids from the corresponding organic acid and hydrogen peroxide. This reaction has been used extensively to synthesize peracids (205,224). Tracer studies show that the mechanism involves cleavage of the acyl oxygen bond of the peracid (238) and is both acid and base catalyzed (239,240). The pseudo first order rate constants (large excess of $H_2O$) take the form:

$$\text{acid} \quad k_A = k_{1A} + k_{2A}\,(H^+)$$

$$\text{base} \quad k_B = k_{1B} + k_{2B}\,(OH^-)$$

Values of the rate constants for peracetic and perbenzoic acids are given in Table 2.8.

Solvent Effects

Only comparatively recently has the understanding of radical-chain reactions advanced to the point where solvent

Table 2.8 Rate Constants for Acidic and Alkaline Hydrolysis of Peracids at 25°C. (238,240)

| Peracid | $k_{1A}$ (1/sec) | $k_{2A}$ (ℓ/mole/sec) | $k_{1B}$ (1/sec) | $k_{2B}$ (ℓ/mole/sec) |
|---|---|---|---|---|
| Perbenzoic acid | $2.8*10^{-7}$ | $5.1*10^{-6}$ | $4.8*10^{-6}$ | $3.3*10^{-4}$ |
| Peracetic acid | $3.8*10^{-6}$ | $1.0*10^{-4}$ | | |

effects can be separated from other factors. It has been shown that the oxidation rate could be very roughly correlated with the dielectric constant (D) of the solvent (209). On the basis of theory which describes the bulk effect of solvents on dipole-forming reactions, the logarithm of the overall oxidation rate constant is expected to be linear with the function $\frac{D-1}{2D+1}$. It is particularly interesting to note that the rates in the hydroxylic solvents are correlated about as well as the rates in aprotic solvents, because dielectric constant is not a very good measure of the greatly enhanced solvent-ionizing power resulting from the hydroxy moiety. This result is presumably because the amount of charge, and charge separation is much less in the autoxidation propagation reaction than in other reactions involving formation of a dipolar transition state, such as solvolysis of t-butyl chloride.

# CHAPTER 3 OXIDATION OF ORGANIC SULFUR COMPOUNDS BY PERACIDS

Oxidation of organic sulfides by peroxides has been demonstrated to be a satisfactory method to produce many of the corresponding sulfoxides and sulfones (301,302,303, 304). Only when this method failed for some organic sulfur compounds, notably thiophenes, was interest generated in stronger oxidizing systems, such as peracids. For example, Gilman and Esmay (305) were the first to oxidize dibenzothiophene to its sulfone using hydrogen peroxide in acetic acid. They attributed the relatively high oxidation rates observed to an acetic acid solvent effect, rather than the formation of peracetic acid by the equilibrium

$$RCO_2H + H_2O_2 \rightleftharpoons RCO_3H + H_2O$$

Overberger and Cummins (306) studied the oxidation of p,p' dichlorobenzyl sulfide to its sulfoxide by perbenzoic acid. The absence of acid catalysis, lack of salt effect, and the large rate enhancement in toluene as opposed to isopropanol solvent led them to propose the following mechanism involving an intramolecularly-hydrogen-bonded form of the peracid:

Later infrared (IR) work demonstrated the direct relationship between the strength of intramolecular hydrogen bonding in

various solvents and reaction rate (307,308). Lack of catalysis by light was taken as evidence of the non-free radical character of the electrophilic attack by peracid. This result was confirmed in our studies (see Appendix A). The Overberger and Cummins mechanism accounted for the main features of the reaction, which also included the observations that 1) an increase in acid strength of the peracid favored the reaction, 2) the rate of oxidation of the sulfide to sulfoxide was increased by electron repelling and decreased by electron-attracting groups, 3) the reaction was first order with respect to both the peracid and the sulfide, i.e., overall second order, and 4) low activation energies (5 - 15 kcal/mole) with a high entropy of activation ($\Delta S^*$ = 20 - 30 entropy units) were found.

Modena and coworkers (309) investigated the oxidation of benzothiophenes and dibenzothiophenes by perbenzoic acid in 1:1 dioxane-water solvent in the temperature range 0-40°C. They found the reaction to be overall second order and suggested that the mechanism of Overberger and Cummins applied to thiophenes as well. It was also noted that the ratio of second-order rate constants for the first stage (to sulfoxide, $k_1$) and the second stage (to sulfone, $k_2$)

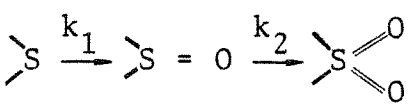

was small for benzothiophene ($k_1/k_2$ = 1.5) and rather more for dibenzothiophene ($k_1/k_2$ = 10), compared with a ratio of $k_1/k_2$ = 50 - 100 for sulfides. In later work (310), they

suggested that two competing mechanisms may contribute to the rate of sulfoxide oxidation in the second stage, one due to the undissociated and the other to the dissociated peracid. Their results were inconclusive, and the sulfide oxidation mechanism of Overberger and Cummins is generally assumed to apply to the peracid oxidation of sulfoxide to sulfone as well.

Ford and Young (311) studied the effect of structure on the rate of reaction of organo-sulfur compounds with peracetic acid. For sulfides, the reaction rates decreased in the sequence: di-n-butyl, tetramethylene > di-sec-butyl> di-t-butyl > phenyl methyl >diphenyl sulfide. These results were explained on the basis of the electron availability on sulfur and steric hindrance. Rate constants for thiophenic compounds were in the increasing sequence: thiophene < 2-methyl thiophene, 3-methyl thiophene < 2,5 dimethyl thiophene, benzothiophene < tetra methyl thiophene, dibenzothiophene << diphenyl sulfide. Two reasons were suggested for the much lower rates of thiophene oxidation versus sulfide oxidation: 1) the lone-pair electrons of the sulfur in thiophene are delocalized by the aromatic character of the molecule, and 2) the increase in configurational strain in the C-S-C bond angles which increases from $91^{o}$ to $100^{o}$ in going from the thiophene to its sulfoxide.

Oxidation of dibenzothiophene in a two-phase system of paraffinic white oil and hydrogen peroxide-acetic acid was investigated by Heimlich and Wallace (312). They observed

a second order dependence on hydrogen peroxide and postulated the mechanism below involving a dimeric oxidizing agent as an explanation.

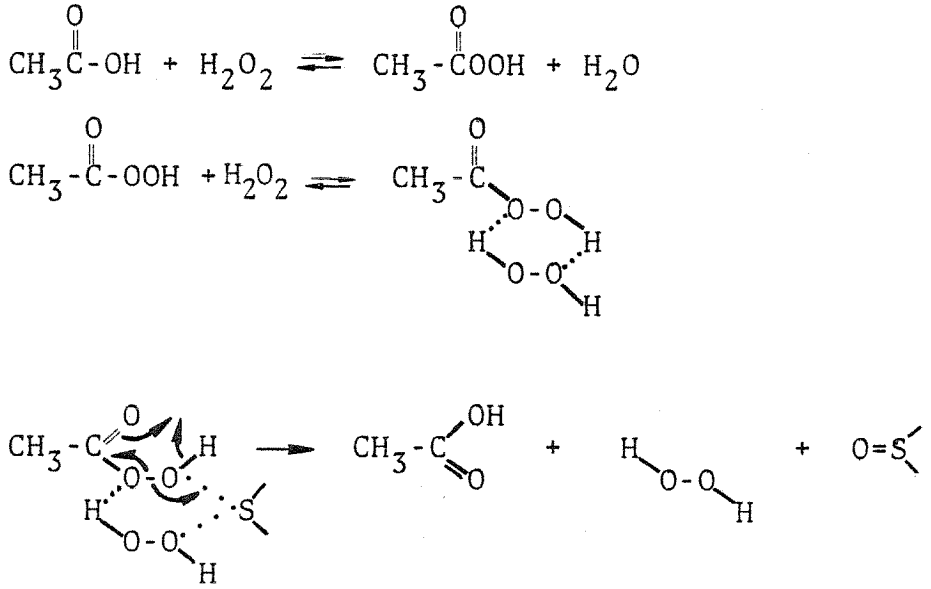

Dibenzothiophene sulfoxide was oxidized 1.4 times faster than dibenzothiophene, in contrast with all other authors. This result may be due to the partial solubility of the sulfoxide in the aqueous phase.

Subsequent work on the peracid oxidation of sulfides and thiophenes has concentrated on the question of participation of the sulfur 3d orbitals (313,314). Quantum mechanical calculations suggest that it is not necessary to invoke conjugation of sulfur 3d orbitals to interpret the large differences in oxidation rates of dibenzothiophene and diphenyl sulfide derivatives (314).

Rate constants which have been obtained for the oxidation of sulfur compounds by peracids are summarized in

Table 3.1.

Table 3.1. Rate Constants for the Oxidation of Sulfur Compounds by Peracids (314,315)

| Sulfur Compound | Acid | Solvent | Temp. °C | k (ℓ/mole/sec) | E kcal/mole | log A (ℓ/mole/sec) |
|---|---|---|---|---|---|---|
| Tetramethylene sulfide | Peracetic | Toluene | -70 | 4 | | |
| Di-n-butyl sulfide | Peracetic | Toluene | -70 | 3.2 | | |
| Di-sec-butyl sulfide | Peracetic | Toluene | -70 | 1.47 | | |
| Di-tert-butyl sulfide | Peracetic | Toluene | -70 | 0.83 | 8.6 | 9.164 |
| Di-tert-butyl sulfide | Peracetic | Toluene | -50 | 5.65 | 8.6 | 9.164 |
| Phenyl methyl sulfide | Peracetic | Toluene | -49 | 0.097 | 9.6 | 8.338 |
| Phenyl methyl sulfide | Peracetic | Toluene | -39.1 | 0.24 | 9.6 | 8.338 |
| Phenyl methyl sulfide | Peracetic | Toluene | -30.0 | 0.53 | 9.6 | 8.338 |
| Phenyl methyl sulfide | Peracetic | Toluene | -20.0 | 1.7 | 9.6 | 8.338 |
| Diphenyl sulfide | Peracetic | Benzene + 10N acetic acid | 0 | 0.268 | 9.6 | 7.166 |

Table 3.1. (contd.)

| Sulfur compound | Acid | Solvent | Temp. °C | k (ℓ/mole/sec) | E kcal/mole | log A (ℓ/mole/sec) |
|---|---|---|---|---|---|---|
| Diphenyl sulfide | Peracetic | Benzene + 10N acetic acid | 10 | 0.4863 | 9.6 | 7.166 |
| Diphenyl sulfide | Peracetic | Toluene | 20 | 0.8880 | 9.6 | 7.166 |
| Dibenzothiophene | Peracetic | Benzene | 15 | 0.0049 | 14.7 | 8.572 |
| Dibenzothiophene | Peracetic | Benzene | 30 | 0.0091 | 14.7 | 8.572 |
| Dibenzothiophene | Peracetic | Benzene | 40 | 0.0168 | 14.7 | 8.572 |
| Dibenzothiophene | Peracetic | Benzene | 50 | 0.0357 | 14.7 | 8.572 |
| Dibenzothiophene | Peracetic | Benzene | 60 | 0.0694 | 14.7 | 8.572 |
| Dibenzothiophene | Peracetic | Benzene + 10N acetic acid | 15 | 0.00433 | 14.8 | 5.8596 |
| Dibenzothiophene | Peracetic | Benzene + 10N acetic acid | 30 | 0.0151 | 14.8 | 5.8596 |
| Dibenzothiophene | Peracetic | Benzene + 10N acetic acid | 40 | 0.0329 | 14.8 | 5.8596 |
| Dibenzothiophene | Peracetic | Benzene + 10N acetic acid | 50 | 0.0725 | 14.8 | 5.8596 |
| Dibenzothiophene | Peracetic | Benzene + 10N acetic acid | 60 | 0.142 | 14.8 | 5.8596 |
| Benzothiophene | Peracetic | Benzene | 40 | 0.0026 | | |
| Benzothiophene | Peracetic | Benzene + 10N acetic acid | 40 | 0.0017 | | |
| Thiophene | Peracetic | Benzene + 10N acetic acid | 40 | $6 \times 10^{-5}$ | | |
| Tetramethylthiophene | Peracetic | Benzene + 10N acetic acid | 40 | 0.0368 | | |

Table 3.1 (contd.)

| Sulfur Compound | Acid | Solvent | Temp. °C | k (ℓ/mole/sec) | E kcal/mole | log A (ℓ/mole/sec) |
|---|---|---|---|---|---|---|
| 2,5-Dimethylthiophene | Peracetic | Benzene + 10N acetic acid | 40 | 0.00186 | | |
| 2-Methylthiophene | Peracetic | Benzene + 10N acetic acid | 40 | $4.1 \times 10^{-4}$ | | |
| 3-Methylthiophene | Peracetic | Benzene + 10N acetic acid | 40 | $3.4 \times 10^{-4}$ | | |
| p,p'-Dichlorobenzyl sulfide | p-Methoxy perbenzoic | Toluene | -65 | 0.61 | 6.6 | 6.6881 |
| p,p'-Dichlorobenzyl sulfide | p-Methoxy perbenzoic | Toluene | -55 | 1.32 | 6.6 | 6.6881 |
| p,p'-Dichlorobenzyl sulfide | p-Methoxy perbenzoic | Toluene | -45 | 2.44 | 6.6 | 6.6881 |
| p,p'-Dichlorobenzyl sulfide | p-Methoxy perbenzoic | Isopropyl alcohol | -35 | 0.19 | 9.9 | 8.362 |
| p,p'-Dichlorobenzyl sulfide | p-Methoxy perbenzoic | Isopropyl alcohol | -25 | 0.44 | 9.9 | 8.362 |
| p,p'-Dichlorobenzyl sulfide | p-Methoxy perbenzoic | Isopropyl alcohol | -15 | 0.95 | 9.9 | 8.362 |
| p,p'-Dichlorobenzyl sulfide | Peroxybenzoic | Toluene | -65 | 1.29 | 5.2 | 5.646 |
| p,p'-Dichlorobenzyl sulfide | Peroxybenzoic | Toluene | -55 | 2.50 | 5.2 | 5.646 |
| p,p'-Dichlorobenzyl sulfide | Peroxybenzoic | Toluene | -45 | 4.17 | 5.2 | 5.646 |
| p,p'-Dichlorobenzyl sulfide | Perbenzoic | Isopropyl alcohol | -40 | 0.15 | 9.6 | 8.2516 |

Table 3.1 (contd.)

| Sulfur Compound | Acid | Solvent | Temp. °C | k (ℓ/mole/sec) | E kcal/mole | log A (ℓ/mole/sec) |
|---|---|---|---|---|---|---|
| p,p'-Dichlorobenzyl sulfide | Perbenzoic | Isopropyl alcohol | -30 | 0.38 | 9.6 | 8.2516 |
| p,p'-Dichlorobenzyl sulfide | Perbenzoic | Isopropyl alcohol | -20 | 0.79 | 9.6 | 8.2516 |
| p,p'-Dichlorobenzyl sulfide | p-Methyl perbenzoic | Isopropyl alcohol | -40 | 0.11 | 11.3 | 9.5979 |
| p,p'-Dichlorobenzyl sulfide | p-Methyl perbenzoic | Isopropyl alcohol | -30 | 0.29 | 11.3 | 9.5979 |
| p,p'-Dichlorobenzyl sulfide | p-Methyl perbenzoic | Isopropyl alcohol | -20 | 0.70 | 11.3 | 9.5979 |
| p,p'-Dichlorobenzyl sulfide | p-Chloroper-benzoic | Isopropyl alcohol | -45 | 0.17 | 9.6 | 8.4687 |
| p,p'-Dichlorobenzyl sulfide | p-Chloroper-benzoic | Isopropyl alcohol | -35 | 0.45 | 9.6 | 8.4687 |
| p,p'-Dichlorobenzyl sulfide | p-Chloroper-benzoic | Isopropyl alcohol | -25 | 0.89 | 9.6 | 8.4687 |
| p,p'-Dichlorobenzyl sulfide | p-Nitroper-benzoic | Isopropyl alcohol | -55 | 0.43 | 6.9 | 6.5578 |
| p,p'-Dichlorobenzyl sulfide | p-Nitroper-benzoic | Isopropyl alcohol | -45 | 0.88 | 6.9 | 6.5578 |
| p,p'-Dichlorobenzyl sulfide | p-Nitroper-benzoic | Isopropyl alcohol | -35 | 1.60 | 6.9 | 6.5578 |
| 3-Methoxybenzothio-phene | Perbenzoic | $CH_2Cl_2$ | 30 | 0.61 | | |
| 3-Methoxybenzothio-phene | Perbenzoic | $CH_2Cl_2$ | 30 | 0.112 | | |

Table 3.1 (contd.)

| Sulfur Compound | Acid | Solvent | Temp. °C | k (ℓ/mole/sec) | E kcal/mole | log A (ℓ/mole/sec) |
|---|---|---|---|---|---|---|
| Benzothiophene | Perbenzoic | $CH_2Cl_2$ | 30 | 0.0051 | | |
| Benzothiophene | Perbenzoic | Dioxane-$H_2O$ | 25 | 0.004 | 14.2 | 7.99 |
| 3-Methoxybenzothiophene | Perbenzoic | $CH_2Cl_2$ | 30 | 0.08 | | |
| 3-Methoxybenzothiophene | Perbenzoic | $CH_2Cl_2$ | 30 | 0.032 | | |
| Benzothiophene sulfoxide | Perbenzoic | $CH_2Cl_2$ | 30 | 0.0095 | | |
| Benzothiophene sulfoxide | Perbenzoic | Dioxane-$H_2O$ | 25 | 0.0029 | | |
| Diphenyl sulfide | Perbenzoic | Dioxane-$H_2O$ | 25 | 5.0 | | |
| Diphenyl suloxide | Perbenzoic | Dioxane-$H_2O$ | 25 | 0.0032 | 13.3 | 8.25 |
| Dibenzothiophene | Perbenzoic | Dioxane-$H_2O$ | 25 | 0.0396 | 13.7 | 8.64 |
| Dibenzothiophene sulfoxide | Perbenzoic | Dioxane-$H_2O$ | 25 | 0.0037 | 13.5 | 7.47 |
| p-Nitrodiphenyl sulfide | Perbenzoic | Dioxane-$H_2O$ | 25 | 0.527 | 10.8 | 7.64 |
| p-Nitrodiphenyl sulfoxide | Perbenzoic | Dioxane-$H_2O$ | 25 | 0.0125 | 12.7 | 5.52 |
| Diphenyl sulfide | Perbenzoic | $CH_2Cl_2$ | 20 | 10.7 | | |
| Dibenzothiophene | Perbenzoic | $CH_2Cl_2$ | 20 | 0.057 | | |

# CHAPTER 4 EXPERIMENTAL APPARATUS AND PROCEDURE

A semi-batch reactor system was chosen for the experimental study because of the preliminary nature of this work. The equipment was modified from that used in previous experiments by Attar (401).

## The Reactor

A schematic of the reactor and peripheral equipment is shown in Figure 4.1. The reactor itself was constructed from a standard 500 ml 3-necked flask to which two additional 24/40 ground glass joints were symmetrically connected, as depicted in Figure 4.2. The central 34/45 joint was used for addition of reagents and stoppered during the run. The other four necks contained 1) a liquid sampling device (see Figure 4.3), 2) a gas bubbler with a cylindrical sintered glass sparger of medium porosity at the tip, through which the oxygen/nitrogen gas mixture was dispersed, 3) a reflux condenser open to the atmosphere and 4) a thermowell in which a YSI No. 632 thermistor and a copper-constantan 24 G thermocouple were inserted. The thermistor was utilized as the input to a Versatherm proportional controller, Model No. 2156, which controlled the 500 ml Glass-Col mantle used to heat the reactor. The temperature was monitored with the previously-mentioned thermocouple read by an electronic thermometer, Bailey Instrument Model Bat 7. The reaction mixture was agitated via a magnetic stirrer placed immediately below the heating mantle. A standard 1 in x 3/8 in teflon-coated stir bar was employed inside the reactor.

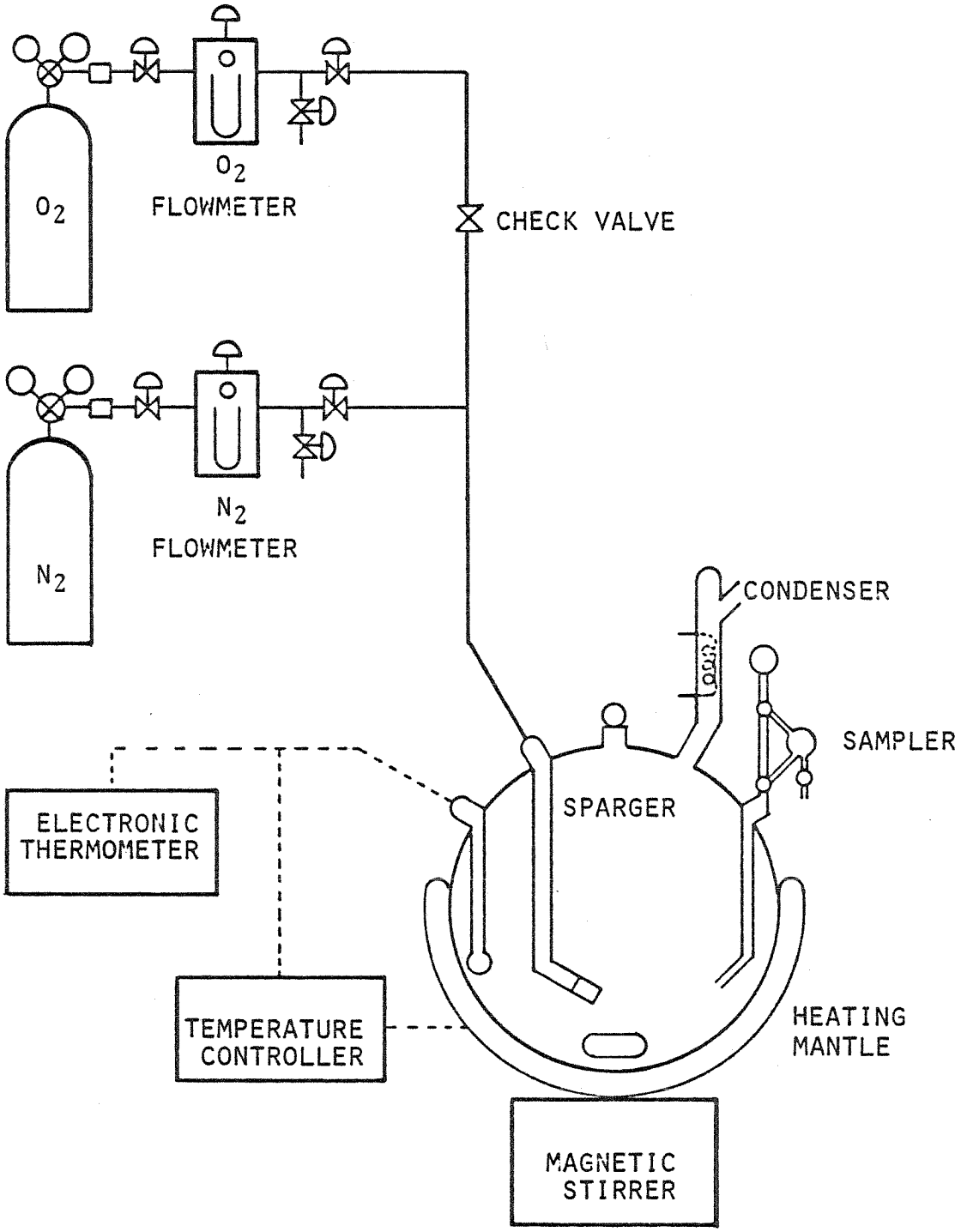


FIGURE 4.1 SCHEMATIC DIAGRAM OF THE REACTOR AND PERIPHERAL EQUIPMENT

FIGURE 4.2 BATCH REACTOR

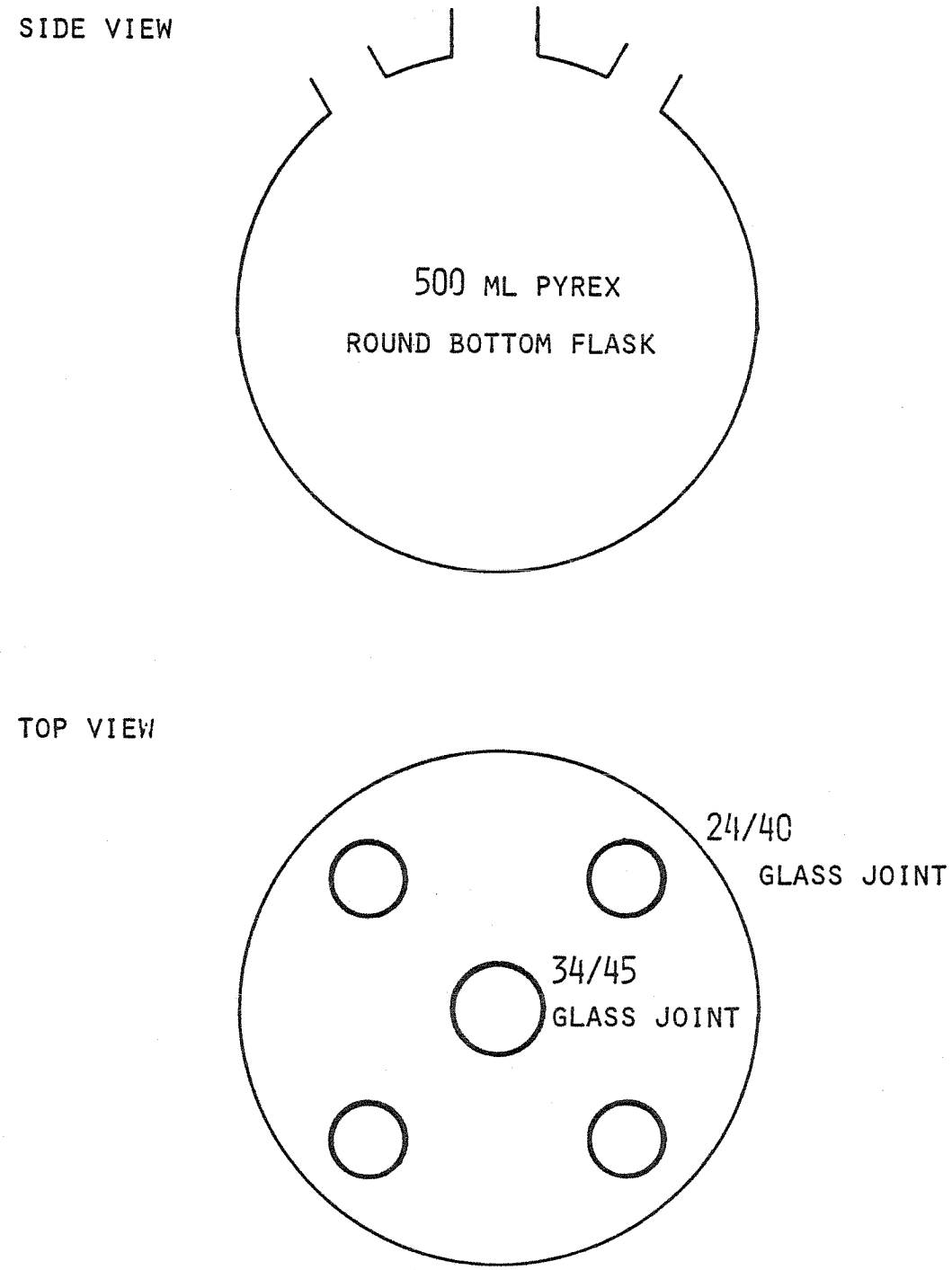

FIGURE 4.3 SAMPLING DEVICE FOR LIQUID SAMPLES

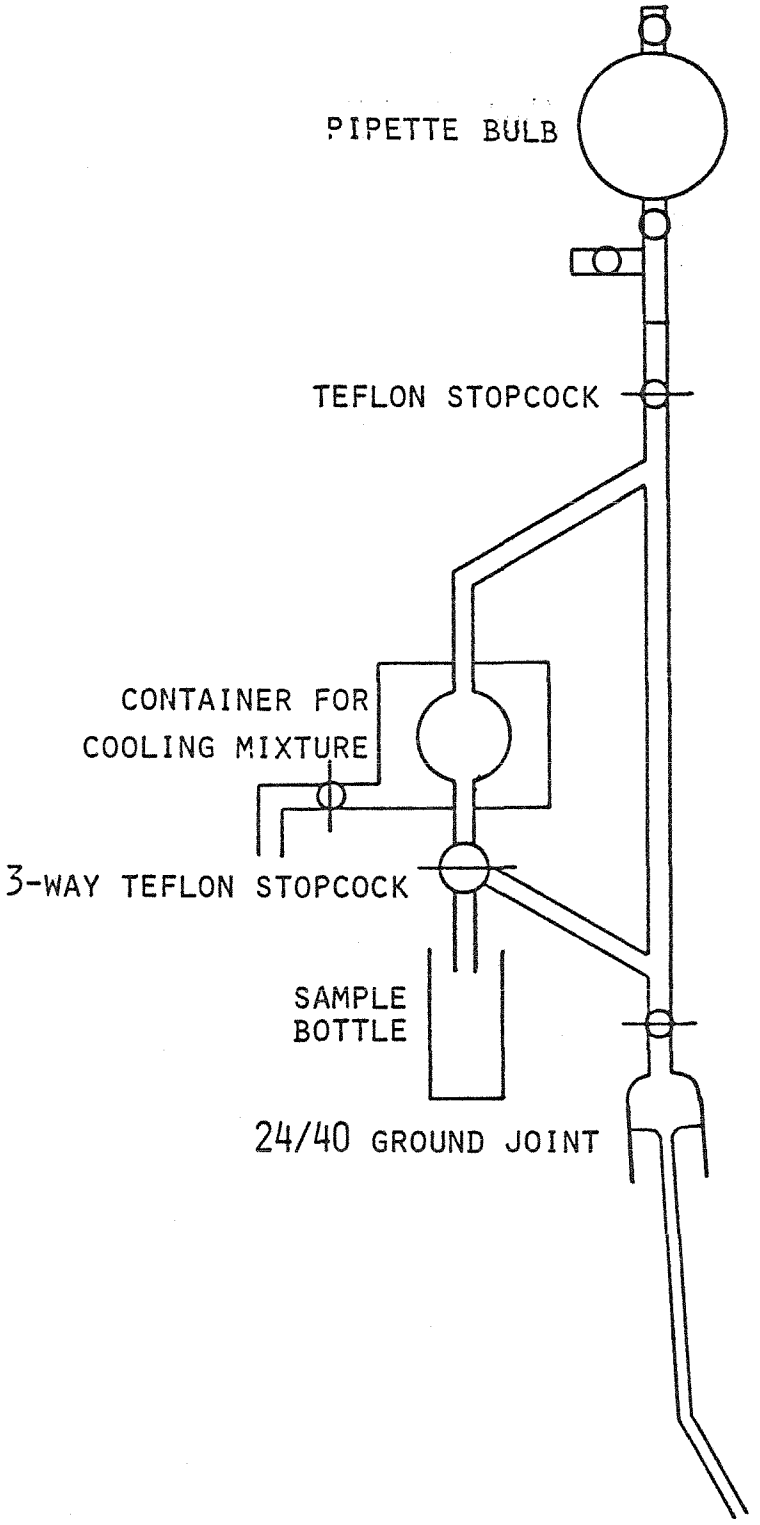

All experiments were run at maximum stirring rate, which was stroboscopically found to be approximately 1800 RPM. Oxygen and nitrogen were fed to the reactor from cylinders of compressed gas through the sintered glass sparger. The delivery pressure of 20 psig was regulated with standard Matheson gas regulators. The flow rate was measured by monitoring the pressure drop created across a fixed bed of small glass beads (see Figure 4.4). The range of flow measurement was determined by the length of the column of glass beads, the length of the manometer u-tube, and the density of the manometer fluid. After calibration by a soap film flowmeter, a linear relationship between volumetric gas flow rate and pressure drop across the glass bead column was obtained with a correlation coefficient greater than 0.99 in all cases. For safety purposes, the entire apparatus was isolated under the hood behind plexiglass shields.

The Chemical System

Two approaches to the choice of a chemical system were possible: 1) selective oxidation of sulfur compounds present in a residual oil fraction, or 2) selective oxidation of model sulfur compounds in a medium which simulates residual oil. The first alternative posed enormous analytical difficulties, whereas the second system was much better defined and held promise of providing basic information on reaction mechanisms which could hopefully be extended to real fuels. This latter approach was chosen for this study.

Dibenzothiopene (DBT) was selected as the sulfur

FIGURE 4.4 GAS FLOWMETER

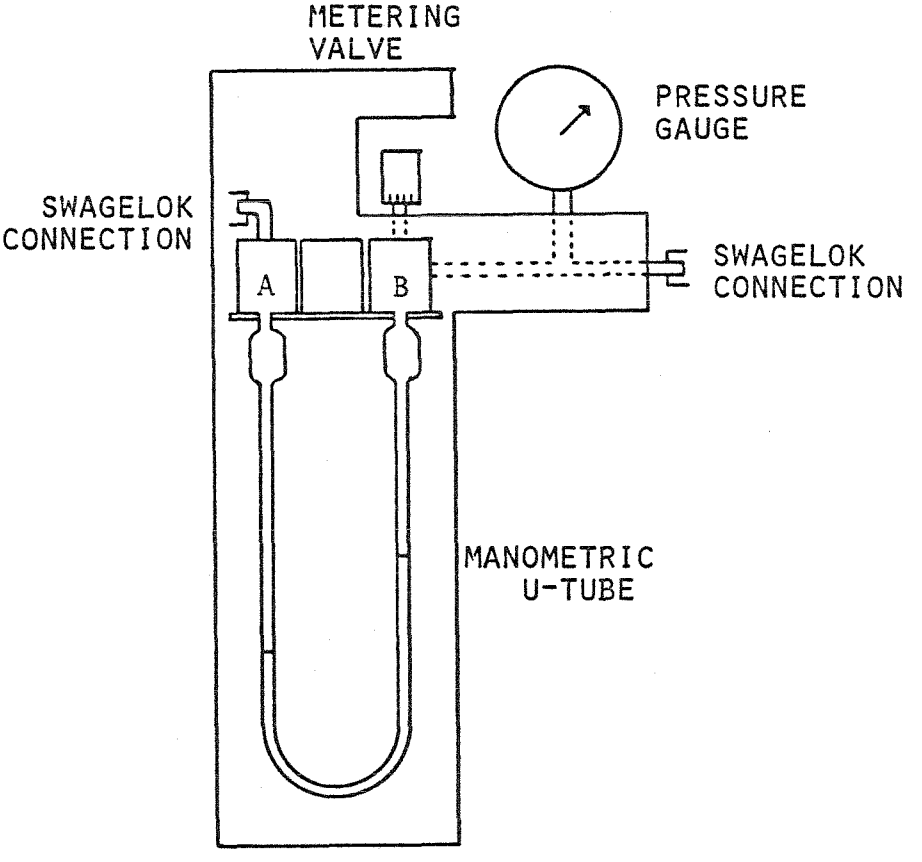


THE MANOMETRIC PRESSURE DIFFERENCE IS PROPORTIONAL TO THE VOLUMETRIC FLOW RATE. POINTS A AND B ARE CONNECTED BY A TUBE PACKED WITH 0.00095 IN GLASS BEADS THROUGH WHICH THE GAS FLOWS.

compound on which the bulk of the experimental work was concentrated; some work was also done with diphenyl sulfide (DPS). Dibenzothiophene, in particular, is a very stable compound because of the resonance character of the central thiophene ring. Many oxidation schemes which have been shown to successfully oxidize sulfides to their corresponding sulfoxides and sulfones have failed for thiophenic sulfur compounds (401). Any oxo-desulfurization process must be able to handle both DBT and DPS since they represent the two most important classes of sulfur compounds found in heavy crude cuts, i.e., thiophenes and sulfides. Both compounds have a symmetric structure, reducing the number of product isomers. Therefore, easier analytical problems were anticipated. Also, these two sulfur compounds, as well as some of their oxidation products are readily available from Aldrich. They were used as received; no impurities were observed on the liquid chromatograph.

Benzaldehyde was chosen as the aldehyde to be used for in situ generation of the peracid. Benzaldehyde has been demonstrated to have reasonable autoxidation rates in the temperature range desired (see Chapter 2). Safety was the primary criterion, however. Many peracids are known to decompose explosively. Perbenzoic acid, while not completely safe, is less reactive. Reagent benzaldehyde was obtained from Aldrich and stored at $0^{o}C$ under argon. Vacuum distillation of the benzaldehyde in an attempt to remove any inhibitors which might be present, resulted in lower rates

of autoxidation instead, as demonstrated in Figure 4.5. Trace metal catalysis was suspected as the cause of this discrepancy. Addition of disodium ethylenedinitrilotetra-acetate (EDTA), a metal-complexing agent, to the original benzaldehyde resulted in no decrease in the rate of autoxidation, however, as can be noted in Figure 4.6. Aldehyde autoxidations are inherently difficult to reproduce (see Chapter 2); in our studies the best results were obtained with benzaldehyde as received without further purification.

Bromobenzene was selected as a solvent which adequately simulated the aromatic, aprotic nature of the hydrocarbons present in residual oil. Reagent grade was utilized without further purification. The atmospheric residual oil used in one experiment was sampled from Newhall Refining Company on June 6, 1980; some of its physical properties are listed below:

SSF. @ 122°F = 1492
Flash = 300°F
Gravity = 12.9 API
pH = 7.2
Cut = ~700°F and not finished

Experimental Procedure

Each experiment was conducted as follows:

1. All glass and Teflon parts which came in contact with the reacting solution were deactivated. The appropriate parts were first rinsed with a mixture of nitric and sulfuric

FIGURE 4.5 EFFECT OF DISTILLATION ON AUTOXIDATION OF BENZALDEHYDE

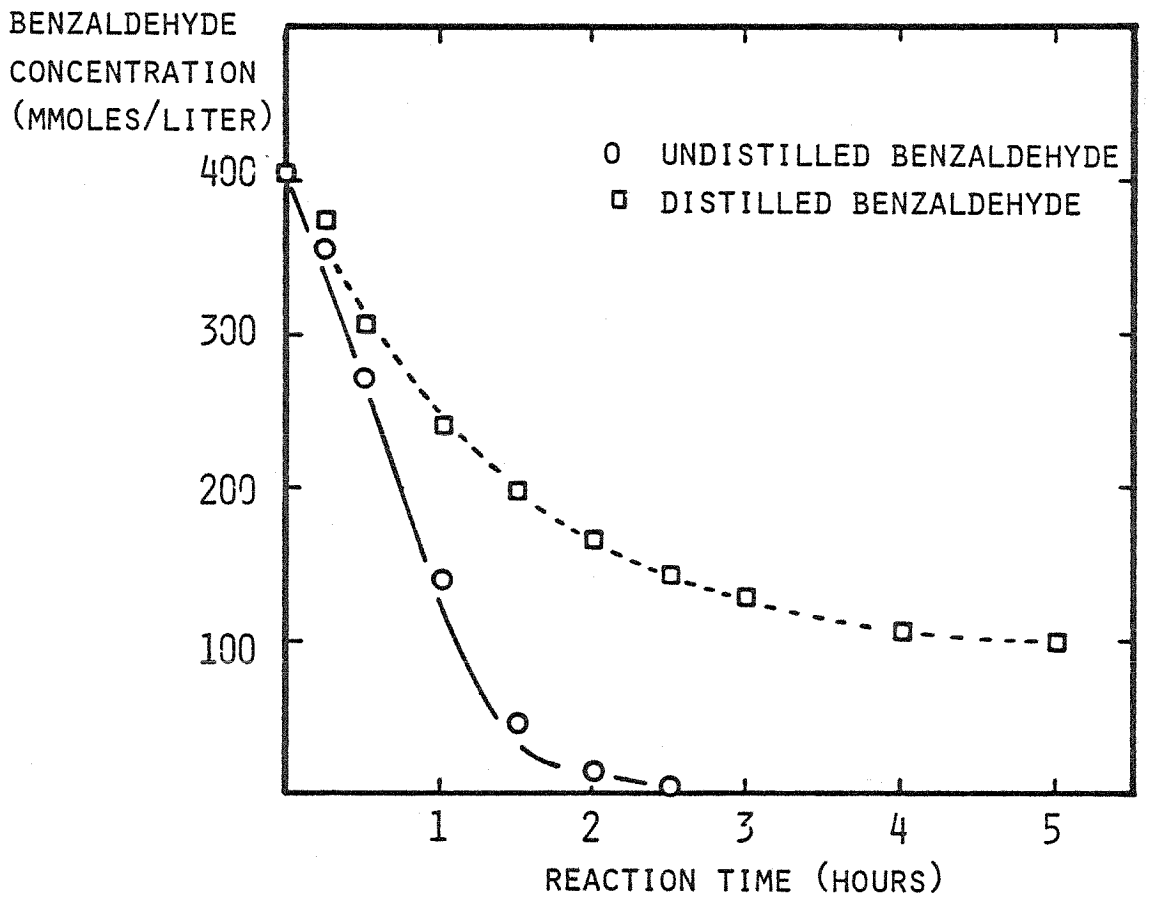


OXIDATION OF 10.5 G BENZALDEHYDE BY 2.6 MMOLES/MIN $O_2$ AT 0.5 ATM. PARTIAL PRESSURE IN 350 G BROMOBENZENE AT 50$^{o}$C, 1 ATM.

FIGURE 4.6 EFFECT OF EDTA ON BENZALDEHYDE AUTOXIDATION

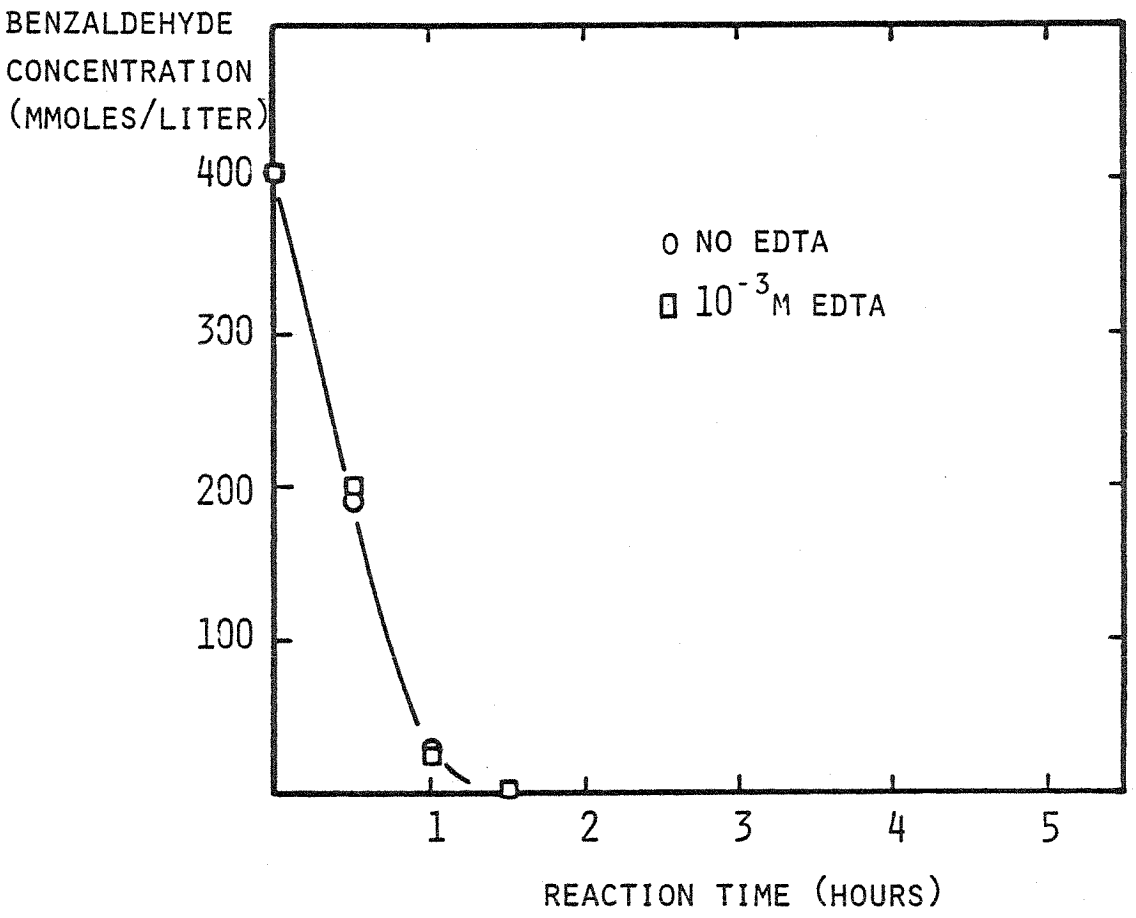


OXIDATION OF 10.5 G BENZALDEHYDE BY 2.6 MMOLES/MIN $O_2$ AT 0.5 ATM. PARTIAL PRESSURE IN 350 G BROMOBENZENE AT 100°C, 1 ATM.

acids, distilled water, acetone, and allowed to dry. The surfaces were then treated with a mixture of 10 ml pyridine, 3 ml trimethylchlorosilane, and 2 ml hexamethyldisilizane. This final deactivation step resulted in the etherification of the active OH groups on the glass surface. The excess solution was rinsed with acetone and the reactor immediately assembled. A minimum amount of Halocarbon 25 - 5S was used to seal the glass joints. A nitrogen purge through the sparger and an argon purge through the condenser were vented through the sampler. Both purges were maintained overnight to dry the remaining acetone.

2. All of the reactants for a particular experiment except the aldehyde were added to the reactor and the magnetic stirrer turned on. The nitrogen purge was maintained; the argon purge was eliminated. A sample of the solvent was taken and checked on the liquid chromatograph for impurities.

3. The mixture was heated to the desired temperature. The top portion of the reaction vessel not covered by heating mantle was insulated with strips of asbestos cloth, which also served to eliminate light and the resulting photo-initiation reactions. This insulation was not used in the experiments reported in Appendix A. The condenser was utilized to keep evaporative losses to a minimum.

4. After the appropriate temperature had been reached, the flows of oxygen and nitrogen were adjusted to the desired rates. The reaction mixture was allowed to equilibrate for ½ hour.

5. An appropriate amount of aldehyde was rapidly transferred from the reagent bottle to the reactor by pipette. The moment at which the pipette had eluted half its contents into the reactor was denoted as time zero. A sample was taken immediately after the addition of the aldehyde.

6. Samples were withdrawn every 15 minutes for the first ½ hour and every ½ hour thereafter. The gas flow rates and reaction temperature were noted just before the sample was taken. Each sample was immediately cooled in an ice bath. A 0.02 ml aliquot was removed by syringe and accurately diluted with 1.98 ml acetonitrile to provide a sample for chromatograph analysis. A second aliquot of approximately 1 ml was rapidly titrated for peracid.

7. The reaction was stopped after 5 hours by turning off the heat and the oxygen. The heating mantle was removed and the reactor was cooled in an ice bath to about $10^{o}C$. The reactor contents were removed and stored in the refrigerator under argon for further analysis. A 10 ml aliquot was weighed in a volumetric flask to provide a density for use in the calculation of peracid concentration.

8. The reactor was dismantled and rinsed with acetone.

Methods of Analysis

High-pressure liquid chromatography (HPLC) was utilized as the primary method of quantitative analysis. This method was chosen over gas chromatography (GC) because the high-boiling nature of some of the compounds studied made vapori-

zation difficult at temperatures below those associated with the onset of GC column degradation. Although high-pressure liquid chromatography has only recently become feasible with the development of a new generation of high-pressure pulse-free liquid pumps, its versatility and power are already well-established. HPLC is rapidly filling the void left by gas chromatography in the analysis of non-volatile compounds, and many excellent reviews on its theory and practice are available (402,405,406,407,408,409). The particular system used in this work consisted of the following components: 1) a Spectraphysics 3500 B liquid chromatograph, 2) a Perkin-Elmer LC-55 Spectrophotometer utilized as a detector, 3) a Spectrum 1021 Filter, 4) a Spectraphysics System I Computing Integrator, 5) a Beckman No. 100506 Recorder, and 6) a Model 1200 Pup Fraction Collector. A schematic is given in Figure 4.7. The reversed-phase separation mode was deemed appropriate for the compounds being analyzed. A stainless-steel column with ID of 3mm and length of 250 mm packed with 10μ particles of Spherisorb octadecyl silica (ODS) used with a mobile-phase gradient of water and acetonitrile resulted in adequate separation. Details of the operation of the liquid chromatograph are given in Appendix B. Similar methods were also used in the analysis of other systems for oxidation of sulfur compounds (see Appendix C). Application of Beer's law to the ultraviolet spectrophotometer used as a detector predicted that the molar concentration of a compound in the spectro-

FIGURE 4.7 SCHEMATIC OF LIQUID CHROMATOGRAPHY SYSTEM

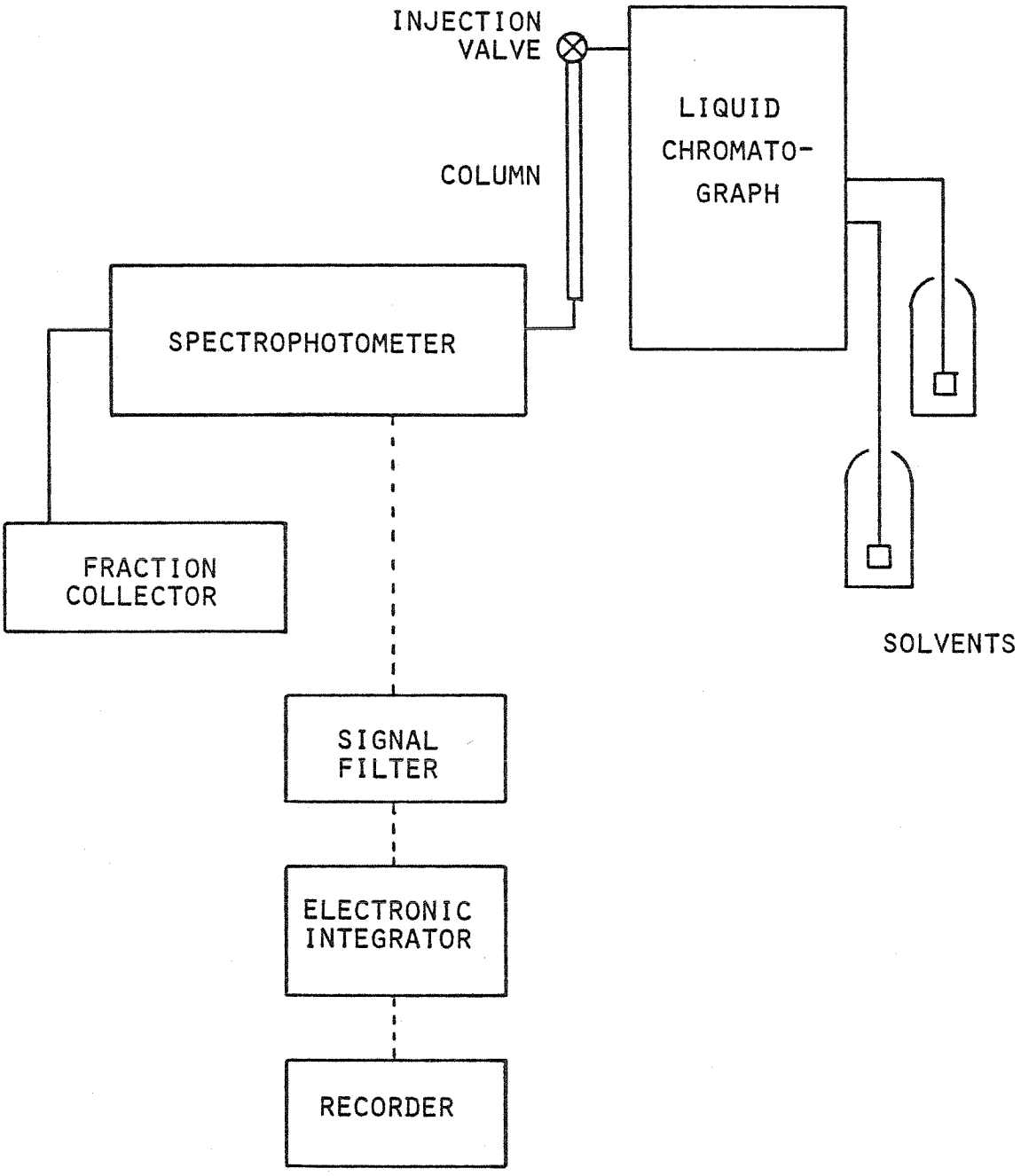

photometer flow-through cell at a given instant is proportional to the absorbance (402). Thus, the area under the peak caused by the detector response to a particular compound is expected to be proportional to the number of moles of that compound in the sample. This linear relation between chromatographic peak area and molar concentration of a given component in the sample was demonstrated for all the major products and reactants in this study except benzoic acid (see Appendix A). The lack of linearity for benzoic acid is presumed to be due to dimerization at higher concentrations. The proportionality constant for the other compounds can be expected to change over time because of fluctuations in the lamp optics and other factors. Therefore, a standard sample of known concentration was run after each set of analyses and a current proportionality constant calculated for those samples.

Peracid was quantitatively determined by the method of Kokatnur and Jelling (403). A recently-taken undiluted sample was rapidly weighed in a 1 ml beaker. The beaker was lowered into a 300 ml Erlenmeyer flask and 50 ml of isopropanol was added, followed by 1 ml of 40% aqueous KI solution and 1 ml glacial acetic acid. The mixture was heated to incipient boiling and titrated with 0.006 N $Na_2S_2O_3$ to the disappearance of the yellow color. The sodium thiosulfate solution was prepared and standardized by well-established methods (404).

Several common techniques for qualitative analysis were

employed, although the dilute nature of the samples and sensitivity of the equipment restricted identification to only the major components. Comparison of retention volumes on the liquid chromatograph with known standard samples was usually employed as the first step in qualitative analysis. These results were then verified by such methods as IR and NMR. Infrared spectroscopy was done on a Perkin-Elmer Model 257 IR spectrophotometer with NaCl sample cells manufactured by Barnes Engineering Co., Model No. 0003-504. Nuclear Magnetic Resonance spectra were taken on a Varian EM 390 NMR spectrometer. Melting points obtained from an Electrothermal Melting Point Apparatus were used to help identify certain derivatives of thiophenic sulfur compounds.

# CHAPTER 5 RESULTS AND DISCUSSION

## Error Analysis

The parameters and quantitative analysis associated with the experiments reported herein were controlled with an error less than:

1. 0.5% in the weight of the solvent medium.
2. 0.05% in the weight of the sulfur compound.
3. 1% in the amount of aldehyde. This relatively large error was because the aldehyde was dispensed rapidly by volumetric pipet to avoid preliminary oxidation rather than weighed.
4. $0.5^{o}C$ in the temperature. The large error was due to cooling of the reactor contents when a sample was withdrawn.
5. 2 mmHg in the pressure.
6. 20 seconds in the time period of sampling.
7. 5% in the flow rates of $O_2$ and $N_2$ and 30 mmHg in the partial pressure of $O_2$.
8. 3% in the quantitative analysis by liquid chromatography. This error resulted primarily from the dilution required to make the sample concentration compatible with the size of the sample loop.
9. 0.5 millimole/ℓ in peracid concentration by iodometric titration.

## Oxygen Diffusion in Aldehyde Autoxidation

Disagreement in the literature over the reaction order

in aldehyde autoxidation led to the suspicion that different diffusion rates for oxygen were obscuring the true reaction kinetics, especially at temperatures greater than 25°C. Therefore, four experiments in the absence of a sulfur compound were designed to observe the effect of oxygen-flow rate on the rate of peracid production. The experimental conditions employed are given in Table 5.1. The depletion of aldehyde monitored by liquid chromatography and the formation of peracid followed by iodometric titration are shown in Tables 5.2 and 5.3, respectively. Figures 5.1 and 5.2 graphically illustrate these results and demonstrate the large dependence of aldehyde autoxidation on oxygen flow rate at this temperature. The assumption of constant oxygen concentration in the liquid phase is obviously not applicable at 100°C. Close examination of the data reveals that the oxygen supplied through the reactor sparger is not sufficient to explain the rates of autoxidation observed. Net diffusion of oxygen back to the reaction mixture through the condenser open to the atmosphere is required to close the oxygen material balance. Additional evidence that the diffusion of oxygen from the gas phase is the rate-controlling step in these four experiments is the zero-order dependence of the autoxidation on aldehyde concentration throughout most of the reaction time. Only when the concentration of benzaldehyde falls below 50 millimoles/liter can a rate dependence on aldehyde be observed. At these low concentrations, least square fitting of the integrated form of

Table 5.1 Parameters for Experiments 1 - 4

| Experiment | 1 | 2 | 3 | 4 |
|---|---|---|---|---|
| Solvent | Bromo-benzene 350 g | Bromo-benzene 350 g | Bromo-benzene 350 g | Bromo-benzene 350 g |
| Sulfur Compound | None | None | None | None |
| Aldehyde | Benzal-dehyde 10.5 g | Benzal-dehyde 10.5 g | Benzal-dehyde 10.5 g | Benzal-dehyde 10.5 g |
| Other | | | | |
| $O_2$ Flow Rate (millimoles/min) | 0.15 | 2.0 | 2.9 | 20.6 |
| $N_2$ Flow Rate (millimoles/min) | 0.71 | 2.0 | 2.9 | 20.2 |
| Temperature ($^oC$) | 100.4 | 100.2 | 100.4 | 99.9 |
| Pressure (mm Hg) | 742.3 | 744.7 | 741.0 | 739.1 |
| $O_2$ Partial Pressure (mm Hg) | 129.2 | 375.3 | 372.7 | 373.2 |

Table 5.2 Quantitative Analysis of Benzaldehyde in Experiments 1 - 4

| | Benzaldehyde Concentration (millimoles/ℓ) | | | |
|---|---|---|---|---|
| Experiment | 1 | 2 | 3 | 4 |
| Reaction Time (min) | | | | |
| 0 | 403 | 402 | 402 | 401 |
| 30 | 367 | 249 | 202 | 158 |
| 60 | 349 | 100 | 47 | 13 |
| 90 | 329 | 35 | 12 | |
| 120 | 291 | 17 | 6 | |
| 150 | 264 | 10 | | |
| 180 | 232 | 7 | | |
| 210 | 204 | | | |
| 240 | 175 | | | |
| 270 | 144 | | | |
| 300 | 117 | | | |
| 360 | 72 | | | |

Table 5.3 Quantitative Analysis of Perbenzoic Acid in Experiments 1 - 4

| | Perbenzoic Acid Concentration (millimoles/ℓ) | | | |
|---|---|---|---|---|
| Experiment | 1 | 2 | 3 | 4 |
| Reaction Time (min) | | | | |
| 0 | 2 | 0 | 4 | 1 |
| 15 | 1 | 10 | 12 | 19 |
| 30 | 1 | 16 | 20 | 23 |
| 60 | 1 | 28 | 36 | 9 |
| 90 | 1 | 27 | 29 | 5 |
| 120 | 1 | 20 | 22 | 5 |
| 150 | 1 | 16 | 16 | 6 |
| 180 | 1 | 11 | 13 | 5 |
| 210 | 1 | 9 | 9 | |
| 240 | 1 | 6 | 7 | 5 |
| 270 | 1 | 5 | 6 | |
| 300 | 1 | 4 | 5 | |
| 360 | 1 | 3 | 4 | |

FIGURE 5.1 BENZALDEHYDE CONCENTRATION PROFILES AS A FUNCTION OF $O_2$ FLOW RATE

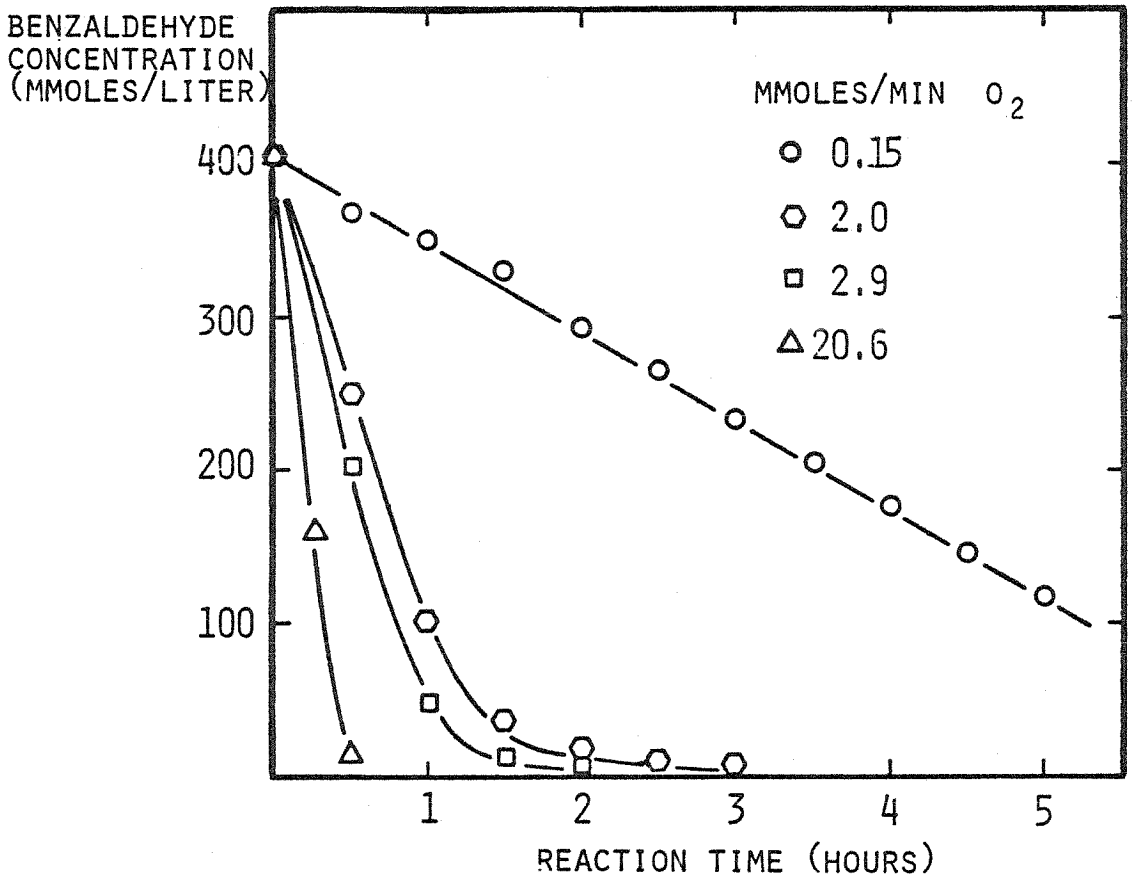


EXPERIMENTS 1-4:

OXIDATION OF 10.5 G BENZALDEHYDE BY $O_2$ IN 350 G BROMOBENZENE AT 100° C, 1 ATM.

FIGURE 5.2 PERBENZOIC ACID CONCENTRATION PROFILES AS AS A FUNCTION OF $O_2$ FLOW RATE

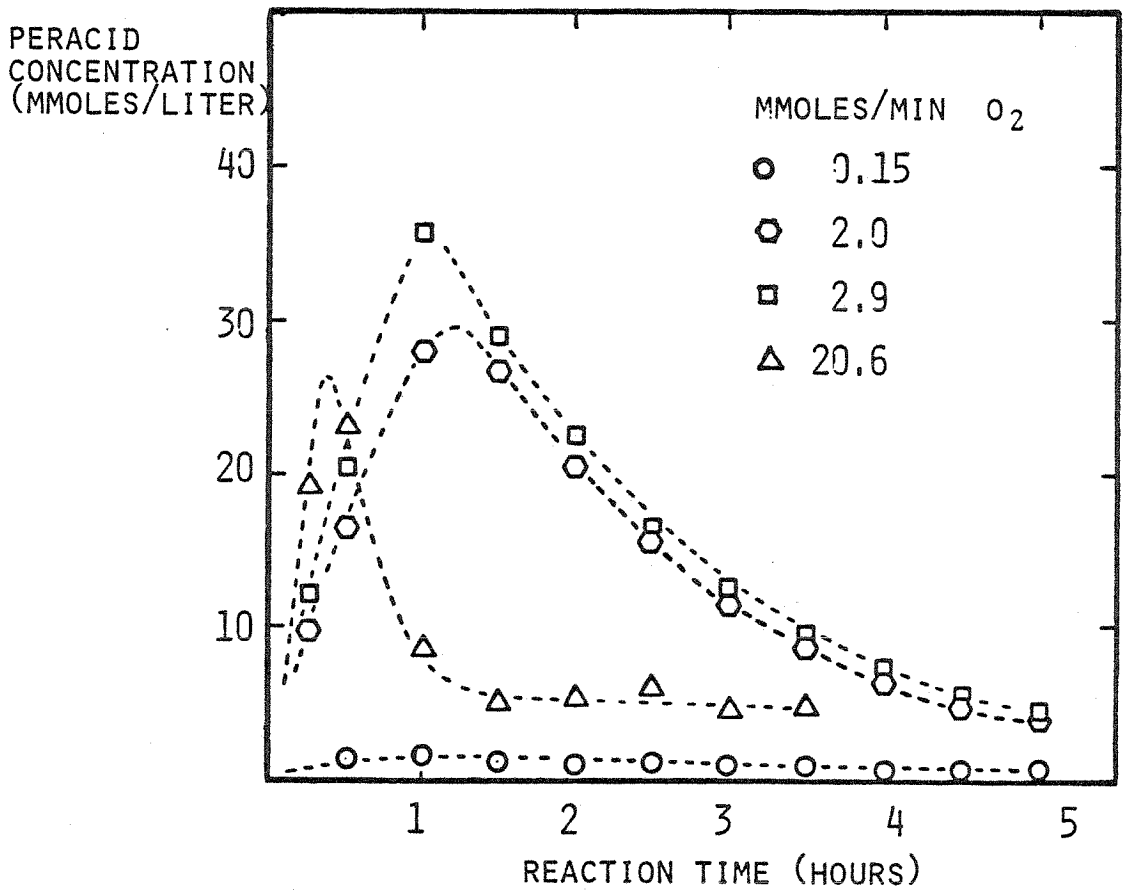


EXPERIMENTS 1-4:

FORMATION OF PERBENZOIC ACID FROM OXIDATION OF 10.5 G BENZALDEHYDE BY $O_2$ IN 350 G BROMOBENZENE AT 100° C, 1 ATM.

the following differential equation representing the rate of aldehyde oxidation as a function of aldehyde concentration yielded the best correlation coefficient for an order of n = 3/2, based on experiments 2 and 3.

$$\frac{-d[RCHO]}{dt} = k[RCHO]^n \qquad (5.1)$$

The following mechanism involving hydrogen abstraction by oxygen as the initiation step has been used (501,502,503, 504) to describe aldehyde thermal autoxidation.

$$RCHO + O_2 \xrightarrow{k_1} RCO\cdot + HO_2\cdot \qquad (i)$$

$$RCO\cdot + O_2 \xrightarrow{k_2} RCO_3\cdot \qquad (ii)$$

$$RCO_3\cdot + RCHO \xrightarrow{k_3} RCO_3H + RCO\cdot \qquad (iii)$$

$$2RCO\cdot \xrightarrow{k_4} \qquad (iv)$$

$$RCO\cdot + RCO_3\cdot \xrightarrow{k_5} \left.\right\} \text{termination products} \qquad (v)$$

$$2RCO_3\cdot \xrightarrow{k_6} \qquad (vi)$$

Application of the long-chain approximation and the steady state assumption to the free radicals yields the following rate expression:

$$\frac{-d[RCHO]}{dt} = \frac{[RCHO]^{3/2}[O_2]^{3/2}}{\frac{1}{k_2}\left(\frac{k_4}{k_1}\right)^{1/2}[RCHO] + \frac{1}{k_3}\left(\frac{k_6}{k_1}\right)^{1/2}[O_2]} \qquad (5.2)$$

If it is assumed that reaction (ii) is extremely rapid (i.e.

$k_2 >> k_3$), the preceding expression reduces to that used by Melville, et. al., (501,502) to fit their data:

$$\frac{-d[RCHO]}{dt} = k_3\left(\frac{k_1}{k_6}\right)^{\frac{1}{2}} [RCHO]^{3/2}[O_2]^{\frac{1}{2}} \qquad (5.3)$$

In the limit of low oxygen concentration, a different overall rate expression is obtained with a much weaker dependence on aldehyde concentration:

$$\frac{-d[RCHO]}{dt} = k_2\left(\frac{k_1}{k_4}\right)^{\frac{1}{2}}[RCHO]^{\frac{1}{2}}[O_2]^{3/2} \qquad (5.4)$$

Experimentally, an oxygen order greater than one has never been observed in aldehyde thermal autoxidation, however. Also, the oxidation rate has been found to be independent of oxygen concentration at high partial pressures of oxygen. If the preceding mechanism is modified by replacing the initiation step with the reaction (not necessarily elementary)

$$RCHO \xrightarrow{k_7} RCO\cdot + H\cdot \qquad (vii)$$

then the overall rate of aldehyde autoxidation is described by

$$\frac{-d[RCHO]}{dt} = \frac{[RCHO]^{3/2}[O_2]}{\left(\frac{k_4}{k_7}\right)^{\frac{1}{2}}\left(\frac{1}{k_2}\right)[RCHO] + \left(\frac{k_6}{k_7}\right)^{\frac{1}{2}}\left(\frac{1}{k_3}\right)[O_2]} = \frac{[RCHO]^{3/2}[O_2]}{\beta[RCHO] + \gamma[O_2]} \qquad (5.5)$$

where

$$\beta = \frac{1}{k_2}\left(\frac{k_4}{k_7}\right)^{\frac{1}{2}}$$

$$\gamma = \frac{1}{k_3}\left(\frac{k_6}{k_7}\right)^{\frac{1}{2}}$$

Thus, equation 5.5 was used to model the results of this work.

The film conversion parameter (505,506) was used to determine the reaction order regime.

$$M = \frac{kC_B\mathcal{D}_{A1}}{\left(k_{A1}\right)^2} \qquad (5.6)$$

where for this application

$k$ = reaction rate constant

$C_B$ = concentration of benzaldehyde

$\mathcal{D}_{A1}$ = diffusivity of oxygen in the liquid

$k_{A1}$ = liquid mass transfer coefficient for oxygen

Typical values of $10^{-5}$ $cm^2/s$ and $10^{-2}$ cm/s were chosen for the diffusivity and mass-transfer coefficient, respectively (507). The rate constant, k, was estimated as $10^{-1}$ $\frac{\ell}{mole \cdot s}$ from the rate equation

$$Rate = k\left[RCHO\right]^{3/2} \qquad (5.7)$$

and the data of experiment 4. Thus, initially M is found to be approximately $4 \cdot 10^{-3}$, corresponding to an intermediate region of both reaction and diffusion control. As the reaction proceeds, however, and the benzaldehyde concentration

is reduced by an order of magnitude, M becomes $4 \cdot 10^{-4}$. At this value of the film conversion parameter, the rate is kinetically controlled; this change in regime is evidenced by the change in the rate dependence on aldehyde seen at low aldehyde concentrations in experiments 2 and 3.

In the intermediate regime where both reaction and diffusion are important, the gas and liquid films act as resistances in series, such that

$$\frac{dC_A}{dt} = ak_{Ag}(p_A - p_{Ai}) = ak_{Al}(C_{Ai} - C_A) \qquad (5.8)$$

for constant liquid volume. In the bulk phase, assume

$$\frac{-dC_A}{dt} = \frac{C_A C_B^{3/2}}{\beta C_B + \gamma C_A} \qquad (5.9)$$

where

$C_A$ = concentration of $O_2$ in the liquid phase

a = ratio of interfacial surface area to liquid volume

$C_B$ = benzaldehyde concentration in the liquid phase

$\beta, \gamma$ = constants from Eqn. 5.5

$p_A$ = partial pressure of $O_2$ in the gas phase

$k_{Ag}$ = oxygen mass transfer coefficient in the gas phase

$k_{Al}$ = oxygen mass transfer coefficient in the liquid phase

and i refers to values at the gas-liquid interface.

Combination of these expressions with Henry's Law:

$$p_{Ai} = HC_{Ai} \qquad (5.10)$$

where H is Henry's Law constant yields the following rate

expression:

$$\frac{-dC_A}{dt} = \frac{-dC_B}{dt} = \frac{p_A C_B^{3/2}}{\frac{1}{K_o a} C_B^{3/2} + \frac{H\beta}{K_o a} C_B + \frac{H\gamma}{K_o a} C_A} \qquad (5.11)$$

where

$$\frac{1}{K_o} = \frac{1}{k_{Ag}} + \frac{H}{k_{Al}}$$

= overall mass transfer coefficient based on the gas phase

The qualitative features of the experimentally observed rate dependence on flow rate can be explained in terms of the preceding overall rate equation for aldehyde autoxidation. The rate is seen to be proportional to the ratio of interfacial surface area to liquid volume, a. This ratio would obviously be expected to decrease as the flow rate decreased, albeit in a complex and non-linear manner for the sparger system employed. The rate is also predicted to be proportional to the partial pressure of oxygen, which is consistent with the extremely slow rate observed in experiment 1. The overall rate expression with diffusional effects included (Eqn. 5.11) is similar in form to the original rate expression (Eqn. 5.5) with an additional term in the denominator. This fact may explain the lack of agreement on elementary rate constants among various investigators.

Temperature Dependence of Aldehyde Autoxidation

Subsequent experiments concentrated in the $O_2$ flow-rate range of about 2-3 millimole/min because this regime resulted

in the maximum production of perbenzoic acid. Before attempting the selective oxidation of sulfur compounds, it was necessary to establish the rate of peracid formation in our reactor configuration. Table 5.4 gives the experimental conditions used in a study of the effect of temperature on the importance of decomposition and other reactions in limiting the formation of peracid. The results of quantitative analysis of benzaldehyde and perbenzoic acid are listed in Tables 5.5 - 8 and plotted in Figures 5.3 and 5.4, respectively. Again, evidence of the oxygen-mass-transfer limitation can be seen in experiments 6 through 8, the increased rate of aldehyde autoxidation at higher temperatures enhancing the rate of oxygen diffusion. The combination of oxygen-diffusion limitations and peracid-depleting reactions cause the maximum formation of peracid to occur near 50°C.

After the aldehyde is completely oxidized, only decomposition contributes to changes in peracid concentration. Thus, rate constants for peracid decomposition can be obtained directly in this region of experiments 6 through 8. The decomposition data are best fitted by a rate equation that is second order in perbenzoic acid,

$$\frac{-d[RCO_3H]}{dt} = k[RCO_3H]^2 \qquad (5.12)$$

which is consistent with the reaction:

$$2RCO_3H \xrightarrow{k_8} 2RCO_2H + O_2 \quad \text{where R=phenyl} \; . \qquad \text{(viii)}$$

Table 5.4 Parameters for Experiments 5 - 8

| Experiment | 5 | 6 | 7 | 8 |
|---|---|---|---|---|
| Solvent | Bromo-benzene 350 g | Bromo-benzene 350 g | Bromo-benzene 350 g | Bromo-benzene 350 g |
| Sulfur Compound | None | None | None | None |
| Aldehyde | Benzal-dehyde 10.5 g | Benzal-dehyde 10.5 g | Benzal-dehyde 10.5 g | Benzal-dehyde 10.5g |
| Other | | | | |
| $O_2$ Flow Rate (millimoles/ min) | 2.63 | 2.61 | 2.64 | 2.62 |
| $N_2$ Flow Rate (millimoles/ min) | 2.56 | 2.56 | 2.58 | 2.58 |
| Temperature ($^{o}C$) | 27.6 | 50.4 | 75.6 | 100.5 |
| Pressure (mm Hg) | 743.2 | 734.6 | 741.2 | 742.2 |
| $O_2$ Partial Pressure (mm Hg) | 376.1 | 371.0 | 374.2 | 374.1 |

Table 5.5 Quantitative Analysis of Samples for Experiment 5

| Reaction Time (min) | Benzaldehyde (millimoles/ℓ) | Perbenzoic Acid (millimoles/ℓ) |
|---|---|---|
| 0 | 402 | 0 |
| 15 | | 0 |
| 30 | 398 | 1 |
| 60 | 389 | 3 |
| 90 | 378 | 9 |
| 120 | 372 | 10 |
| 150 | 367 | 10 |
| 180 | 365 | 9 |
| 210 | 357 | 8 |
| 240 | 361 | 6 |
| 300 | 357 | 5 |

Table 5.6 Quantitative Analysis of Samples for Experiment 6

| Reaction Time (min) | Benzaldehyde (millimoles/ℓ) | Perbenzoic Acid (millimoles/ℓ) |
|---|---|---|
| 0 | 404 | 0 |
| 15 | 354 | 17 |
| 30 | 270 | 36 |
| 60 | 138 | 83 |
| 90 | 45 | 120 |
| 120 | 13 | 129 |
| 150 | 4 | 128 |
| 180 | | 118 |
| 210 | | 120 |
| 240 | | 120 |
| 300 | | 113 |

Table 5.7 Quantitative Analysis of Samples for Experiment 7

| Reaction Time (min) | Benzaldehyde (millimoles/ℓ) | Perbenzoic Acid (millimoles/ℓ) |
|---|---|---|
| 0 | 404 | 0 |
| 15 | 321 | 13 |
| 30 | 226 | 25 |
| 60 | 63 | 57 |
| 90 | 5 | 61 |
| 120 | | 51 |
| 150 | | 44 |
| 180 | | 40 |
| 210 | | 35 |
| 240 | | 33 |
| 300 | | 29 |

Table 5.8 Quantitative Analysis of Samples for Experiment 8

| Reaction Time (min) | Benzaldehyde (millimoles/ℓ) | Perbenzoic Acid (millimoles/ℓ) |
|---|---|---|
| 0 | 404 | 2 |
| 15 | | 4 |
| 30 | 190 | 12 |
| 60 | 25 | 31 |
| 90 | | 19 |
| 120 | | 13 |
| 150 | | 8 |
| 180 | | 5 |
| 210 | | 4 |
| 240 | | 3 |
| 300 | | 3 |

FIGURE 5.3 OXIDATION RATE OF BENZALDEHYDE AS A FUNCTION OF TEMPERATURE

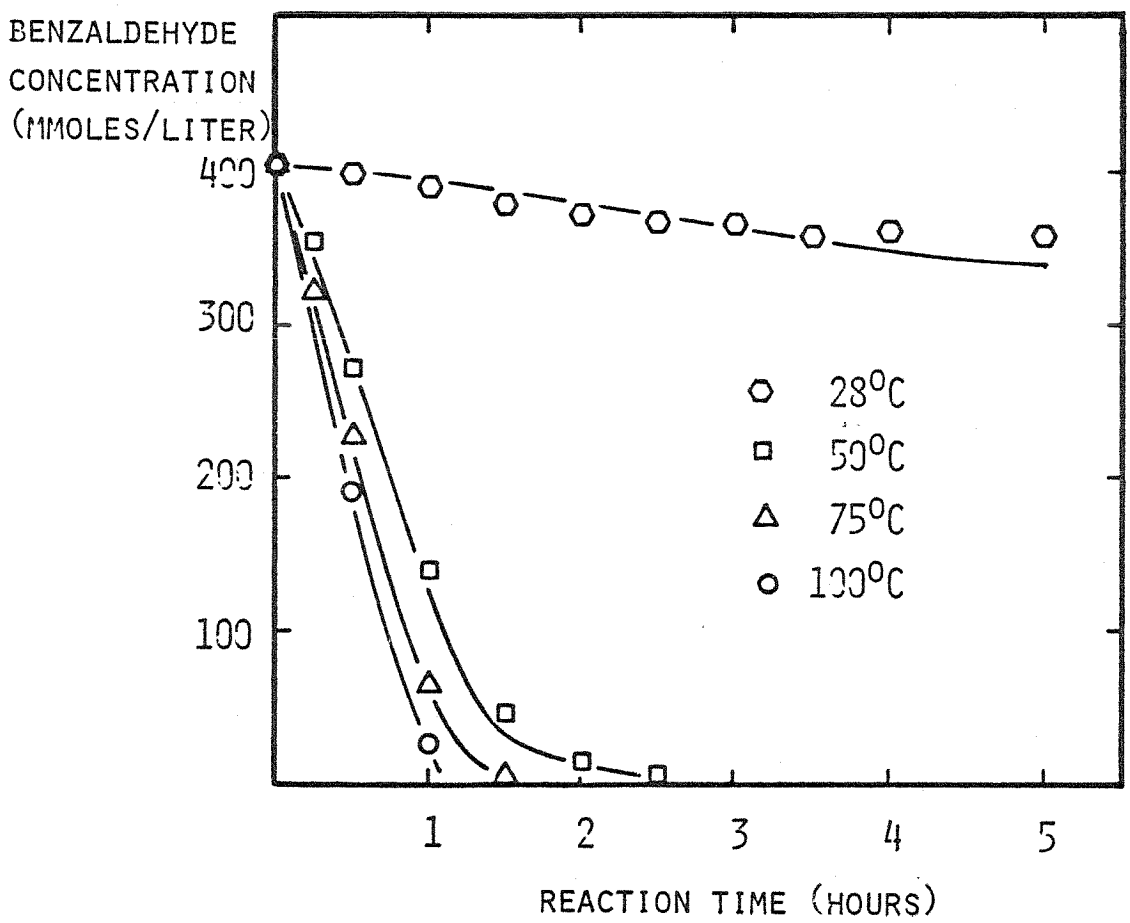


EXPERIMENTS 5-8:

OXIDATION OF 10.5 G BENZALDEHYDE BY 2.6 MMOLES/MIN $O_2$ AT 0.5 ATM. PARTIAL PRESSURE IN 350 G BROMOBENZENE AT 1 ATM.

FIGURE 5.4 FORMATION OF PERBENZOIC ACID FROM AUTOXIDATION OF BENZALDEHYDE AS A FUNCTION OF TEMPERATURE

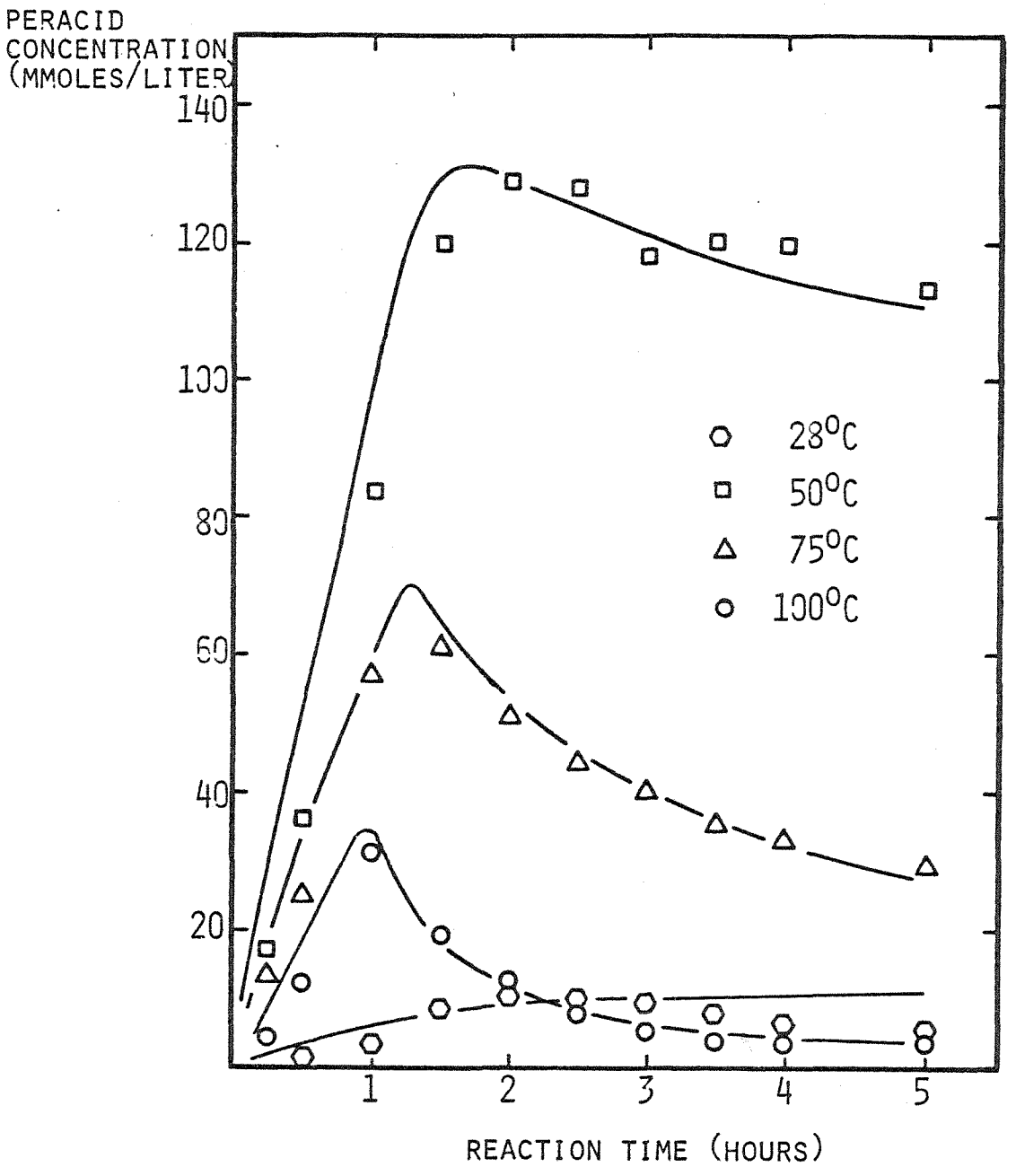


EXPERIMENTS 5-8:

FORMATION OF PERBENZOIC ACID FROM OXIDATION OF 10.5 G BENZALDEHYDE BY 2.6 MMOLES/MIN $O_2$ AT 0.5 ATM. PARTIAL PRESSURE IN 350 G BROMOBENZENE AT 1 ATM.

Table 5.9 is a compilation of these decomposition rate constants obtained by least square analysis from various experiments; they are combined in an Arrhenius plot in Figure 5.5. The corresponding activation energy is found to be approximately 24 $\frac{kcal}{mole}$.

The other reactions participating in aldehyde autoxidation cannot be separated and evaluated in this manner. The complex and coupled nature of this reaction system requires that the integration, rather than differentiation method of determination of rate constants be used.

In addition to the decomposition reaction of peracid and the mechanism for peracid formation already discussed, the direct oxidation of aldehyde by peracid also contributes to the concentration profiles observed.

$$RCO_3H + RCHO \xrightarrow{k_9} 2RCO_2H \qquad \text{(ix)}$$

The aldehyde oxidation in the absence of sulfur compound was therefore modeled by the following rate expressions:

$$\frac{-d[RCHO]}{dt} = \frac{[RCHO]^{3/2}}{\alpha'[RCHO]^{3/2} + \beta'[RCHO] + \gamma'[O_2]} + k_9[RCHO][RCHO_3H] \qquad (5.13)$$

$$\frac{-d[RCHO]}{dt} = \frac{[RCHO]^{3/2}}{\alpha'[RCHO]^{3/2} + \beta'[RCHO] + \gamma'[O_2]} - k_9[RCHO][RCHO_3H] - 2k_8[RCO_3H]^2 \qquad (5.14)$$

Table 5.9 Second Order Rate Constants for Peracid Decomposition

| Experiment | Temperature ($^{o}C$) | $\kappa$ ($\ell$/mole·min) |
|---|---|---|
| 4 | 100 | $6.5*10^{-4}$ |
| 8 | 100 | $6.95*10^{-4}$ |
| 12 | 100 | $6.16*10^{-5}$ |
| 7 | 75 | $4.3*10^{-5}$ |
| 11 | 75 | $1.74*10^{-5}$ |
| 6 | 50 | $4.33*10^{-6}$ |

FIGURE 5.5 ARRHENIUS PLOT OF THE SECOND ORDER RATE CONSTANT FOR PERBENZOIC ACID DECOMPOSITION, $k_8$

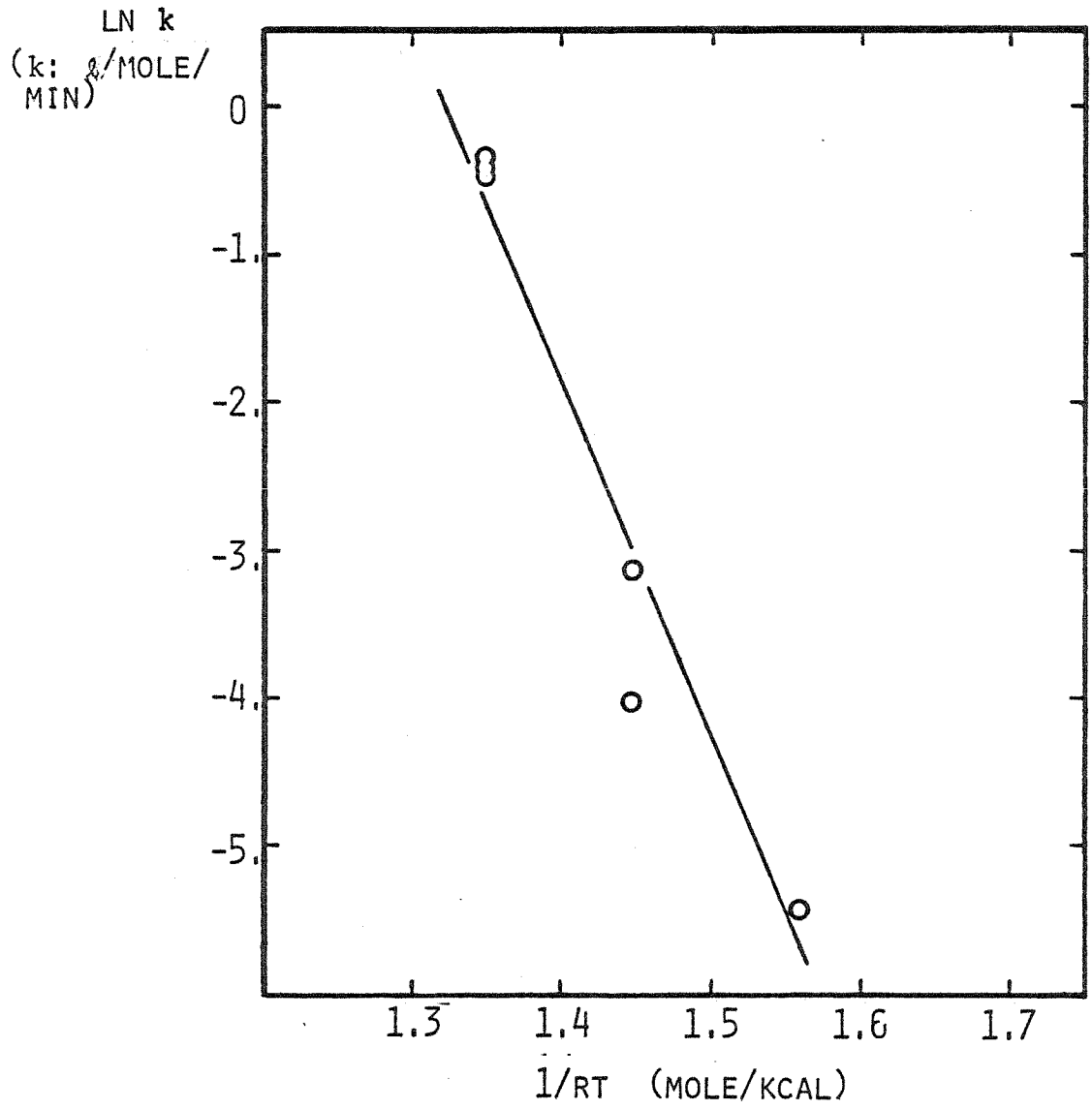

where $\alpha' = (K_o a P_{o_2})^{-1}$

$\beta' = H\beta\ (K_o a P_{o_2})^{-1}$

$\gamma' = H\gamma\ (K_o a P_{o_2})^{-1}$

Appropriate values of $\alpha'$, $\beta'$, $\gamma'$, $k_8$ and $k_9$ were chosen, and the differential equations above were integrated by a fourth-order Runge-Kutta scheme. The constants $\alpha'$, $\beta'$, $\gamma'$, and $k_9$ were varied until a reasonable fit with the experimental data was obtained. Note that $k_8$ was obtained directly from decomposition data. The assumption that $\beta'=0$ (i.e., $k_2 >> k_3$) was also used to reduce the number of variables.

In light of previous comments, constant oxygen concentration is not a good assumption for the reactor configuration employed. The oxygen concentration required for evaluation of the rates was obtained by simultaneously integrating the differential equation:

$$\frac{d[O_2]}{dt} = aK_oP_{o_2} - aK_oH[O_2] + k_8[RCO_3H]^2 - \frac{[RCHO]^{3/2}}{\alpha'[RCHO]^{3/2} + \gamma'[O_2]} \qquad (5.15)$$

$$= \frac{1}{\alpha'}\left(1 - \frac{[O_2]}{[O_2]_{eq}}\right) + k_8[RCO_3H]^2 - \frac{[RCHO]^{3/2}}{\alpha'[RCHO]^{3/2} + \gamma'[O_2]}$$

where $[O_2]_{eq}$ is the solubility of oxygen in the liquid phase

at the given temperature and partial pressure of oxygen. Oxygen solubilities were estimated from the Shair correlation (508) which resulted in the following relationship:

$$\ell n \frac{P_{O_2}}{[O_2]_{eq}} = 3.3282 + \frac{413.46}{T} \qquad (5.16)$$

where $P_{O_2}$ = partial pressure of $O_2$ in atm.

$[O_2]_{eq}$ = oxygen solubility in mole/ℓ

T = temperature, K

This correlation gave values of oxygen solubility in bromobenzene between 4 and 6 mmole/ℓ under the conditions employed in experiments 5-8. The little data available on oxygen solubility in aromatic solvents in this temperature range falls between $10^{-2}$ and $10^{-3}$ mole/ℓ; therefore, these values were considered reasonable. During the course of integration of equations 5.13 - 5.15, the oxygen concentration was not allowed to increase above the appropriate saturation value. The solid lines in Figures 5.3 and 5.4 are the results of this modeling procedure for experiments 5 through 8.

The direct oxidation of aldehyde by peracid significantly limits the amount of peracid formed under given conditions. The competing route for peracid removal is decomposition and can be calculated independently. Thus, the contribution of reaction (ix) in limiting the maximum concentration of peracid can be readily evaluated. Figure 5.6 is a plot of the temperature dependence of the second order rate constant,

FIGURE 5.6 ARRHENIUS PLOT OF THE RATE CONSTANT FOR THE PERBENZOIC ACID-BENZALDEHYDE REACTION

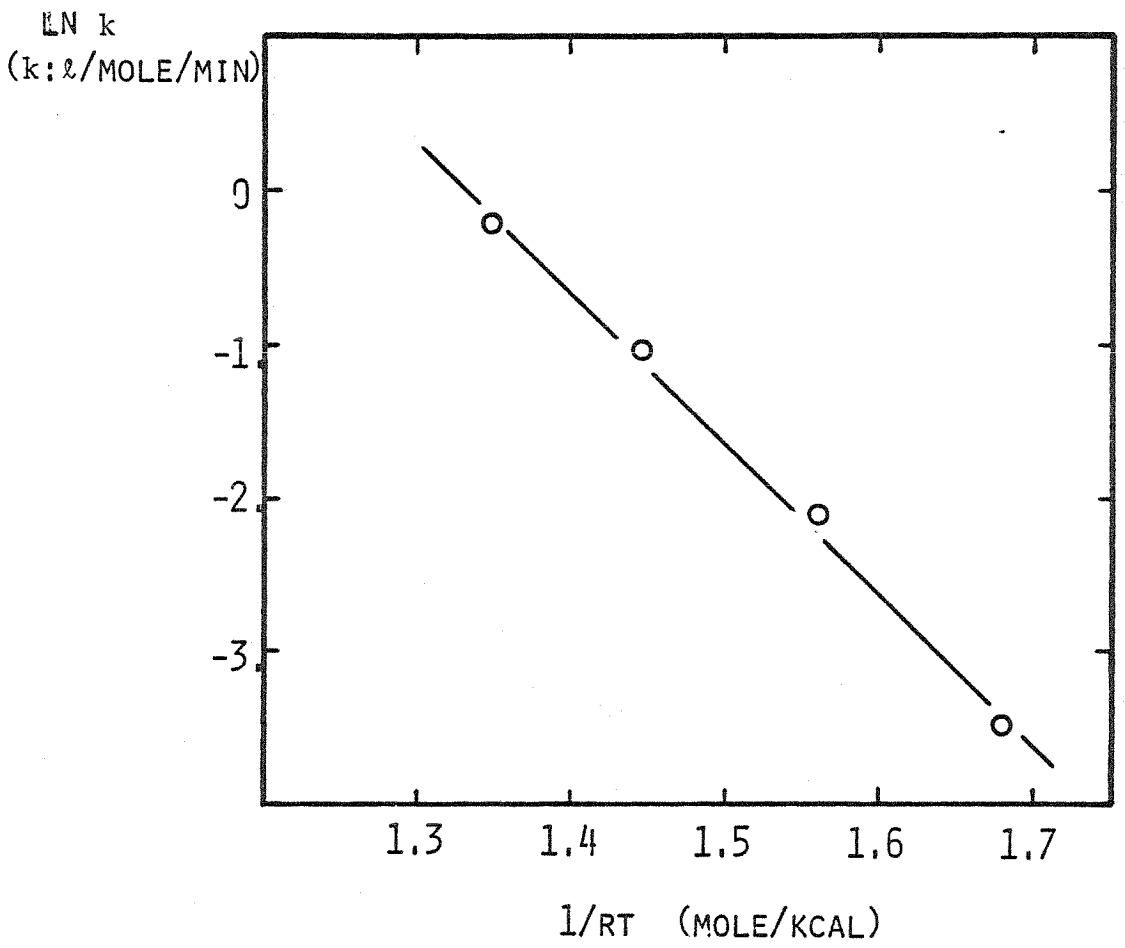

$k_9$, for the perbenzoic acid-benzaldehyde reaction. The corresponding activation energy is 9.6 kcal/mole. Comparison of this value with that for peracid decomposition leads to the conclusion that as the temperature increases the peracid-aldehyde reaction becomes less important in limiting the peracid concentration obtainable.

The constants $\alpha'$ and $\gamma'$ obtained from the rate expression for benzaldehyde autoxidation (Eqn. 5.5) are listed in Table 5.9a. The constant $\alpha'$ which contains only parameters related to oxygen diffusion is seen to have a weak dependence on temperature, the resistance to diffusion decreasing slightly with increasing temperature. The constant $\gamma'$ contains both diffusion and kinetic parameters, although these two factors may be separated once $\alpha'$ is known to calculate a rate constant for aldehyde autoxidation ($\frac{1}{\gamma}$). These constants were obtained with the assumption that $\beta'=0$ (i.e., $k_2 >> k_3$); therefore the appropriate kinetic rate expression for aldehyde autoxidation from equation 5.5 reduces to:

$$\frac{-d[RCHO]}{dt} = \left(\frac{1}{\gamma}\right)[RCHO]^{3/2} \qquad (5.17)$$

where $\frac{1}{\gamma} = k_3\left(\frac{k_7}{k_6}\right)^{\frac{1}{2}}$

The extremely low value of $\frac{1}{\gamma}$ at 28°C may be indicative of the operation of a different mechanism for autoxidation at this temperature.

Table 5.9a Temperature Dependence of Constants in Equation 5.13 Describing Benzaldehyde Oxidation

| Temperature | $\alpha' = (k_o a P_{O_2})^{-1}$ | $\gamma' = H\gamma(k_o a P_{O_2})^{-1}$ | $\frac{1}{\gamma} = k_3\left(\frac{k_7}{k_6}\right)^{\frac{1}{2}}$ | $k_9$ |
|---|---|---|---|---|
| ($^oC$) | $\left(\frac{\ell \cdot min}{mole}\right)$ | $\left(\frac{\ell \cdot min^2}{mole}\right)$ | $\left(\frac{\ell}{mole \cdot min^2}\right)^{\frac{1}{2}}$ | $\left(\frac{\ell}{mole \cdot min}\right)$ |
| 28 | 400 | $3.8*10^5$ | 0.12 | 0.03 |
| 50 | 320 | $1.6*10^3$ | 20. | 0.12 |
| 75 | 280 | $7.9*10^2$ | 32. | 0.35 |
| 100 | 250 | $3.8*10^2$ | 57. | 0.80 |

Oxidation of Dibenzothiophene

Experimental conditions for the counterparts of experiments 5 through 8 with the sulfur compound dibenzothiophene present are given in Table 5.10. The results of quantitative analysis of the batch reactor samples are tabulated in Tables 5.11 - 5.14 and plotted in Figures 5.7 - 5.13. One qualitative feature of the oxidation of dibenzothiophene by the products of aldehyde autoxidation is immediately apparent; the rate of aldehyde autoxidation is significantly inhibited by the presence of dibenzothiophene. Forty to over 95% reductions in initial autoxidation rates were observed. This inhibition is particularly evident in experiments 11 and 12, where the oxidation of benzaldehyde is seen to rapidly increase after all of the dibenzothiophene has been converted to its sulfone. This result cannot be explained by assuming that dibenzothiophene eliminates the direct oxidation of aldehyde by peracid as an aldehyde oxidation path by scavenging peracid. This slowing of the rate of benzaldehyde autoxidation has the additional effect of raising the temperature at which the mass-transfer limitation for oxygen appears. Thus, because of the varying effect of the diffusion of oxygen at higher temperatures, no general trends in the inhibition of autoxidation by dibenzothiophene could be discerned. The concentration of perbenzoic acid is kept below the level of detection by its rapid reaction with dibenzothiophene, or alternatively, the acyl peroxy radical may oxidize the dibenzothiophene directly, partially inhibiting

Table 5.10 Parameters for Experiments 9 - 12

| Experiment | 9 | 10 | 11 | 12 |
|---|---|---|---|---|
| Solvent | Bromo-benzene 350 g | Bromo-benzene 350 g | Bromo-benzene 350 g | Bromo-benzene 350 g |
| Sulfur Compound | DBT 5.036 | DBT 5.034 | DBT 5.036 | DBT 5.029 |
| Aldehyde | Benzal-dehyde 10.5 g | Benzal-dehyde 10.5 g | Benzal-dehyde 10.5 g | Benzal-dehyde 10.5 g |
| Other | | | | |
| $O_2$ Flow Rate (millimoles/min) | 2.67 | 2.64 | 2.65 | 2.62 |
| $N_2$ Flow Rate (millimoles/min) | 2.58 | 2.59 | 2.56 | 2.56 |
| Temperature ($^oC$) | 26.6 | 50.2 | 75.5 | 100.0 |
| Pressure (mm Hg) | 746.4 | 740.6 | 741.7 | 736.0 |
| $O_2$ Partial Pressure (mm Hg) | 379.9 | 374.0 | 377.5 | 371.7 |

DBT = Dibenzothiophene

Table 5.11 Quantitative Analysis of Samples for Experiment 9

| Reaction Time (min) | Benzaldehyde | Perbenzoic Acid | DBT | DBTO | $DBTO_2$ |
|---|---|---|---|---|---|
| | | | (millimoles/ℓ) | | |
| 0 | 404 | 0 | 108 | | |
| 15 | | 0 | | | |
| 30 | 389 | 0 | 108 | | |
| 60 | 388 | 0 | 108 | | |
| 90 | 381 | 0 | 106 | | |
| 120 | 388 | 0 | 106 | | |
| 150 | 386 | 0 | 107 | 2 | |
| 180 | 385 | 0 | 106 | 3 | |
| 210 | 387 | 0 | 106 | 5 | |
| 240 | 390 | 0 | 106 | 9 | |
| 300 | 367 | 0 | 95 | 13 | 0 |

DBT = Dibenzothiophene

DBTO = Dibenzothiophene sulfoxide

$DBTO_2$ = Dibenzothiophene sulfone

Table 5.12 Quantitative Analysis of Samples for Experiment 10

| Reaction Time (min) | Benzaldehyde | Perbenzoic Acid | DBT | DBTO | $DBTO_2$ |
|---|---|---|---|---|---|
| | | | (millimoles/ℓ) | | |
| 0 | 404 | 0 | 112 | | |
| 15 | | 0 | | | |
| 30 | 397 | 0 | 112 | | |
| 60 | 361 | 0 | 87 | 22 | 2 |
| 90 | 356 | 0 | 81 | 28 | 3 |
| 120 | 341 | 0 | 73 | 32 | 4 |
| 150 | 335 | 0 | 68 | 36 | 6 |
| 180 | 329 | 0 | 63 | 40 | 7 |
| 210 | 323 | 0 | 59 | 43 | 9 |
| 240 | 313 | 0 | 54 | 44 | 10 |
| 300 | 309 | 0 | 49 | 48 | 13 |

DBT = Dibenzothiophene

DBTO = Dibenzothiophene sulfoxide

$DBTO_2$ = Dibenzothiophene sulfone

Table 5.13 Quantitative Analysis of Samples for Experiment 11

| Reaction Time (min) | Benzaldehyde | Perbenzoic Acid | DBT | DBTO | $DBTO_2$ |
|---|---|---|---|---|---|
| | | | (millimoles/ℓ) | | |
| 0 | 404 | 0 | 110 | 0 | 0 |
| 15 | 353 | 0 | 77 | 30 | 4 |
| 30 | 319 | 0 | 56 | 45 | 11 |
| 60 | 263 | 0 | 25 | 53 | 32 |
| 90 | 221 | 1 | 9 | 44 | 56 |
| 120 | 187 | 1 | 2 | 27 | 76 |
| 150 | 164 | 2 | | 9 | 96 |
| 180 | 61 | 48 | | | 94 |
| 210 | 5 | 65 | | | 99 |
| 240 | | 59 | | | 103 |
| 300 | | 54 | | | 103 |

DBT = Dibenzothiophene

DBTO = DBT sulfoxide

$DBTO_2$ = DBT sulfone

Table 5.14 Quantitative Analysis of Samples for Experiment 12

| Reaction Time (min) | Benzaldehyde | Perbenzoic Acid | DBT | DBTO | $DBTO_2$ |
|---|---|---|---|---|---|
| | | | (millimoles/ℓ) | | |
| 0 | 404 | 0 | 115 | 0 | |
| 15 | 329 | 0 | 66 | 38 | 8 |
| 30 | 294 | 0 | 42 | 49 | 21 |
| 60 | 245 | 0 | 19 | 48 | 43 |
| 90 | 217 | 0 | 9 | 39 | 60 |
| 120 | 188 | 0 | 3 | 26 | 77 |
| 150 | 163 | 1 | 0 | 5 | 97 |
| 180 | 19 | 37 | | | 81 |
| 210 | 5 | 30 | | | 101 |
| 240 | 3 | 14 | | | 100 |
| 300 | 2 | 7 | | | 103 |

DBT = Dibenzothiophene

DBTO = DBT sulfoxide

$DBTO_2$ = DBT sulfone

FIGURE 5.7 BENZALDEHYDE AUTOXIDATION AS A FUNCTION OF TEMPERATURE DURING THE CO-OXIDATION OF DIBENZOTHIOPHENE AND BENZALDEHYDE

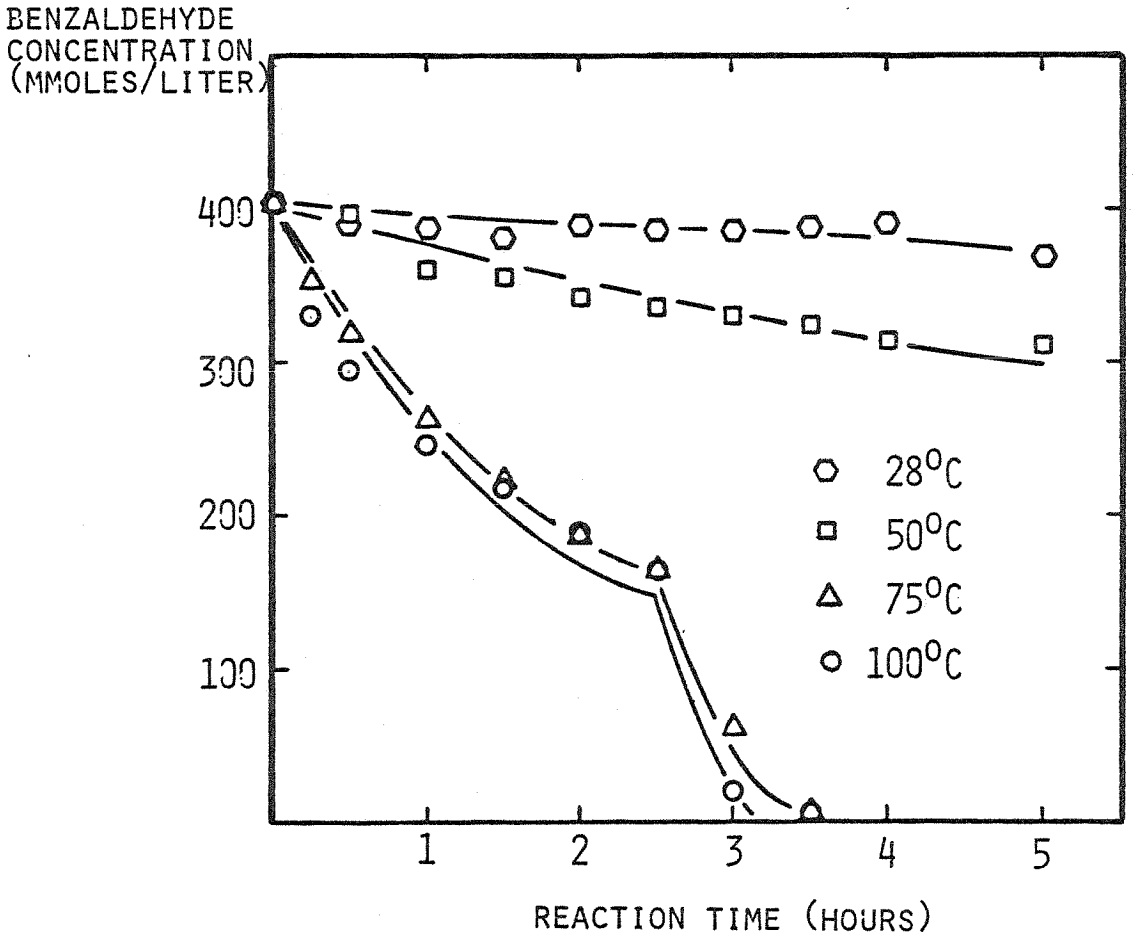


EXPERIMENTS 9-12:

OXIDATION OF 10.5 G BENZALDEHYDE BY 2.6 MMOLES/MIN $O_2$ AT 0.5 ATM. PARTIAL PRESSURE IN 350 G BROMOBENZENE AND 5.0 G DIBENZOTHIOPHENE AT 1 ATM.

FIGURE 5.8 FORMATION OF PERBENZOIC ACID AS A FUNCTION OF TEMPERATURE DURING THE CO-OXIDATION OF DIBENZO-THIOPHENE AND BENZALDEHYDE

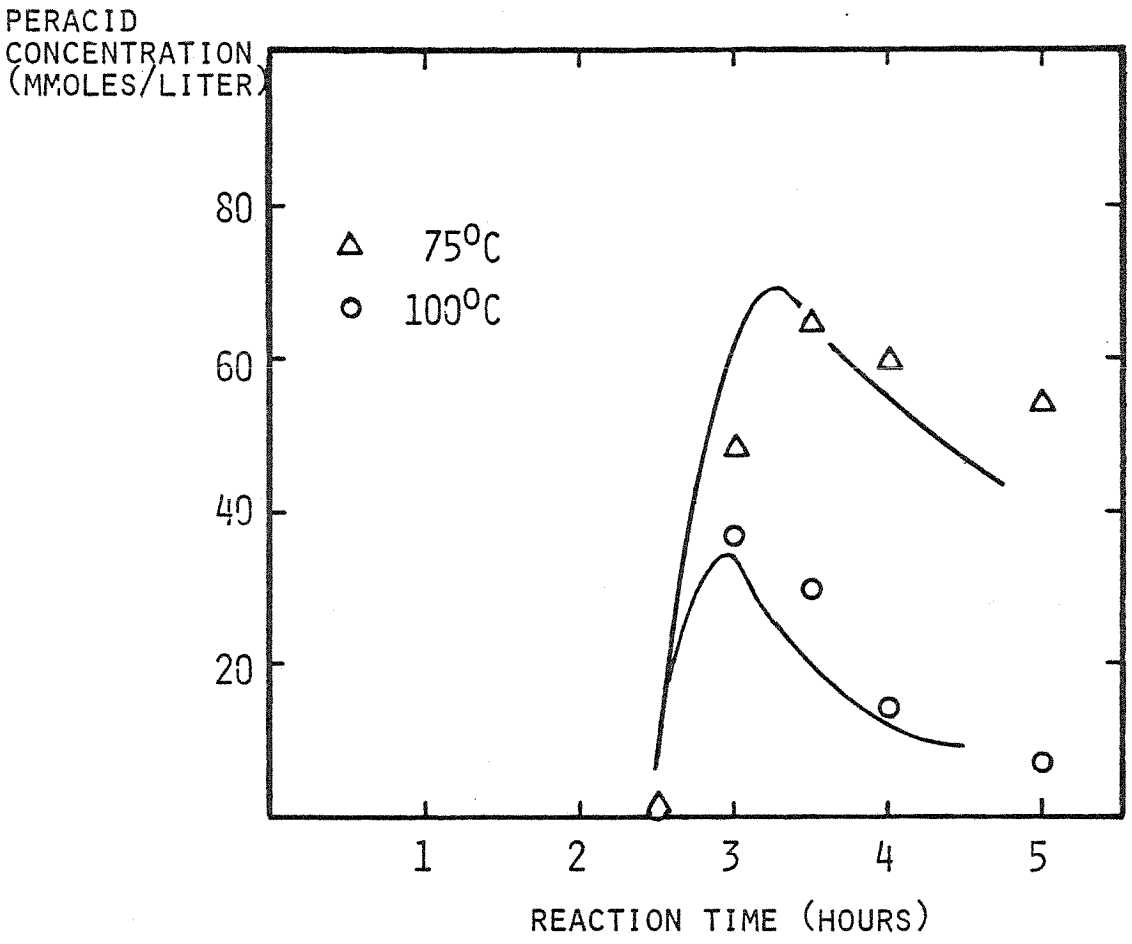


EXPERIMENTS 9-12:

FORMATION OF PERBENZOIC ACID FROM THE OXIDATION OF 10.5 G BENZALDEHYDE BY 2.6 MMOLES/LITER AT 0.5 ATM. PARTIAL PRESSURE IN 350 G BROMOBENZENE AND 5.0 G DIBENZOTHIOPHENE AT 1 ATM.

FIGURE 5.9 OXIDATION OF DIBENZOTHIOPHENE AS A FUNCTION OF TEMPERATURE

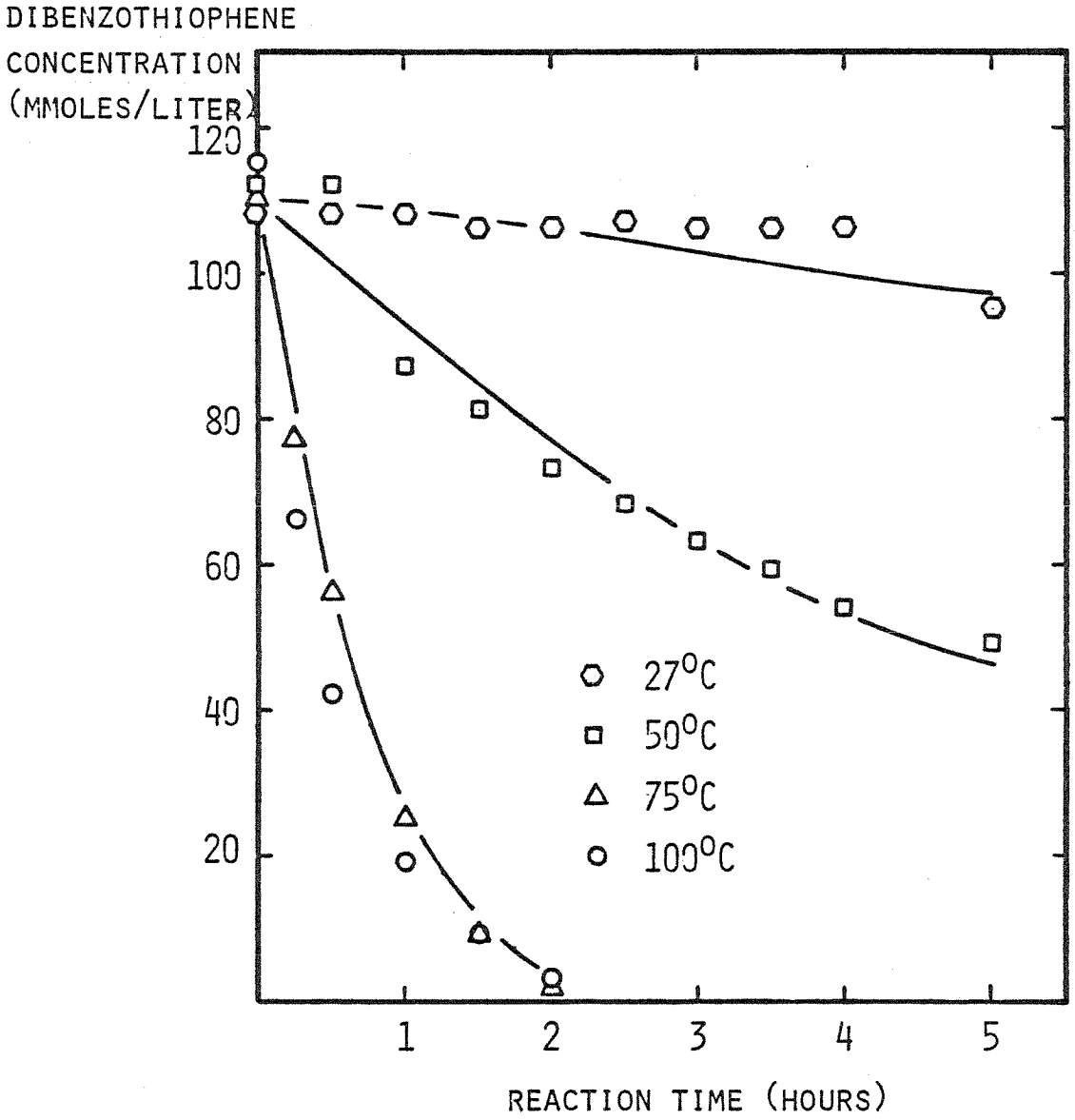


EXPERIMENTS 9-12:

OXIDATION OF 5.0 G DIBENZOTHIOPHENE BY 10.5 G BENZALDEHYDE AND 2.6 MMOLES/MIN $O_2$ AT 0.5 ATM. PARTIAL PRESSURE IN 350 G BROMOBENZENE AT 1 ATM.

FIGURE 5.10 CONCENTRATION PROFILES OF DIBENZOTHIOPHENE AND ITS OXIDATION PRODUCTS AT 27$^{0}$C

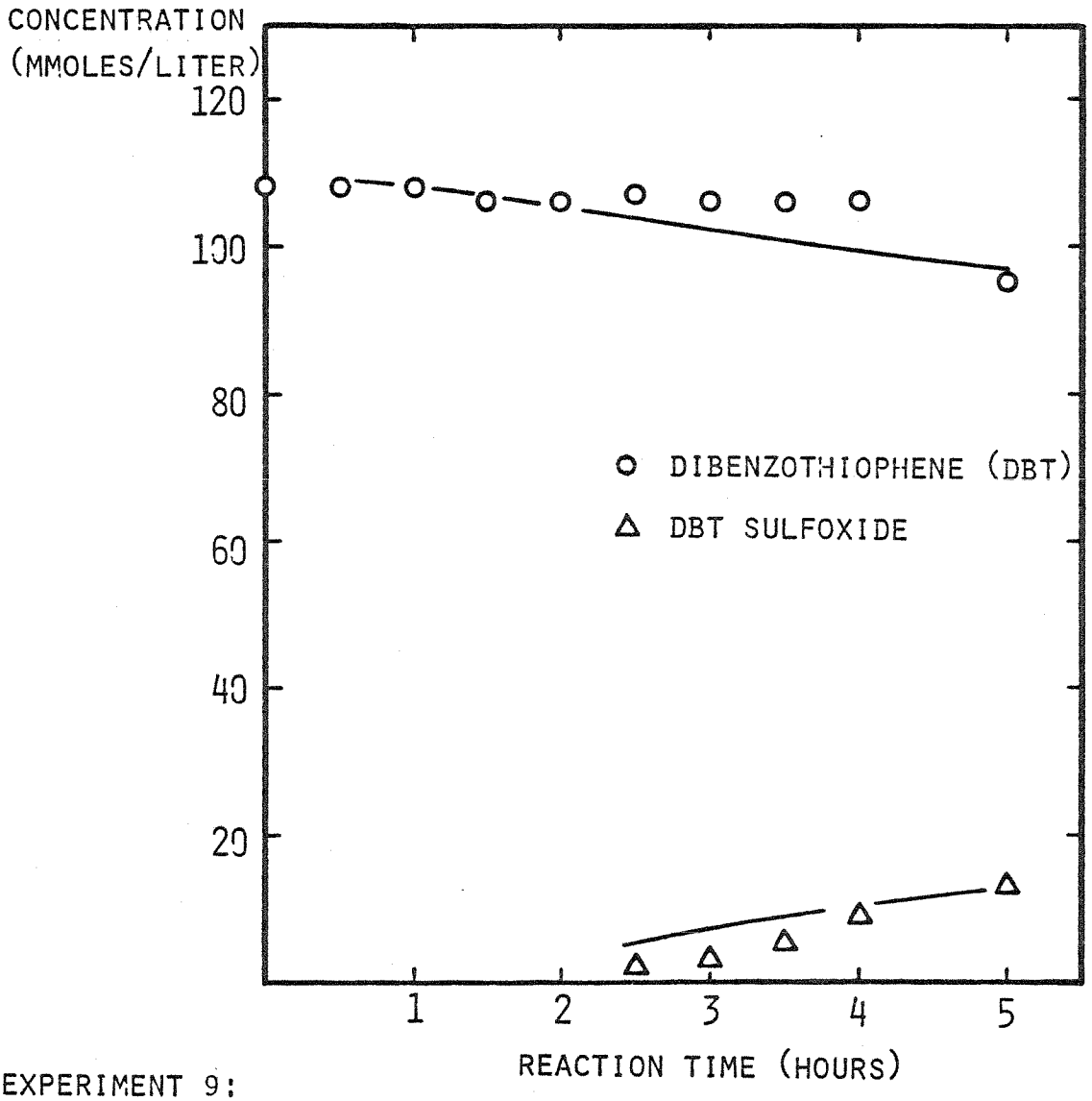


EXPERIMENT 9:

OXIDATION OF 5.0 G DIBENZOTHIOPHENE BY 10.5 G BENZALDEHYDE AND 2.6 MMOLES/MIN $O_2$ AT 0.5 ATM. PARTIAL PRESSURE IN 350 G BROMOBENZENE AT 27$^{0}$C, 1 ATM.

FIGURE 5.11 CONCENTRATION PROFILES OF DIBENZOTHIOPHENE AND ITS OXIDATION PRODUCTS AT $50^{o}C$

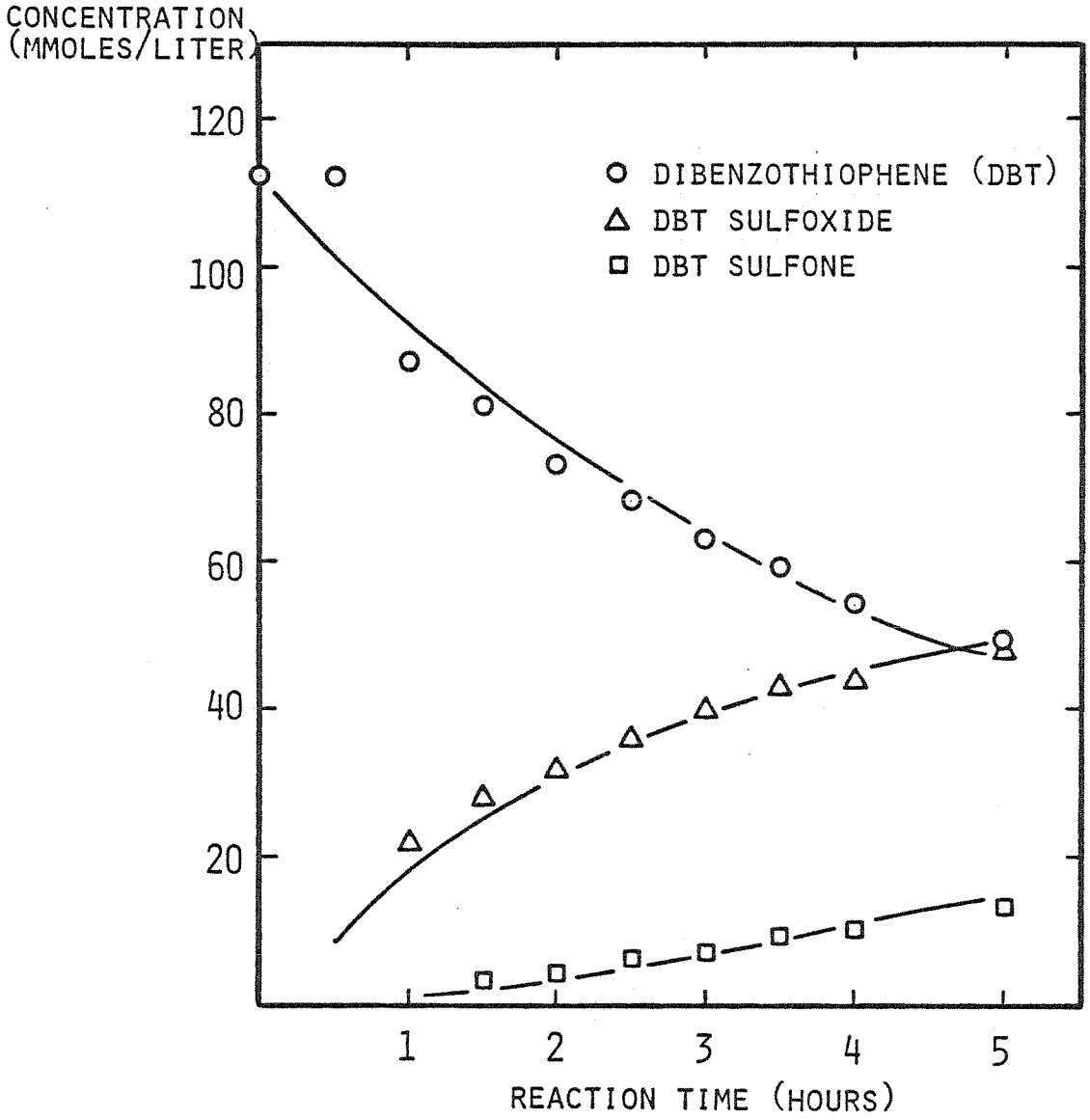


EXPERIMENT 10:

OXIDATION OF 5.0 G DIBENZOTHIOPHENE BY 10.5 G BENZALDEHYDE AND 2.6 MMOLES/MIN $O_2$ AT 0.5 ATM. PARTIAL PRESSURE IN 350 G BROMOBENZENE AT $50^{o}C$, 1 ATM.

FIGURE 5.12 CONCENTRATION PROFILES OF DIBENZOTHIOPHENE AND ITS OXIDATION PRODUCTS AT 75°C

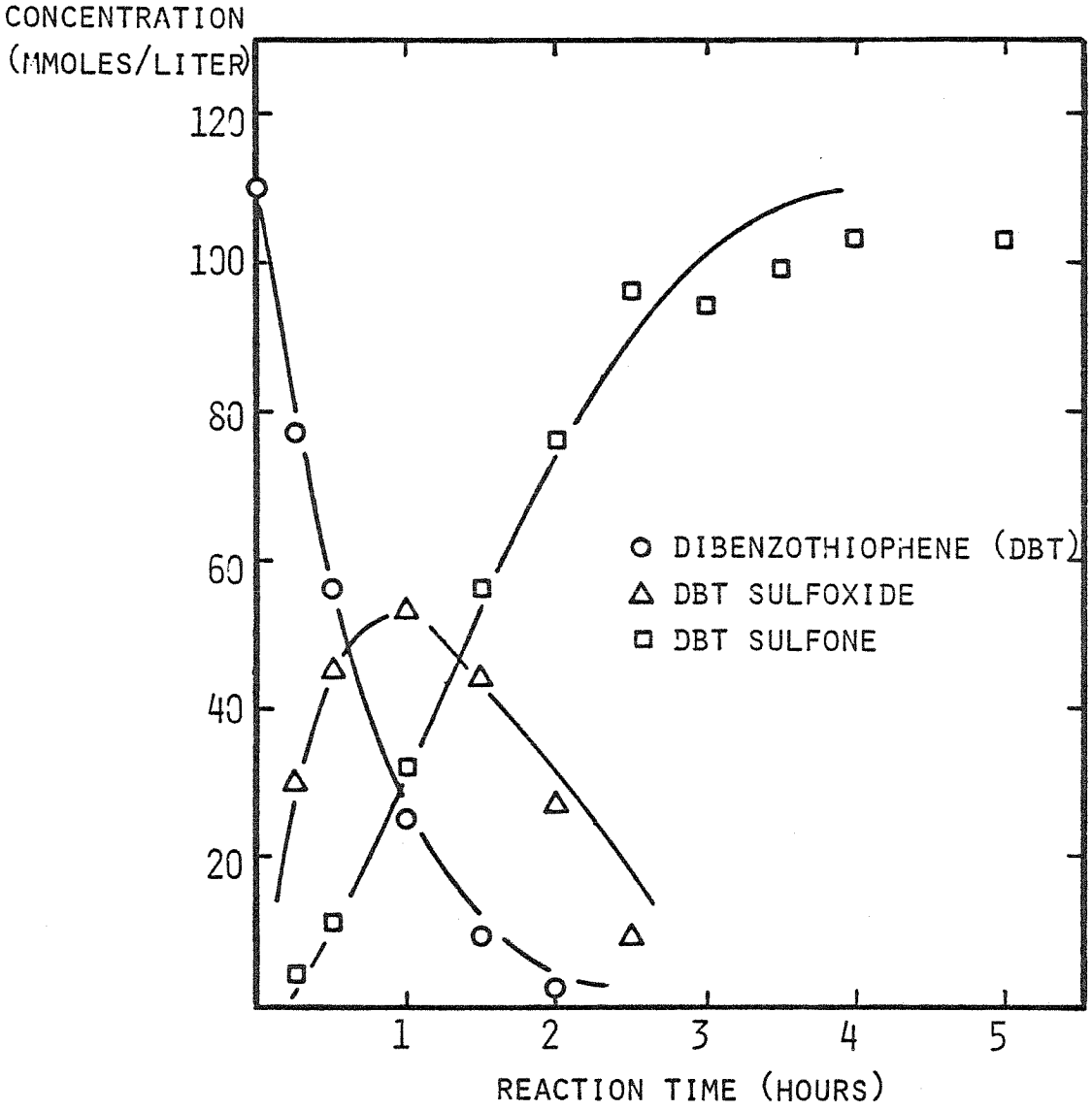


EXPERIMENT 11 :
OXIDATION OF 5.0 G DIBENZOTHIOPHENE BY 10.5 G BENZALDEHYDE AND 2.6 MMOLES/LITER $O_2$ AT 0.5 ATM. PARTIAL PRESSURE IN 350 G BROMOBENZENE AT 75°C, 1 ATM.

FIGURE 5.13 CONCENTRATION PROFILES OF DIBENZOTHIOPHENE AND ITS OXIDATION PRODUCTS AT 100°C.

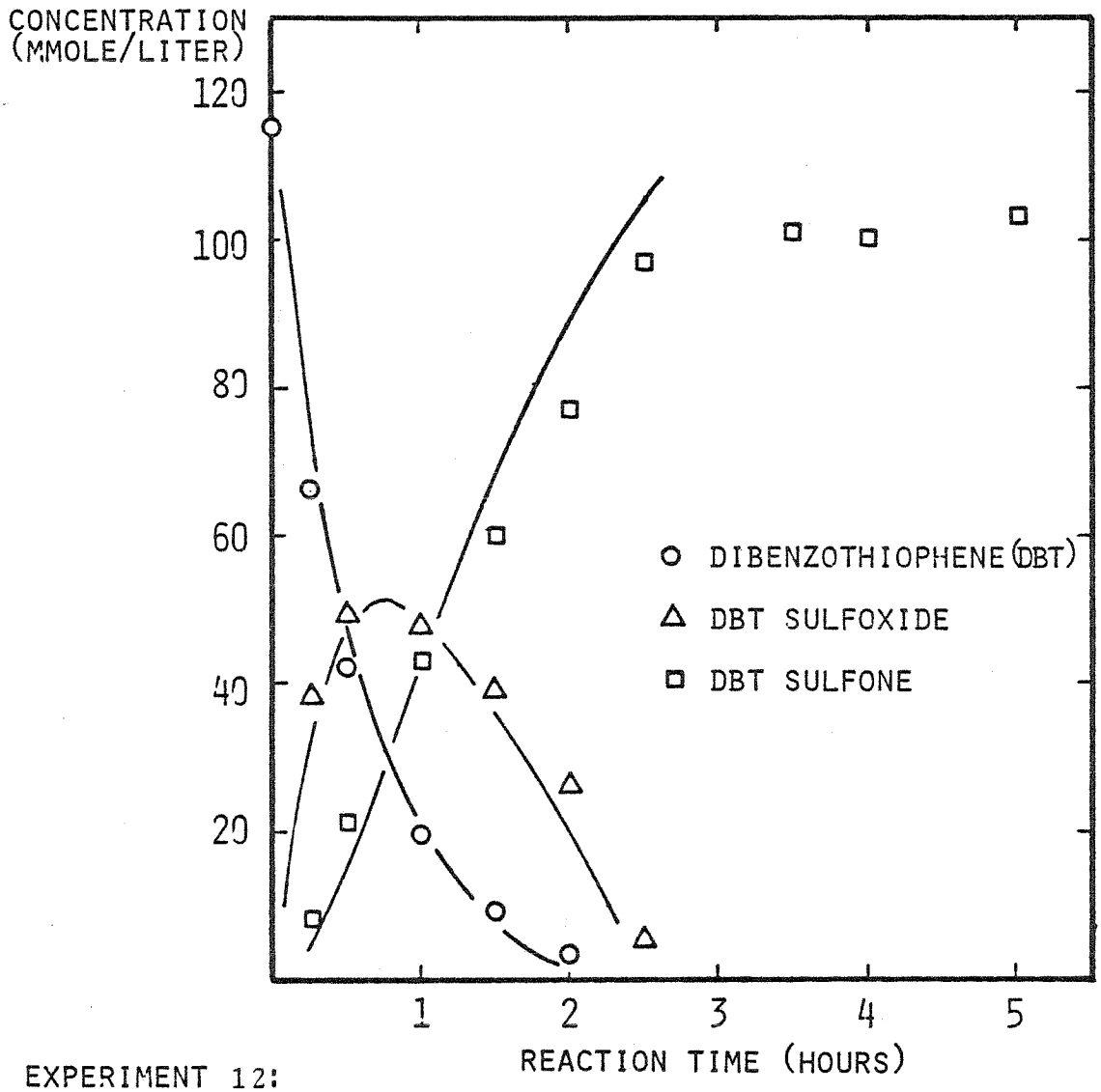


EXPERIMENT 12:

OXIDATION OF 5.0 G DIBENZOTHIOPHENE BY 10.5 G BENZALDEHYDE AND 2.6 MMOLE/LITER $O_2$ AT 0.5 ATM. PARTIAL PRESSURE IN 350 G BROMOBENZENE AT 100°C, 1 ATM.

benzaldehyde autoxidation as well as reducing peracid formation by breaking the radical chain, as follows:

$$RCHO \xrightarrow{k_7} RCO\cdot + H\cdot \qquad \text{(vii)}$$

$$RCO\cdot + O_2 \xrightarrow{k_2} RCO_3\cdot \qquad \text{(ii)}$$

$$RCO_3\cdot + RCHO \xrightarrow{k_3} RCO_3H + RCO\cdot \qquad \text{(iii)}$$

$$RCO_3\cdot + DBT \xrightarrow{k_{10}} DBTO + \text{inert product} \qquad \text{(x)}$$

$$RCO_3\cdot + DBTO \xrightarrow{k_{11}} DBTO_2 + \text{inert product} \qquad \text{(xi)}$$

This latter mechanism has been postulated to explain the action of other inhibitors (see Chapter 2) and is substantiated by the return to more rapid autoxidation rates once the sulfur compound is in the form of sulfone. Only after the dibenzothiophene is completely oxidized does the concentration of perbenzoic acid build up as in the previous set of experiments with no sulfur compound present. Application of the steady-state approximation to the free radicals in the preceding mechanism involving reactions (vii),(ii),(iii), (x) and (xi) results in the following overall rate expression:

$$\frac{d[RCHO]}{dt} = \frac{k_7 [RCHO]^2}{k_{10}[DBT] + k_{11}[DBTO]} \qquad (5.18)$$

This type of rate dependence is not consistent with the data, however, and therefore the oxidation of dibenzothiophene by acyl peroxy radical is not the primary reaction path under these conditions.

Other authors (509) have suggested that the actual inhibitor during the oxidation of sulfides is sulfur dioxide

obtained from decomposition of sulfones. This hypothesis can be rejected as an explanation in the case of dibenzothiophene; such inhibition would be expected to continue past the point of complete oxidation of dibenzothiophene to sulfone.

The complexity of the reaction network again precluded determination of the rate constants by the differentiation of the concentration data, and dictated the use of an integration method. The following set of reactions was used to model the system:

$$RCHO + O_2 \longrightarrow RCO_3H \qquad \text{(xii)}$$

$$RCHO + RCO_3H \xrightarrow{k_9} 2RCO_2H \qquad \text{(ix)}$$

$$2RCO_3H \xrightarrow{k_8} 2RCO_2H + O_2 \qquad \text{(viii)}$$

$$DBT + RCO_3H \xrightarrow{k_{13}} DBTO + RCO_2H \qquad \text{(xiii)}$$

$$DBTO + RCO_3H \xrightarrow{k_{14}} DBTO_2 + RCO_2H \qquad \text{(xiv)}$$

These reactions were assumed to be irreversible, second-order, and elementary except for reaction (xii), where the rate expression (5.11) for autoxidation including diffusion was used. The appropriate differential equations for each species were integrated by a fourth-order Runge-Kutta scheme in a similar manner as for the set of experiments in the absence of sulfur compound. The rate constants for perbenzoic acid decomposition and the perbenzoic acid-benzaldehyde reaction were obtained from the corresponding sulfur-free experiments.

This procedure could not be extended to $\gamma'$ in the overall rate expression for benzaldehyde autoxidation in light of the partial inhibition of this oxidation by dibenzothiophene. The trial-and-error search for the rate constants $k_{13}$ and $k_{14}$ was aided by analysis of the non-linear differential equations associated with these consecutive reactions

$$\frac{d[DBT]}{dt} = -k_{13}[DBT][RCO_3H] \qquad (5.19)$$

$$\frac{d[DBTO]}{dt} = k_{13}[DBT][RCO_3H] - k_{14}[DBTO][RCO_3H] \qquad (5.20)$$

These differential equations are better handled on a time-free basis:

$$\frac{d[DBTO]}{d[DBT]} = -1 + \frac{k_{14}}{k_{13}}\frac{[DBTO]}{[DBT]} \qquad (5.21)$$

This expression is equivalent to that for the consecutive first order system (510). The maximum concentration of dibenzothiophene sulfoxide (DBTO) occurs when the derivative is zero; the following relationship between the rate constants is obtained at this point:

$$\frac{[DBTO]_{max}}{[DBT]_{max\ DBTO}} = \frac{k_{13}}{k_{14}} \quad . \qquad (5.22)$$

This ratio was used to reduce the number of degrees of freedom in the search for the rate constants which gave the best fit to the experimental data. The solid lines in Figures 5.7 - 5.13 are the result of fitting with the model

outlined by reactions (viii), (ix), (xii), (xiii), (xiv). Arrhenius plots of the rate constants for dibenzothiophene and dibenzothiophene sulfoxide oxidation by perbenzoic acid obtained by this method are shown in Figure 5.14. The corresponding activation energies are 17.7 kcal/mole and 18.4 kcal/mole, respectively. These values are slightly higher than those obtained by other authors (see Appendix A), and thus may add credence to participation of the alternative mechanism of sulfur attack by the acyl peroxy radical in addition to the peracid itself.

To insure that non-radical species other than perbenzoic acid did not also contribute to the oxidation of dibenzothiophene, two blank experiments were run. Table 5.15 gives the experimental conditions and the results of quantitative analysis are listed in Tables 5.16 and 5.17. No products of dibenzothiophene oxidation were detected on the liquid chromatograph for either experiment. Experiment 13 demonstrates that the primary product of benzaldehyde autoxidation, benzoic acid, cannot effect the oxidation of dibenzothiophene even in the presence of oxygen. That benzaldehyde itself is not the dibenzothiophene oxidizing agent is shown in experiment 14, where only nitrogen gas was delivered through the sparger. Although obscured by scatter in the analysis, there is some evidence that a slight amount of oxygen diffusion back through the condenser may have occurred.

FIGURE 5.14 ARRHENIUS PLOT OF THE RATE CONSTANTS FOR THE OXIDATION OF DIBENZOTHIOPHENE (DBT) AND DIBENZOTHIOPHENE SULFOXIDE (DBTO) BY PERBENZOIC ACID ($\phi CO_3H$)

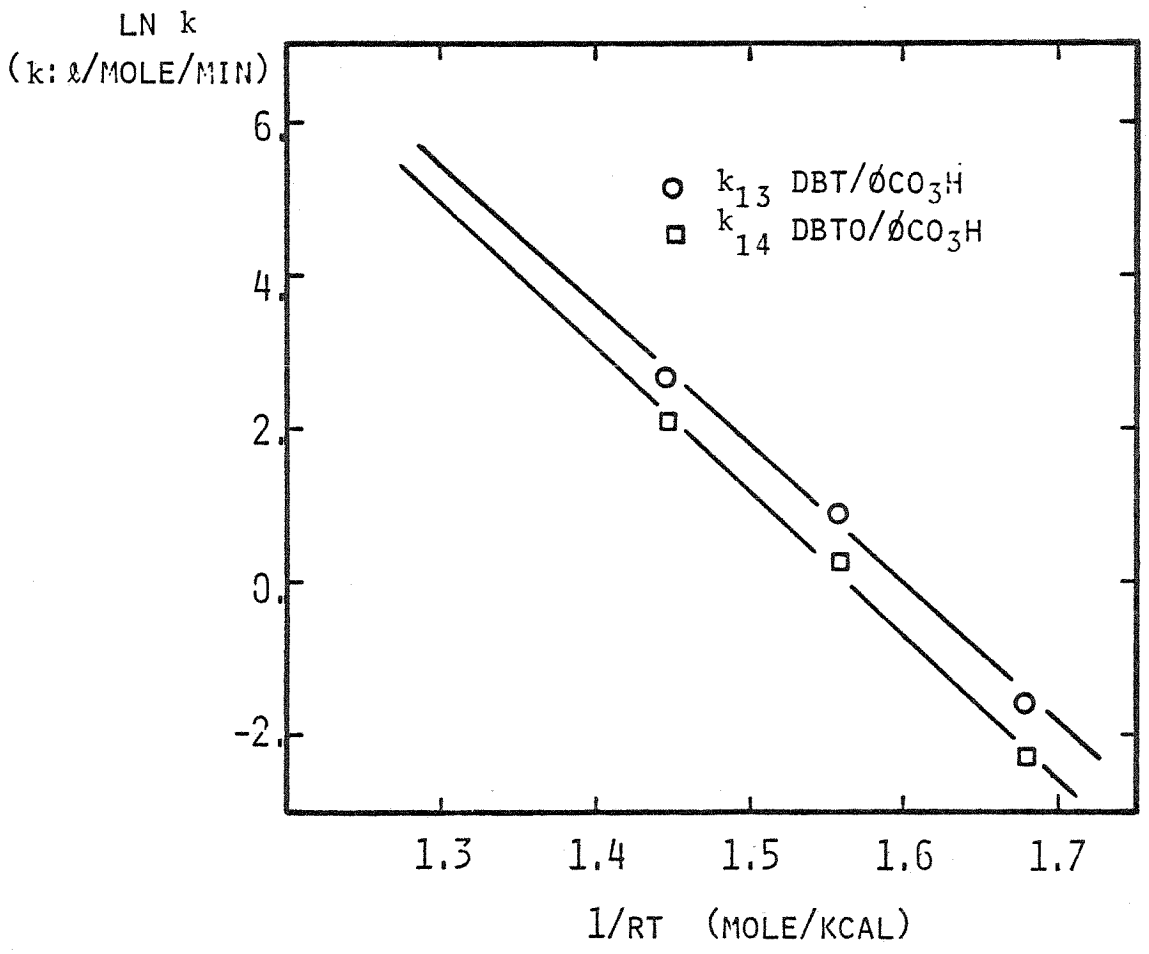

Table 5.15 Parameters for Experiments 13 - 14

| Experiment | 13 | 14 |
|---|---|---|
| Solvent | Bromobenzene 350 g | Bromobenzene 350 g |
| Sulfur Compound | DBT 5.041 g | DBT 5.040 g |
| Aldehyde | None | Benzaldehyde |
| Other | | |
| $O_2$ Flow Rate (millimoles/min) | 2.63 | 0.0 |
| $N_2$ Flow Rate (millimoles/min) | 2.58 | 5.20 |
| Temperature ($^{o}C$) | 75.5 | 75.4 |
| Pressure (mm Hg) | 745.1 | 745.7 |
| $O_2$ Partial Pressure (mm Hg) | 376.3 | 0.0 |

DBT = Dibenzothiophene

Table 5.16 Quantitative Analysis of Samples for Experiment 13

| Reaction Time (min) | DBT | Perbenzoic Acid | DBTO |
|---|---|---|---|
| | | (millimoles/ℓ) | |
| 0 | 111 | 0 | 0 |
| 30 | 109 | 0 | 0 |
| 60 | 113 | 0 | 0 |
| 90 | 108 | 0 | 0 |
| 120 | 112 | 0 | 0 |
| 150 | 110 | 0 | 0 |
| 180 | 110 | 0 | 0 |
| 240 | 119 | 0 | 0 |
| 300 | 109 | 0 | 0 |

DBT = Dibenzothiophene

DBTO = DBT sulfoxide

Table 5.17 Quantitative Analysis of Samples for Experiment 14

| Reaction Time (min) | Benzaldehyde | Perbenzoic Acid | DBT | DBTO |
|---|---|---|---|---|
| | | (millimoles/ℓ) | | |
| 0 | 404 | 0 | 118 | 0 |
| 30 | 398 | 0 | 116 | 0 |
| 60 | 356 | 0 | 106 | 0 |
| 90 | 394 | 0 | 118 | 0 |
| 120 | 408 | 0 | 124 | 0 |
| 150 | 381 | 0 | 116 | 0 |
| 180 | 402 | 0 | 122 | 0 |
| 240 | 382 | 0 | 114 | 0 |
| 300 | 372 | 0 | 112 | 0 |

DBT = Dibenzothiophene

DBTO = Dibenzothiophene sulfoxide

Selectivity of Dibenzothiophene Oxidation

One of the outstanding features of the perbenzoic acid oxidation of dibenzothiophene is the selectivity of the attack. In none of the experiments was there any evidence in the liquid chromatogram of dibenzothiophene derivatives resulting from oxidation of the carbon structure. This conclusion is substantiated by the closure of the material balance on dibenzothiophene, its sulfoxide, and sulfone within the scatter of the analysis. Although the reaction mixture turned to a yellow color during the course of the experiment which deepened to rosé at higher temperatures, there was no evidence of attack on the solvent at the level of detection of the liquid chromatograph. This observation is also valid for decane and toluene as well as bromobenzene (see Appendix A). The yellow color is presumed to be due to termination products from autoxidation of aldehydes since it also occurred in the absence of sulfur compound. In experiments 7, 8, 11 and 12, some highly-retained (non-polar) compounds were observed in small amounts in the liquid chromatogram; these were attributed to the decomposition of the unstable termination products.

A second factor of importance is closely related to selectivity, yet is more accurately described as efficiency of oxidation. For this purpose, it shall be defined as the percentage of aldehyde oxidized which is effective in oxidizing dibenzothiophene, as opposed to being consumed in the peracid decomposition or peracid-aldehyde reactions.

This factor may be easily calculated at any time, t, during the course of the reaction from the formula:

$$\% \text{ efficiency} = \frac{[DBTO]_t + 2[DBTO_2]_t}{[RCHO]_o - [RCHO]_t} \times 100 \qquad (5.23)$$

The efficiencies were calculated for experiments 9 through 12 and plotted in Figure 5.15. Although the efficiency is seen to increase rapidly with temperature at first, it reaches a maximum between 75°C and 100°C. This result is as to be expected from the activation energies involved. The activation energy of the reaction of perbenzoic acid with dibenzothiophene and its sulfoxide is intermediate between that of the peracid-aldehyde reaction and peracid decomposition. Thus, at low temperatures, the aldehyde competes effectively for the perbenzoic acid with the DBT, whereas at high temperature peracid decomposition will be preferred. A second consequence of the relative rates involved is that dibenzothiophene will be more efficiently oxidized in situations where the concentrations of aldehyde and peracid are kept low.

Oxidation of Diphenyl Sulfide

Diphenyl sulfide, a model compound representing another important class of sulfur compounds present in fossil fuels, was studied in experiment 15; the experimental conditions are outlined in Table 5.18. Diphenyl sulfide was observed to inhibit benzaldehyde autoxidation even more than dibenzothiophene; therefore, a larger initial benzaldehyde concentration was used. Over 99% reduction in benzaldehyde autoxi-

FIGURE 5.15 EFFICIENCY OF PERBENZOIC ACID ATTACK ON DIBENZOTHIOPHENE AS A FUNCTION OF TEMPERATURE

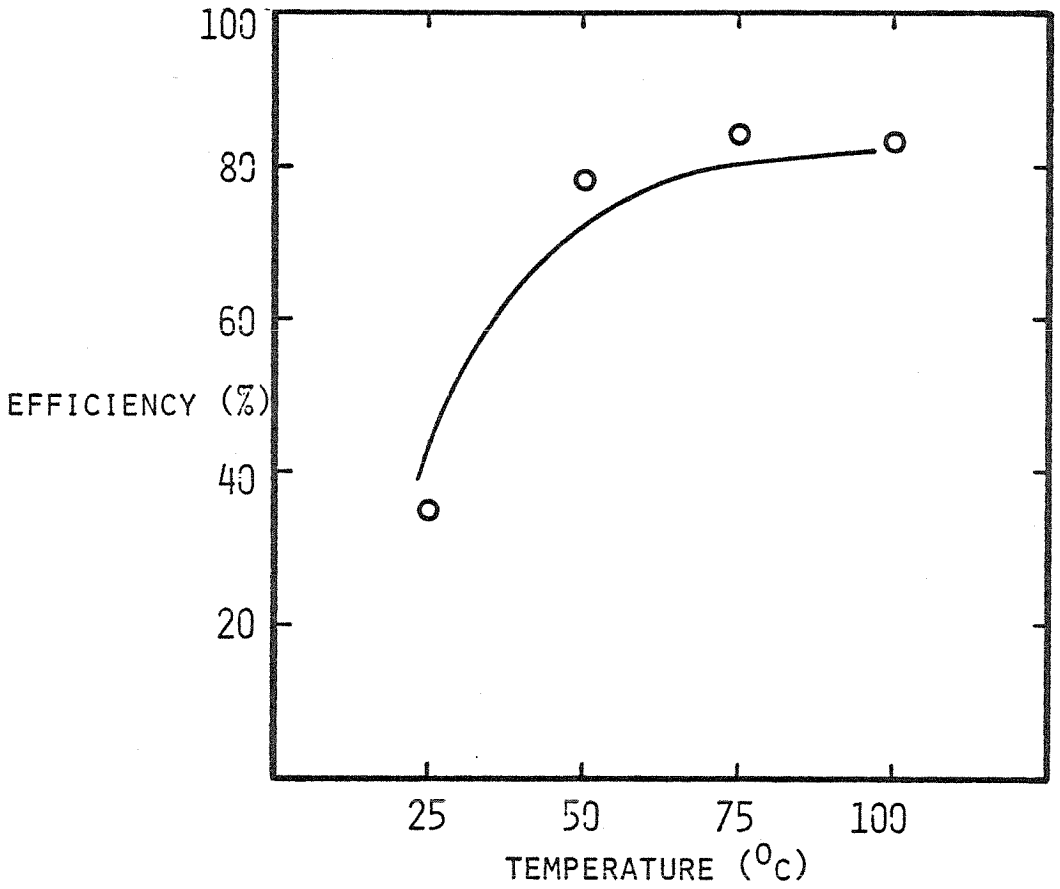

Table 5.18 Parameters for Experiments 15 -17

| Experiment | 15 | 16 | 17 |
|---|---|---|---|
| Solvent | Bromobenzene 350 g | Bromobenzene 350 g | Bromobenzene 200 g |
| Sulfur Compound | DPS 5.001 g | DBT 2.049 g | DBT 5.039 g |
| Aldehyde | Benzaldehyde 26.15 g | Benzaldehyde 10.5 g | Benzaldehyde 26.15 g |
| Other | | Napthalene 2.009 g | Atmospheric Resid 100 g |
| $O_2$ Flow Rate (millimoles/min) | 2.63 | 2.63 | 2.66 |
| $N_2$ Flow Rate (millimoles/min) | 2.54 | 2.60 | 2.57 |
| Temperature ($^{o}C$) | 75.2 | 75.6 | 75.3 |
| Pressure (mm Hg) | 736.9 | 745.6 | 743.2 |
| $O_2$ Partial Pressure (mm Hg) | 375.1 | 375.0 | 378.3 |

DPS = Diphenyl sulfide

DBT = Dibenzothiophene

dation rate was found. The quantitative results are given in Table 5.19 and plotted in Figures 5.16 and 5.17. A mechanism analogous to the one developed for oxidation of dibenzothiophene was used to model the concentration profiles. The solid lines in Figures 5.16 and 5.17 represent this fit. The second order rate constants for the oxidation of diphenyl sulfide and its sulfoxide were 25. $\frac{\ell}{\text{mole}\cdot\text{min}}$ and 5.0 $\frac{\ell}{\text{mole}\cdot\text{min}}$ compared with values of 12. $\frac{\ell}{\text{mole}\cdot\text{min}}$ and 7.0 $\frac{\ell}{\text{mole}\cdot\text{min}}$ obtained for dibenzothiophene and its sulfoxide at the same temperature. The aromatic character of the central ring probably made the thiophenic sulfur more difficult to oxidize initially, although the difference was not as great as expected. Previous workers have noted that the ratio of rate constants for oxidation to sulfoxide is over 100 (see Chapter 3). Once oxidized, the dibenzothiophene sulfoxide was slightly more susceptible to subsequent oxidation to sulfone than the diphenyl sulfoxide. This finding is also contrary to other data for the attack of perbenzoic acid on these sulfoxides, although the rate constants are reported to be the same order of magnitude (511). This observation may again be caused by the operation of a different mechanism of sulfur oxidation where the peracid is formed by in situ aldehyde autoxidation (i.e., attack by the acyl peroxy radical).

Oxidation in the Presence of Napthalene

It was considered desirable to investigate the oxidation of sulfur compounds in the presence of condensed aromatic

Table 5.19 Quantitative Analysis of Samples for Experiment 15

| Reaction Time (min) | Benzaldehyde | Perbenzoic Acid | DPS | DPSO | $DPSO_2$ |
|---|---|---|---|---|---|
| | | | (millimoles/ℓ) | | |
| 0 | 948 | 0 | 105 | 6 | |
| 15 | 926 | 0 | 98 | 15 | |
| 30 | 936 | 0 | 92 | 19 | |
| 60 | 923 | 0 | 84 | 27 | |
| 90 | 895 | 0 | 73 | 34 | |
| 120 | 893 | 0 | 66 | 41 | |
| 150 | 893 | 0 | 60 | 48 | |
| 180 | 882 | 0 | 52 | 53 | |
| 240 | 859 | 0 | 20 | 67 | 2 |
| 300 | 770 | 0 | 10 | 68 | 32 |

DPS = Diphenyl sulfide

DPSO = Diphenyl sulfoxide

$DPSO_2$ = Diphenyl sulfone

FIGURE 5.16 RATE OF BENZALDEHYDE AUTOXIDATION DURING THE CO-OXIDATION OF DIPHENYL SULFIDE

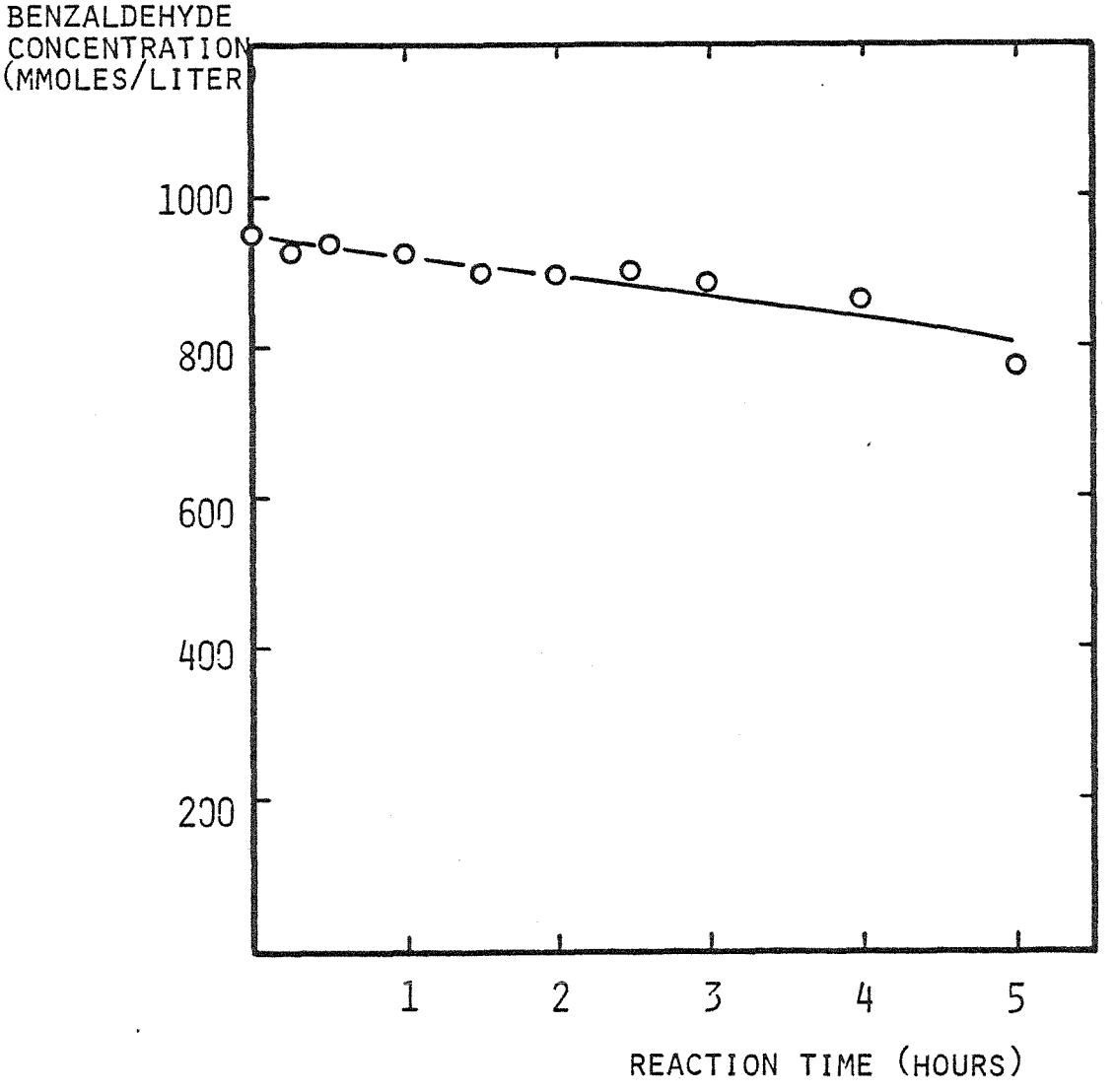


EXPERIMENT 15:

OXIDATION OF 26.2 G BENZALDEHYDE BY 2.6 MMOLES/MIN $O_2$ AT 0.5 ATM. PARTIAL PRESSURE IN 350 G BROMOBENZENE AND 5.0 G DIPHENYL SULFIDE AT $75^{O}C$, 1 ATM.

FIGURE 5.17 CONCENTRATION PROFILES OF DIPHENYL SULFIDE AND ITS OXIDATION PRODUCTS AT 75°C

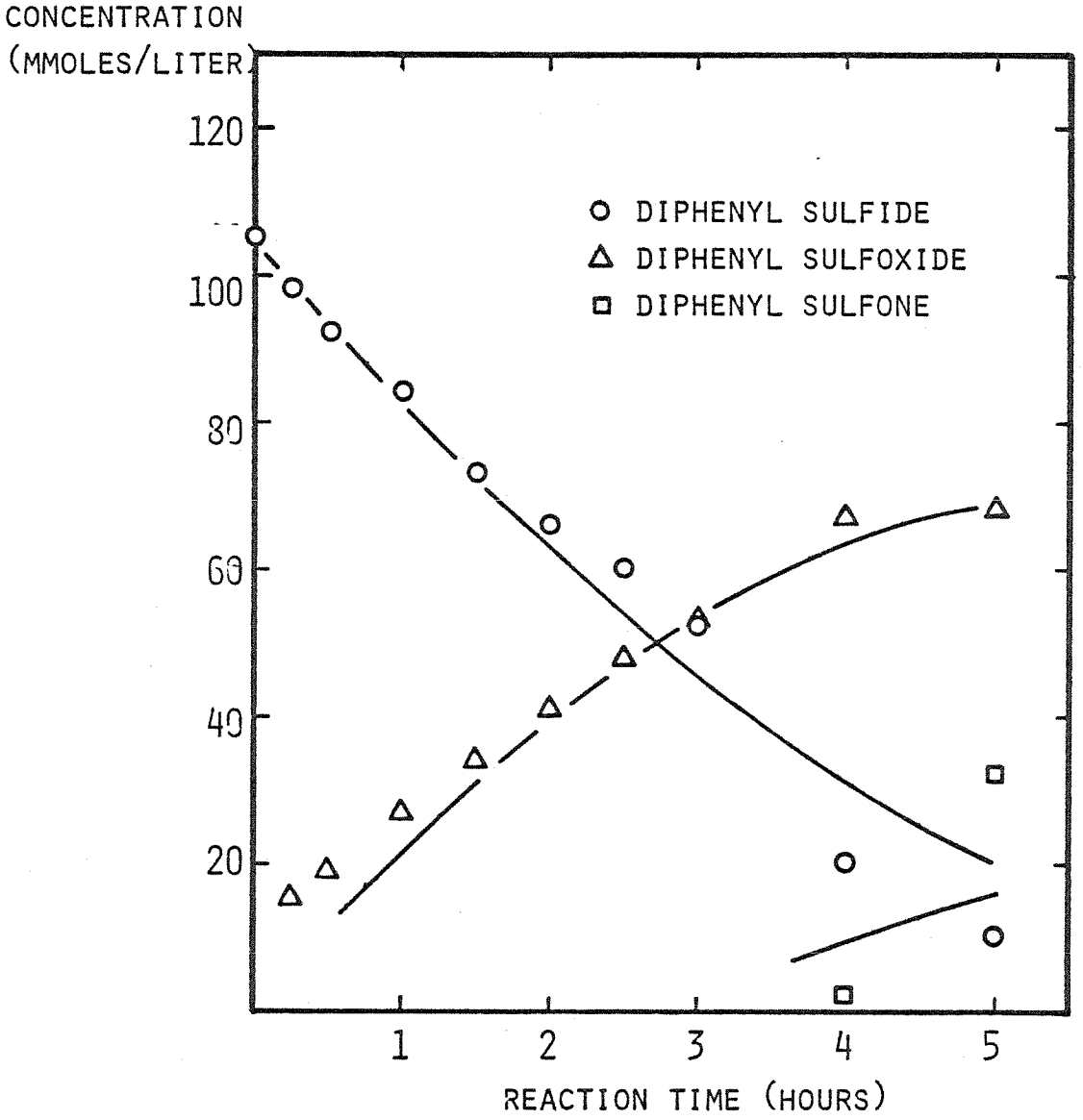


EXPERIMENT 15:

OXIDATION OF 5.0 G DIPHENYL SULFIDE BY 26.2 G BENZALDEHYDE AND 2.6 MMOLES/MIN $O_2$ AT 0.5 ATM. PARTIAL PRESSURE IN 350 G BROMOBENZENE AT 75°C, 1 ATM.

rings, because these types of compounds are a major constituent in fossil fuels. The experimental conditions selected are given in Table 5.18. The results of quantitative analysis are given in Table 5.20 and plotted in Figures 5.18 and 5.19. It was not possible to follow the concentration of naphthalene accurately because its retention time on the liquid chromatograph was approximately that of the bromobenzene solvent. None of the oxidation products of naphthalene, including 1,4 naphthoquinone were observed, however. Despite this evidence of a lack of an inhibitory mechanism, what appears to be about an hour induction period is seen in Figure 5.18. The rate of benzaldehyde autoxidation is severely curtailed in the presence of naphthalene after the induction period as well. Thus, naphthalene exhibits both inhibitor and retarder characteristics in the benzaldehyde autoxidation. The oxidation of dibenzothiophene seems to be unaffected by naphthalene the solid lines in Figure 5.18 are a fit with the rate constants from experiment 11.

Solvent Effects

Dramatic solvent effects have been observed previously for both aldehyde autoxidation and peracid oxidation of organic sulfur compounds. Differences in rate observed during aldehyde autoxidation have been correlated with dielectric constant (see Chapter 2) and explained in terms of stabilization of the radical electron. The reduction in the rate of oxidation of sulfides by peracids in polar solvents has been attributed to solvent interference with

Table 5.20 Quantitative Analysis of Samples for Experiment 16

| Reaction Time (min) | Benzaldehyde | Perbenzoic Acid | DBT | DBTO | $DBTO_2$ |
|---|---|---|---|---|---|
| | | | (millimoles/ℓ) | | |
| 0 | 404 | 0 | 46 | | |
| 30 | 400 | 0 | 46 | | |
| 60 | 395 | 0 | 46 | | |
| 90 | 400 | 0 | 46 | 1 | |
| 120 | 385 | 0 | 40 | 6 | 0 |
| 150 | 383 | 0 | 38 | 8 | 1 |
| 180 | 384 | 0 | 37 | 9 | 1 |
| 210 | 377 | 0 | 35 | 10 | 2 |
| 240 | 362 | 0 | 32 | 11 | 2 |
| 300 | 372 | 0 | 31 | 13 | 3 |

DBT = Dibenzothiophene

DBTO = Dibenzothiophene sulfoxide

$DBTO_2$ = Dibenzothiophene sulfone

FIGURE 5.18 CONCENTRATION PROFILES OF DIBENZOTHIOPHENE AND ITS OXIDATION PRODUCTS IN THE PRESENCE OF NAPHTHALENE AT $75^{o}C$

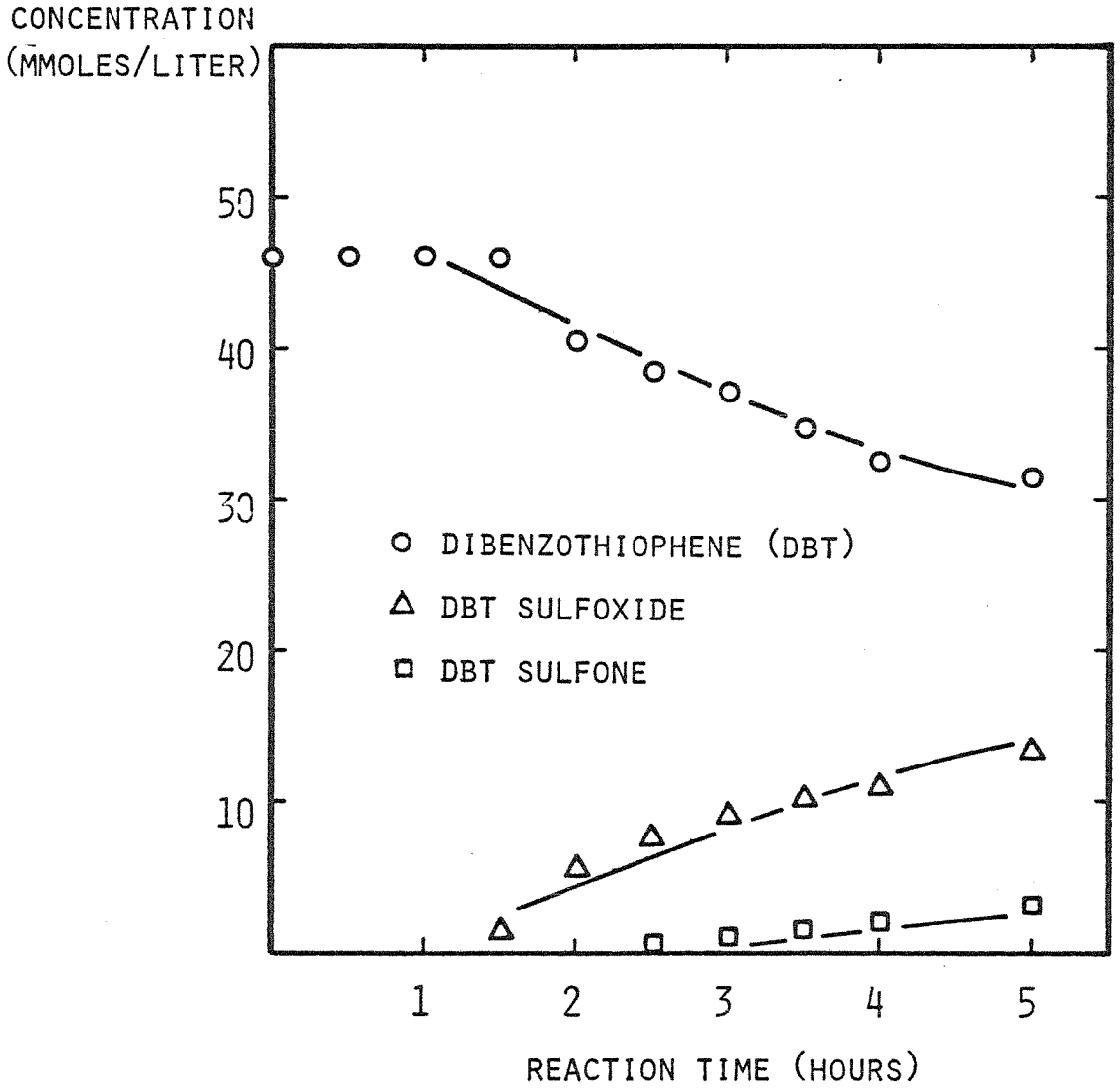


EXPERIMENT 16:
OXIDATION OF 2.0 G DIBENZOTHIOPHENE BY 10.5 G BENZALDEHYDE AND 2.6 MMOLES/MIN $O_2$ AT 0.5 ATM. PARTIAL PRESSURE IN 350 G BROMOBENZENE AND 2.0 G NAPHTHALENE AT $75^{o}C$, 1 ATM.

FIGURE 5.19 RATE OF BENZALDEHYDE AUTOXIDATION DURING THE CO-OXIDATION OF DIBENZOTHIOPHENE IN THE PRESENCE OF NAPHTHALENE AT $75^{o}C$

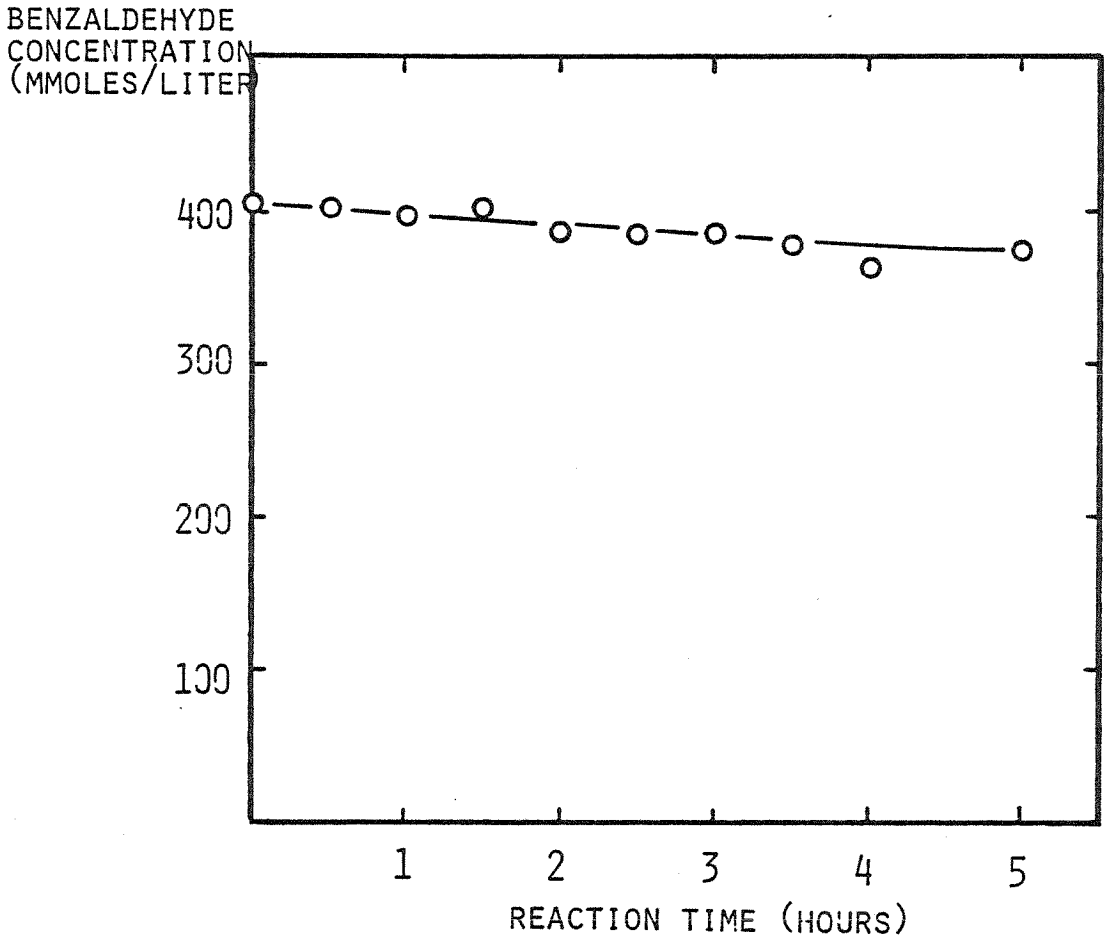


EXPERIMENT 16:

OXIDATION OF 10.5 G BENZALDEHYDE BY 2.6 MMOLES/MIN $O_2$ AT 0.5 ATM. PARTIAL PRESSURE IN 350 G BROMOBENZENE, 2.0 G DIBENZOTHIOPHENE, AND 2.0 G NAPHTHALENE AT $75^{o}C$, 1 ATM.

the intramolecular hydrogen bond of the peracid (see Chapter 3). Thus, a solvent appropriate for each separate oxidation process may not be suitable for the co-oxidation. Decane was demonstrated as an excellent medium for obtaining high oxidation rates for both aldehyde autoxidation and oxidation of dibenzothiophene by peracid (see Appendix A). In order to complement the work with bromobenzene, derivatives of benzene were selected to represent the three primary classes of solvents: 1) polar, protic; 2) polar, non-protic, and 3) non-polar. The solvents used were benzyl alcohol, acetophenone, and toluene, respectively; the reaction conditions employed are presented in Table 5.21.

No oxidation of dibenzothiophene was observed in benzyl alcohol. Although fifty percent of the initial aldehyde charge reacted during the course of 5 hours, only a trace of benzoic acid, the primary product of benzaldehyde autoxidation, was detected. In addition, an unidentified component with retention time greater than dibenzothiophene was observed on the liquid chromatograph. These results are consistent with the replacement of aldehyde autoxidation by the competing mechanism of acetal formation.

$$\text{ØCHO} + \text{ØCH}_2\text{OH} \rightleftharpoons (\text{Ø} - \underset{\text{OH}}{\overset{\text{H}}{\text{C}}} - \text{OCH}_2\text{Ø}) \qquad \text{(xv)}$$

$$(\text{Ø} - \underset{\text{OH}}{\overset{\text{H}}{\text{C}}} - \text{OØ}) + \text{ØCH}_2\text{OH} \rightleftharpoons \underset{\text{Acetal}}{\text{Ø} - \underset{\text{OCH}_2\text{Ø}}{\overset{\text{H}}{\text{C}}} - \text{OCH}_2\text{Ø}} + \text{H}_2\text{O} \qquad \text{(xvi)}$$

Table 5.21 Parameters for Experiments 18 - 20

| Experiment | 18 | 19 | 20 |
|---|---|---|---|
| Solvent | Benzyl Alcohol 250 g | Acetophenone 250 g | Toluene 200g |
| Sulfur Compound | DBT 5.035 g | DBT 5.036 g | DBT 5.042 g |
| Aldehyde | Benzaldehyde 10.5 g | Benzaldehyde 10.5 g | Benzaldehyde 10.5 g |
| Other | | | |
| $O_2$ Flow Rate (millimoles/min) | 2.62 | 2.62 | 2.64 |
| $N_2$ Flow Rate (millimoles/min) | 2.58 | 2.57 | 2.57 |
| Temperature ($^oC$) | 75.0 | 75.0 | 75.0 |
| Pressure (mm Hg) | 739.1 | 739.3 | 739.6 |
| $O_2$ Partial Pressure (mm Hg) | 372.1 | 373.3 | 374.6 |

DBT = Dibenzothiophene

Similarly, no oxidation of dibenzothiophene, as well as only trace amounts of benzoic acid were observed when acetophenone was used as the solvent. Acetophenone and benzaldehyde were found to elute at the same time under the chromatographic conditions employed; this peak increased almost 50% in area during the course of the 5-hour reaction period. These observations can best be explained by the substitution of aldol condensation for benzaldehyde autoxidation.

$$\text{ØCHO} + \text{ØCOCH}_3 \longrightarrow \text{Ø} - \overset{\text{H}}{\underset{|}{\text{C}}} = \overset{\text{H}}{\underset{|}{\text{C}}} - \overset{\text{O}}{\overset{\|}{\text{C}}} - \text{Ø} + \text{H}_2\text{O} \qquad \text{(xvii)}$$

The ketone formed would be expected to have a retention time on the liquid chromatograph very similar to the reactants. Peracid generation via aldehyde autoxidation has been successfully carried out in such solvents as acetic acid (503,504) and acetone (512); thus, it is the reactive nature of these two solvents rather than their polarity which are assumed responsible for the apparent lack of peracid formation.

Toluene also did not support the co-oxidation of dibenzothiophene and benzaldehyde; no change was observed in the initial concentration of either reactant for five hours. This result can be attributed to chain-transfer retardation by the following reactions in conjunction with the previously demonstrated inhibitory action of dibenzothiophene.

$$\text{RCO}\cdot + \text{ØCH}_3 \longrightarrow \text{RCHO} + \text{ØCH}_2\cdot \qquad \text{(xviii)}$$

$$\text{ØCH}_2\cdot + \text{ØCH}_3 \longrightarrow \text{ØCH}_3 + \text{ØCH}_2\cdot \qquad \text{(xix)}$$

The approximately 1 millimole/liter of peroxidic product detected by iodometric titration after four hours is probably due to the formation of tolyl hydroperoxide.

Dibenzothiophene Oxidation in the Presence of Residual Oil

The experiments discussed to this point reveal that although perbenzoic acid is a selective oxidant for sulfur compounds, mass-transfer limitations for oxygen and inhibition of autoxidation combine to reduce the effectiveness of its in situ generation from benzaldehyde. A final experiment was designed to approximate a fuel environment more closely, yet still maintain the ability to follow the course of the reaction with the analytical mtehods previously developed. Atmospheric residual oil was added to the reaction mixture as detailed in the compilation of experimental conditions in Table 5.18. The results of quantitative analysis are given in Table 5.22. Titration of perbenzoic acid was not possible due to the presence of residual oil. As expected, no benzaldehyde autoxidation or dibenzothiophene oxidation was observed within the scatter of the analysis. This result is attributed to the autoxidation-inhibiting compounds present in the residual oil.

Table 5.22 Quantitative Analysis of Samples for Experiment 17

| Reaction Time (min) | Benzaldehyde | DBT | DBTO |
|---|---|---|---|
| | (millimoles/ℓ) | | |
| 0 | 891 | 91 | 0 |
| 30 | 909 | 91 | 0 |
| 60 | 815 | 96 | 0 |
| 90 | 894 | 94 | 0 |
| 120 | 921 | 97 | 0 |
| 150 | 923 | 99 | 0 |
| 180 | 917 | 99 | 0 |
| 240 | 921 | 99 | 0 |
| 300 | 896 | 93 | 0 |

DBT = Dibenzothiophene

DBTO = Dibenzothiophene sulfoxide

# CHAPTER 6 SUMMARY AND RECOMMENDATIONS

## Summary and Conclusions

The most important result of this investigation is the demonstration that thiophenic sulfur compounds as well as sulfides can be selectively oxidized at low temperature (25 - 100$^{o}$C) and pressure (1 atm.) to their corresponding sulfoxides and sulfones by peracids formed in situ via the autoxidation of aldehydes. Although oxidation of aldehydes by molecular oxygen to form peracids (i.e. autoxidation) has been studied separately, combination of this process with the co-oxidation of sulfur compounds by the peracid generated has not been investigated previously.

Several factors are shown to limit the rate of in situ formation of peracid. In the reactor configuration employed, a variation in benzaldehyde autoxidation rates with oxygen flow rate was observed, indicating a mass-transfer limitation for oxygen. Mathematical analysis of the appropriate regime where both reaction and diffusion are important demonstrates that the resulting overall rate equation is similar in form to that obtained by the consideration of aldehyde autoxidation alone. From the overall rate expression derived, it is concluded that the increase in aldehyde autoxidation rates is probably caused by the higher surface-to-volume ratio induced by the increased oxygen flow rate through the sparger. Thus, oxygen flow rate and partial pressure are effective in controlling the rate of peracid formation.

Two reactions were also found to limit the rate of peracid formation: decomposition and the direct oxidation of aldehyde by peracid. In contrast with previous work where the emphasis was placed on the measurement of the oxygen absorption rate, quantitative analysis of benzaldehyde and perbenzoic acid allowed the rates of these two reactions to be evaluated. Decomposition of perbenzoic acid is dominated by a second order mechanism between 25°C and 100°C with an activation energy of approximately 24 kcal/mole. At 100°C, the rate of the benzaldehyde-perbenzoic acid reaction is the same order of magnitude as the perbenzoic decomposition reaction; however, its activation energy is only 9.6 kcal/mole. At an $O_2$ flow rate of 2.6 mmole/min, the maximum formation of peracid was observed at 50°C.

The perbenzoic acid generated via benzaldehyde autoxidation is very selective in oxidizing dibenzothiophene and diphenyl sulfide. No oxidation of the carbon structure was observed. In addition to being selective, the in situ oxidation was also efficient; at 75°C, 84% of the aldehyde oxidized contributed to the oxidation of dibenzothiophene. The activation energies for perbenzoic acid oxidation of dibenzothiophene and dibenzothiophene sulfoxide were found to be 17.7 kcal/mole and 18.4 kcal/mole, respectively. These values are between those found for the perbenzoic acid-benzaldehyde reaction and perbenzoic acid decomposition. Therefore, perbenzoic acid generated by benzaldehyde autoxidation is most effective in oxidizing dibenzothiophene

at intermediate temperatures.

The second order rate constants for the oxidation of diphenyl sulfide and its sulfoxide at 75°C were 25 $\frac{\ell}{\text{mole}\cdot\text{min}}$ and 5 $\frac{\ell}{\text{mole}\cdot\text{min}}$ compared with 12 $\frac{\ell}{\text{mole}\cdot\text{min}}$ and 7 $\frac{\ell}{\text{mole}\cdot\text{min}}$ obtained for dibenzothiophene and its sulfoxide at the same temperature. A value of two for the ratio of diphenyl sulfide to dibenzothiophene oxidation rates is in marked contrast to previous work, where a value of 100 has been reported. This discrepancy could be the result of a variety of factors, including solvent effects and the degree of participation of alternate oxidation mechanisms.

Dibenzothiophene was observed to inhibit the rate of benzaldehyde autoxidation, causing reductions in autoxidation rate ranging from 40 to over 95%. Diphenyl sulfide and naphthalene were even more effective inhibitors, reducing the rate of benzaldehyde autoxidation over 99%. Although the concentration of perbenzoic acid remained below the level of detection (<0.5 mmole/ℓ) in the presence of these compounds, the corresponding reduction in the rate of the peracid-aldehyde reaction does not account for the reduction in aldehyde autoxidation observed. In the case of dibenzothiophene in particular, the benzaldehyde autoxidation was found to return to its uninhibited rate upon complete oxidation of DBT to its sulfone, eliminating $SO_2$ production as a possible explanation for the inhibition. These observations are consistent with the participation of the acyl peroxy radical in the oxidation of dibenzothiophene, thereby breaking

the radical chain. This mechanism also accounts for 3-5 kcal/mole discrepancy with previous investigators over the activation energy of the perbenzoic acid-dibenzothiophene reaction and the order of magnitude lower rate at 25°C. Oxidation by acyl peroxy radical is not the principal path for dibenzothiophene oxidation, however, because the resulting rate expression cannot be reconciled with the data. Since no oxidation products were observed, naphthalene presumably acts as a chain-transfer retarder. The lack of autoxidation of benzaldehyde as well as the lack of subsequent oxidation of dibenzothiophene in the presence of residual oil is probably due to the action of similar inhibitors and retarders.

The solvent medium has been demonstrated to have a large effect on both the rate of benzaldehyde autoxidation and the rate of perbenzoic acid oxidation of dibenzothiophene. Autoxidation rates are known to be enhanced by increased dielectric constant whereas oxidation by peracids is reduced by solvents which interfere with the intramolecular hydrogen bonding in peracid. Decane has been shown to be an excellent solvent for maintaining high rates during the co-oxidation of benzaldehyde and dibenzothiophene. Bromobenzene was used to more closely approximate the aromatic character of a fuel oil or coal medium. Although benzaldehyde autoxidation did not occur as rapidly as in decane, the oxidation rate of dibenzothiophene by the perbenzoic acid generated was very similar in both solvents. The second order rate constant

at 50°C was 2.3 $\frac{\ell}{\text{mole}\cdot\text{min}}$ in decane compared with 2.4 $\frac{\ell}{\text{mole}\cdot\text{min}}$ in bromobenzene. The large differences in the corresponding sulfoxide oxidation rates, 6.3 $\frac{\ell}{\text{mole}\cdot\text{min}}$ and 1.3 $\frac{\ell}{\text{mole}\cdot\text{min}}$, respectively, were probably caused by solubility effects. Dibenzothiophene sulfoxide is only slightly solvated by decane, exposing it to more rapid attack by the peracid. Solvents may also affect the co-oxidation of aldehydes and sulfur compounds by providing alternate pathways for reaction such as acetal formation, aldol condensation, and radical chain-transfer in the cases of benzyl alcohol, acetophenone, and toluene, respectively.

In addition, high pressure liquid chromatography was demonstrated to be a valuable tool in the analysis of higher molecular weight compounds typically found in residual oil. With an appropriate choice of spectrophotometer wavelength, reproducibility can be maintained with less than 2% scatter, as evidenced by the material balances obtained for sulfur compounds. The reverse-phase mode is particularly appropriate for analysis of oxidation products; different degrees of oxidation result in large differences in retention time.

## Recommendations

One of the more obvious areas for future work is the elucidation of the mechanism for inhibition of aldehyde autoxidation by organic sulfur compounds. This type of investigation would not only contribute to the understanding of co-oxidation of aldehydes and sulfur compounds, but also

to the mechanisms of free-radical chains in general. An extension of this type of work to include studies of retardation by common solvents and other compounds would also be appropriate.

Previous studies of aldehyde autoxidation should be re-evaluated in the light of the mass-transfer effects observed here. The similar forms of the rate expressions for the chain mechanism including and excluding oxygen diffusion may be responsible for the lack of progress in this area. In particular, the controversy over thermal initiation versus photochemical initiation mechanisms should be resolved conclusively. In this regard, electron-spin-resonance studies may prove fruitful.

Infrared studies have hinted at the importance of the intramolecular hydrogen bond of peracids in their effectiveness as an oxidizing agent for sulfur compounds. Nuclear-magnetic-resonance studies of the peracidic proton may shed some additional light on the details of the specific oxidation mechanism.

Application of this co-oxidation to the sulfur compounds in coal or coal liquids would also be interesting. Of course, for this information to be useful in development of a desulfurization process, the decomposition of oxidized sulfur compounds also needs further investigation.

Chapter 1 References

101. Nealon, J. (ed.), "Monthly Energy Review", DOE/EIA-0035 (80/09) (1980).

102. Sharko, J.R. and Wolfe, L., "Availability of Low Sulfur Coal and Oil", Decision Sciences Corporation Research Paper #171 (1972).

103. Coleman, H.J., et al., J. Chem. and Eng. Data 6, 3 (1961) 464.

104. Thompson, C.J., et al., J. Chem. and Eng. Data 9, 3 (1964) 473.

105. Thompson, C.J., et al., J. Chem. and Eng. Data 10, 3 (1965) 27.

106. Tabler, S.K., J. Air Poll. Con. Assoc. 29 (1979) 803.

107. Maurin, P.E. and Jonakin, J., Chem. Engg. 77, 9 (1970) 173.

108. Anon., Env. Sci, and Technology 6, 8 (1972) 688.

109. Slack, A.V., Chem Eng. Prog. 72, 8 (1976) 94.

110. Asssociation Staff, "Modern Energy Technology", Vol. 2, Research and Education Assoc.: New York (1975).

111. Kalvinskas, J., et al., "Coal Desulfurization by Low Temperature Chlorinolysis, Phase II", JPL80-15 (1980).

112. McKinley, J.B., "Catalysis", Vol. 5, Reinhold: New York (1957) 405.

113. Schuman, S.C. and Shalit, H., Catalysis Rev. 4, 2 (1970) 245.

114. Schuitt, G.C.A. and Gates, B.C., AIChE J. 19, 3 (1973) 417.

115. Watkins, C.H. and Czajkowski, C.J., Chem. Eng. Prog. 67, 8 (1971) 75.

116. Attar, A. and Corcoran, W.H., Ind. Eng. Chem. Prod. Res. Dev. 17 (1978) 102.

117. Wallace, T.J. and Heimlich, B.N., Tetrahedron 24 (1968) 1311.

118. La Count, R.B. and Friedman, S., J. Org. Chem. 42 16 (1977) 2751.

119. Friedman, S., et al., Prep. Div. Fuel. Chem. ACS 22, 2 (1977) 100.

120. Kralik, J.G., PhD thesis, California Institute of Technology (1981).

121. Vasilakos, N.P., PhD thesis, California Institute of Technology (1981).

122. Vasilakos, N.P., et al., "Oxidative Chlorination of Dibenzothiophene", to be published.

123. Heimlich, B.N. and Wallace, T.J., Tetrahedron 22 (1966) 3571.

124. Overberger, C.G. and Cummins, R.W., J. Am. Chem. Soc. 75 (1953) 4250.

125. Bateman, L. and Hargrave, K.R., Proc. Roy. Soc. (London) A224 (1954) 389.

126. Attar, A., PhD thesis, California Institute of Technology (1977).

Chapter 2

201. Attar, A., Ph.D. thesis, California Institute of Technology (1977).

202. Emanuel, N.M., et al. "Liquid Phase Oxidation of Hydrocarbons", Plenum: New York (1967).

203. Sheldon, R.A., and Kochi, J.K., Oxid. and Combustion Revs. 5 (1973) 135.

204. Walling, C., "Free Radicals in Solution", Wiley: New York (1957).

205. Swern, D. (ed.), "Organic Peroxides", Vol. 1, Wiley-Interscience: New York (1970).

206. McNesby, J.R. and Heller, C.A., Chem. Rev. 54 (1954) 325.

207. Backstrom, H.L.J., Z. Physik. Chem. B25 (1934) 99.

208. Waters, W.A. and Wickham-Jones, C., J. Chem. Soc. (1951) 812.

209. Howard, J.A., and Ingold, K.U,, Can. J. Chem. 42 (1964) 1044.

210. Bawn, C.E.H., Hobin, T.P., and Raphael, L., Proc. Roy. Soc. (London), A237 (1956) 313.

211. Tezuka, M., et. al., Bull. Chem. Soc. Japan 49 (1976) 2765.

212. Boga, E., et. al., Acta Chim. Acad, Sci. Hungar. 78 (1973) 75.

213. Marta, F., Boga, E. and Matok, M., Discuss. Faraday Soc. 46 (1968) 173.

214. Bawn, C.E.H., and Jolley, J.E., Proc. Roy. Soc. (London) A237 (1956) 297.

215. Cooper, H.R., and Melville, H.W., J. Chem. Soc.(1951) 1984.

216. Ingles, T.A., and Melville, H.W., Proc. Roy. Soc. (London) A218 (1953) 175.

217. Dick, C.R. and Hanna, R.F., J. Org. Chem. 29 (1964) 1218.

218. McDowell, C.A., and Thomas, J.H., J. Chem. Soc. (1949) 2208.

219. McDowell, C.A., and Thomas, J.H., J. Chem. Soc. (1950) 1462.

220. McDowell, C.A., and Thomas, J.H., Trans. Faraday Soc. 46 (1950) 1030.

221. Pease, Robert N., J. Am. Chem. Soc. 55 (1933) 2753.

222. Hay, J.M., "Reactive Free Radicals", Academic: New York (1974).

223. Koubek, E., et al. J. Am. Chem. Soc. 85 (1963) 2263.

224. Swern, D., Chem. Rev. 45 (1949) 1.

225. Briner, E., Ad. Chem. Ser. 21 (1959) 184.

226. Komissarova, I.N., et. al., Izv. Akad. Nauk. SSR, Ser. Khim. 9 (1978) 1991.

227. Mulcahy, M.F.R. and Watt, I.C., Proc. Roy. Soc. (London) A216 (1953) 10, 30.

228. Bennett, J.E., et al., Trans. Faraday Soc. 66, (1970) 386, 397.

229. Russell, G.A., J. Am. Chem. Soc. 79 (1957) 3871.

230. Bateman, L., Quart. Revs. Chem. Soc. (London) 8 (1954) 147.

231. Santini, D.G., Chem. Eng. Prog. 57 (1961) 61.

232. Donaldson, C.R., "Safety in High Pressure Polyethylene Plants", AICHE: New York (1973) 31.

233. Goodman, J.F., et. al., Trans. Far. Soc. 58 (1962) 1846.

234. Starcher, P.S., et. al., J. Org. Chem. 26 (1961) 3568.

235. Phillips, B., et. al., J. Am. Chem. Soc. 79 (1957) 5982.

236. Kagan, M.J., and Lubarsky, G.D., J. Phys. Chem. 39 (1935) 837.

237. Ogata, Y. and Sawaki, Y., J. Org. Chem. 34 (1969) 3985.

238. Bunton, C.A., et. al., J. Chem. Soc. (1956) 1226.

239. Secco, F. and Celsi, S., J. Chem. Soc. (B) (1971) 1792.

240. Secco, F., et.al, J. Chem. Soc. Perkin Trans. 2 (1973) 1544.

Chapter 3

301. Kharasch, N. (ed.), "Organic Sulfur Compounds", Vol. 1, Pergamon: New York (1961).

302. Hargrave, K.R., Proc. Roy. Soc. A235 (1956) 55.

303. Bateman, L. and Hargrave, K.R., Proc. Roy. Soc. A224 (1954) 389, 399.

304. Attar, A., Phd thesis, California Institute of Technology, (1977).

305. Gilman, H. and Esmay, D.L., J. Am. Chem. Soc. 74 (1952) 2021.

306. Overberger, G.G., and Cummins, R.W., J. Am. Chem. Soc. 75 (1953) 4250.

307. Curci, R., et. al., J. Org. Chem. 35, 3 (1970) 740.

308. Kavcic, R., and Plesnicar, B., J. Org. Chem. 35, 6 (1970) 2033.

309. Greco, A., et. al., Gaz. Chim. Italiana 90 (1960) 671.

310. Curci, et. al., Tetrahedron 22 (1966) 1235.

311. Ford, J.F., and Young, V.O., Prep. Div. Pet. Chem. ACS 10, 2 (1965) c111.

312. Heimlich, B.N., and Wallace, T.J., Tetrahedron 22 (1966) 3571.

313. Kucharczyk, N. and Horak, V., Coll. Czech. Chem. Commun. 34 (1969) 2417.

314. Ponec, R. and Prochazka, M., Coll. Czech. Chem. Commun. 39 (1974) 2081.

315. Attar, A. and Corcoran, W.H., Ind. Eng. Chem. Prod. Res. Dev. 17, 2 (1978) 102, and references therein.

Chapter 4

401. Attar, A., PhD thesis, California Institute of Technology, 1977.

402. Bauman, F., Hadden, N., et. al., "Basic Liquid Chromatography", Varian Aerograph (1971).

403. Kokatnur, V.R., and Jelling, M., J. Am. Chem. Soc. 63 (1941) 1432.

404. Skoog, D.A., and West, D.M., "Fundamentals of Analytical Chemistry", Holt: New York (1969).

405. Kirkland, J.J. (ed.), "Modern Practice of Liquid Chromatography", Wiley: New York (1971).

406. Simpson, C.F. (ed.), "Practical High Performance Liquid Chromatography", Heyden: New York (1976).

407. Mikes, O. and VesPalec, R., J. Chromatogr. Lib. 3 (1975) 233.

408. Snyder, L.R., and Kirkland, J.J., "Introduction to Modern Liquid Chromatography", Wiley: New York (1974).

409. Bakalyar, S.R., Am. Lab. 10, 6 (1978) 43.

Chapter 5

501. Cooper, H.R. and Melville, H.W., J. Chem. Soc. (1951) 1984.

502. Ingles, T.A. and Melville, H.W., Proc. Roy. Soc. (London) A218 (1953) 175.

503. Hendricks, C.F., et al., Ind. Eng. Chem. Prod. Res. Dev. 16, 4 (1977) 270.

504. Hendricks, C.F., et al., Ind. Eng. Chem. Prod. Res. Dev. 27, 3 (1978) 260.

505. Levenspiel, O., "Chemical Reaction Engineering", Wiley: New York (1972) 409 - 419.

506. Danckwerts, P.V., "Gas-Liquid Reactions", McGraw Hill: New York (1970) 96 - 151.

507. Astarita, G., "Mass Transfer with Chemical Reaction", Elsevier: New York (1967).

508. Pravnitz, J.M., "Molecular Thermodynamics of Fluid-Phase Equilibria", Prentice-Hall: Englewood Cliffs, N.J. (1969).

509. Bamford, C.H. and Tipper, C.F.H., "Comprehensive Chemical Kinetics", Vol. 16, Elsevier: New York (1980).

510. Carberry, J.J., "Chemical and Catalytic Reaction Engineering", McGraw-Hill: New York (1976) 46.

511. Greco, A., et al., Gaz. Chim. Italiana 90 (1960) 671.

512. Swern, D., Chem. Rev. 45 (1949) 1.

# APPENDIX A SELECTIVE OXIDATION OF DIBENZOTHIOPHENE IN DECANE BY PERBENZOIC ACID FORMED IN SITU


## Abstract

Perbenzoic acid (POB) was formed by oxidation of benzaldehyde in the presence of ultraviolet light. The POB which was formed selectively oxidized dibenzothiophene (DBT) to sulfoxide (DBTO) and sulfone ($DBTO_2$) under the experimental conditions. DBT sulfoxide was converted to sulfone at a substantially greater rate than DBT to sulfoxide.


## Introduction

The principal objective of this research was to examine a system to oxidize selectively the thiophenic compounds in fuel oil as an initial step in desulfurization. There have been several successful attempts in oxidizing sulfur in organic sulfides (A1,A4,A8,A13), but selective oxidation of sulfur in thiophenic compounds has been more difficult. According to Ford and Young (A5), the stability of the thiophenic compounds and their resistance to oxidation can be explained by: 1) the slightly strained thiophenic nucleus that opposes further strain caused by oxidation, and 2) the delocalization of the lone-pair electrons of the sulfur because of the aromatic structure (A12) of the thiophene. The resonance character of the ring becomes more restricted by adding a conjugated substituent to the molecule. For this reason, dibenzothiophene is oxidized more easily than thiophene. Furthermore, selectivity

*Appendix A is essentially an article by A. Paybarah, R.L. Bone, and W.H. Corcoran to be submitted for publication.

of the oxidation of the thiophenic compounds can also be explained in terms of the electron delocalization of the aromatic rings due to their resonance character. The validity of this interpretation is demonstrated by addition of an electron-donating group such as a methyl moiety to an aromatic ring. This addition promotes more electron localization which makes the molecule more susceptible to an electrophilic attack by an oxidizing agent. In general, to reduce the difficulty of oxidation of thiophenic compounds, a very strong oxidizing agent is required, and peracids show promise (A5, A11). Performic and peracetic acids, although the two most powerful oxidizers of their kind, were rejected because of their extreme explosive potential when subjected to shock or strong light. Perbenzoic acid, a weaker oxidizer, and accordingly a safer one, was considered instead. If thiophenic compounds in fuel oil were oxidized on a commercial scale by addition of peracid, an enormous amount would be required, which in turn would necessitate great care in storage and handling. Therefore, for the sake of safety and economy, it was decided to consider oxidation by way of perbenzoic acid formed in situ as a substitute for addition of a concentrated peracid.

Liquid-phase oxidation of aldehydes by $O_2$ to the peracid and then the selective oxidation of dibenzothiophene by perbenzoic and peracetic acids have been treated separately in the past by different authors (A9,A5,A6,A3). The combination of these two processes, however, has not been studied. In the

study by Ingles and Melville (A9), oxidation of benzaldehyde in the presence of UV light gave a substantial conversion to POB as the primary product. A free-radical mechanism gave the best fit for their rate data. The sequence may be written as:

initiation

$$RCHO \xrightarrow{I} RCO\cdot + H\cdot \quad \text{photochemical effect} \quad (1)$$

$$RCHO + O_2 \xrightarrow{k_1} RCO\cdot + HO_2\cdot \quad \text{thermal effect} \quad (2)$$

propagation

$$RCO\cdot + O_2 \xrightarrow{k_2} RCO_3\cdot \quad (3)$$

$$RCO_3\cdot + RCHO \xrightarrow{k_3} RCO_3H + RCO\cdot \quad (4)$$

termination

$$2RCO_3\cdot \xrightarrow{k_4} \text{inert product} \quad (5)$$

Besides the free-radical mechanism, there are other reactions that take place in the oxidation of benzaldehyde, such as

$$RCO_3H + RCHO \xrightarrow{k_5} 2RCO_2H \quad (6)$$

$$2RCO_3H \xrightarrow{k_6} 2ROH + O_2 \quad (7)$$

In both cases, part of the POB formed is converted to benzoic acid (A.14).

In the selective oxidation of the organic sulfides by peracids, Overberger and Cummins (A11) suggested that the oxidation takes place via a nucleophilic attack by the lone-pair electrons of the sulfur on the intramolecularly bonded peracid.

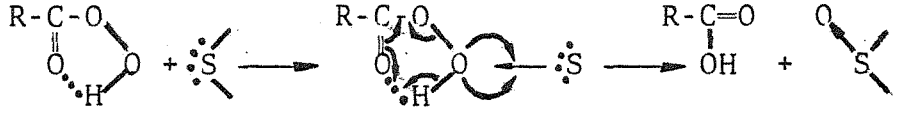

Formation of the intramolecularly bonded complex of the peracid was later confirmed by other authors (e.g. A15). Charges and bond orders of the elements in the complexes of performic and peracetic acid have been measured and are given by Brooks and Haas (A2). Because of the existing similarities between the thiophenic compounds and their sulfoxides, both share lone-pair electrons of sulfur, they likely follow the same mechanism as discussed above (A6). Inasmuch as dibenzothiophene and its derivatives comprise an important part of the thiophenic compounds in fuel oil, we have in this work considered in particular the selective oxidation of this compound. The stoichiometry equations of the oxidation of DBT and its sulfoxide by perbenzoic acid are given as

$$\begin{aligned} RCO_3H + DBT &\xrightarrow{k_7} RCO_2H + DBTO \\ RCO_3H + DBTO &\xrightarrow{k_8} RCO_2H + DBTO_2 \end{aligned} \qquad (9)$$

The kinetics of the simultaneous oxidation of benzaldehyde to POB and the oxidation of DBT and DBT sulfoxide by POB are given by

$$-d(RCHO)/dt = k'\ (RCHO) + k_5(RCHO)(RCO_3H) \qquad (10)$$

$$-d(DBT)/dt = k_7\ (RCO_3H)(DBT) \qquad (11)$$

$$d(DBTO_2)/dt = k_8\ (RCO_3H)(DBTO) \qquad (12)$$

$$d(\Sigma)/dt = k'\ (RCHO) - k_5(RCHO)(RCO_3H - R' \qquad (13)$$

where k' represents the combined effects of Equations (1) and

(2), $(\Sigma) = (RCO_3H) - (DBT) + (DBTO_2)$, and R' is the combined rate of the peracid decomposition from both thermal and photochemical effects.

## Experimental

### Reagent and Solvents

As mentioned in the foregoing section, dibenzothiophene was chosen as the thiophenic compound due to its relative abundance in the fuel oil. Benzaldehyde was selected as the precursor for the perbenzoic acid. The latter compound is a strong oxidizer and at the same time is relatively safe when produced in situ.

A solvent was selected to give the highest yield of POB for a fixed period of time. In preliminary and later, more detailed tests, benzene, toluene, cyclohexane, n-hexane and n-decane were compared. Potassium iodide was added as a reagent to the solutions of benzaldehyde in the individual solvents. Under the experimental conditions of oxidation, the POB formed then oxidized the colorless $I^-$ ions to the colored iodine. Of the solvents, n-decane provided the most promising results. N-hexane offered more or less comparable results, but it was rejected because of its relatively high volatility.

### Equipment

The reactions were carried out in a 500 ml, 3-necked, spherical reaction flask. The flask necks contained a thermometer, a tap-water-cooled condenser, and a glass tube for an oxygen inlet. Flow of oxygen was manually controlled from

a supply tank. It bubbled through an evaporator filled with the same solvent as in the flask and then entered the reaction vessel. Two U-tube manometers showed the relative rate of flow of oxygen and were attached to the oxygen line before and after the evaporator. The solution in the flask was continuously mixed by using a magnetic stirrer, and the speed of stirring was periodically measured by a stroboscope. As necessary the flask was heated with an electrical mantle. Ultraviolet light (UV) was obtained from a fluorescent-type blacklite bulb, Sylvania #F15T8-BL, placed approximately 4 inches from the reaction flask. Measurements taken by a pyroelectric radiometer indicated that approximately 85 μ watts/ $cm^2$ of radiation was transmitted through the pyrex flask, primarily in the soft UV region (300-400 nm). For comparison, some experiments were run in ordinary fluorescent room light, designated by "white".

Iodometric Titration

A method modified from that of Kokatnur and Jelling (A10) was used to measure the concentration of POB in samples taken from the reacting solution. A 1-ml aliquot was drawn from the reaction flask and mixed with 20 ml of a 1 per cent aqueous solution of potassium iodide. The mixture was put under argon blanket to stop further oxidation and stirred for about five minutes to ensure total reaction of POB with the excess KI. The mixture was titrated, depending upon the POB concentration, with a sodium thiosulfate solution having a concentration of 0.04 N or less.

Liquid Chromatography

A model 3500 Spectra Physics liquid chromatograph (LC) was also used in analysis of the samples from the reaction vessel. The mobile liquid phase was controlled to vary from pure water to pure acetonitrile in 15 minutes. In sequence the peaks from the LC unit were benzoic acid, benzaldehyde, DBT sulfoxide, DBT sulfone, and DBT as shown in Figure A.1. Quantitative LC responses for individual constitutents were calibrated by measurement of several known samples in n-decane. N-octanol was added to certain samples to improve solubilities of benzoic acid, DBT sulfoxide, and DBT sulfone in n-decane. The relationships between LC output and concentration were linear except for benzoic acid as may be noted in Figure A.2.

POB and benzoic acid had the same retention time under the LC conditions employed. In the analysis of the samples from the reaction vessel, therefore, this peak indicated the reacted benzaldehyde rather than individual constituents.

Melting Point

To ensure the purity of the crystalline reactants and products, that is DBT, sulfoxide, sulfone, and benzoic acid, their melting points were measured and compared to the equivalent values in the literature. The ratios of measured to literature values are given as: DBT, $100^{o}C/100^{o}C$; benzoic acid, $123^{o}C/122.3^{o}C$; DBT sulfoxide, $188^{o}C/188.5^{o}C$; DBT sulfone, $236^{o}C/235^{o}C$.

Results and Discussion

The first set of experiments was made to study the formation

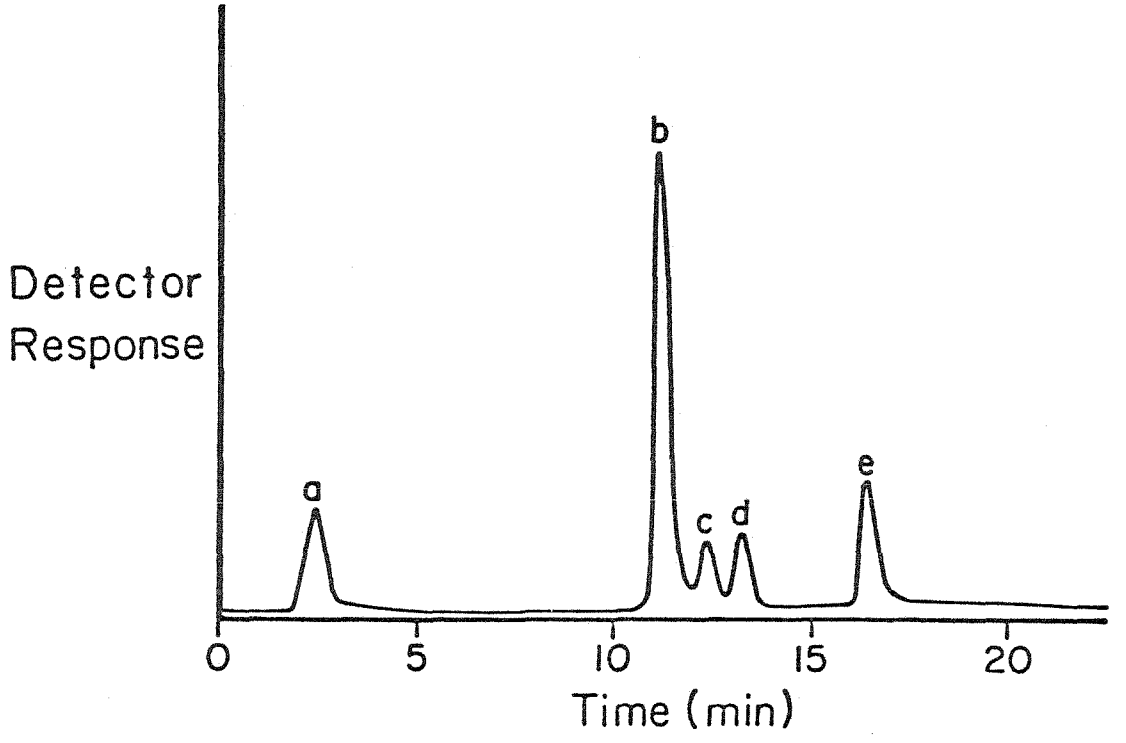


Figure A.1 Sequence and relative retention times of the components in the LC output: a, benzoic acid; b, benzaldehyde; c, DBT sulfoxide; d, DBT sulfone; e, DBT.

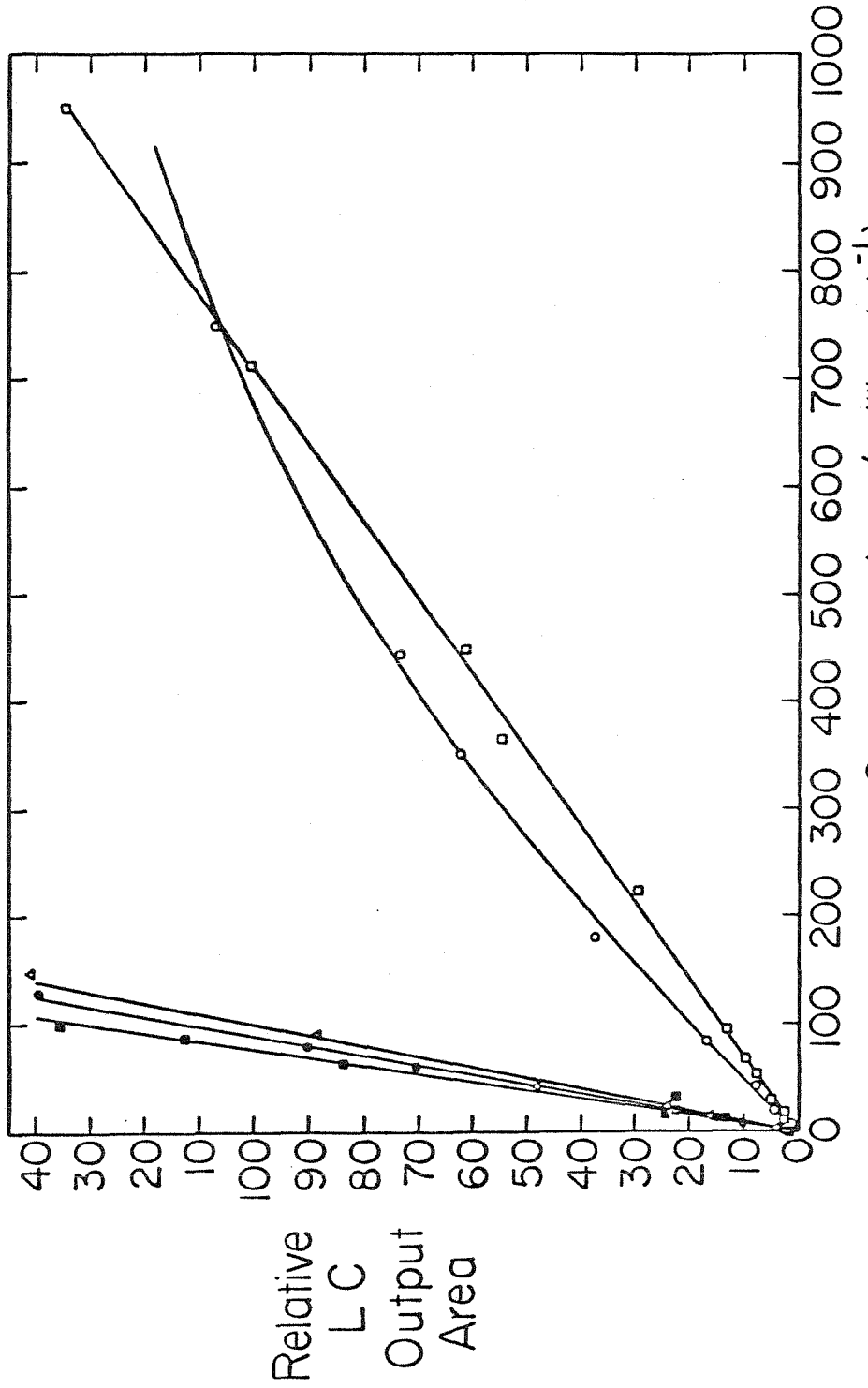


Figure A.2. Calibration of the liquid chromatograph: □, benzaldehyde; ○, benzoic acid; △, DBT; ●, DBT sulfoxide; ■, DBT sulfone.

of POB at atmospheric pressure and room temperatures (22-28$^{o}$C) as shown in Table A.1. Figure A.3 shows the POB concentration profiles.

The results show that the rate of formation of POB depends upon the initial benzaldehyde concentration. Flow rate of oxygen and stirring speed do not practically affect the course of oxidation and so the reaction was not diffusion controlled. Ultraviolet light substantially promotes the rate of oxidation, and n-decane was the solvent that allowed the highest yield of POB.

In the second set of experiments, different solutions of benzaldehyde and DBT in n-decane were used in order to study the simultaneous oxidation of benzaldehyde and DBT. These runs were made at atmospheric pressure and details on conditions are given in Table A.2. Figures A.4ab show the amounts of benzaldehyde reacted and the concentrations of POB. Figure A.5 gives the rates of formation of POB, and Figures A.6ab provide concentration data for the sulfur compound.

Figures A.4ab show that the rate of reaction for benzaldehyde is initially almost constant and then gradually drops. The rate of formation of the peracid is originally equivalent to that of benzaldehyde reaction but then drops depending upon the experimental conditions. The concentration of the peracid remains at a relatively low level when oxidation of DBT is in progress. Then it sharply rises, indicating the termination of DBT oxidation.

Figures A.6ab show that initially there is no marked

Table A.1

Experimental Conditions for Run 1-9

| Run | 1 | 2 | 3 | 4 | 5 | 6 | 8 | 9 |
|---|---|---|---|---|---|---|---|---|
| $(RCHO)_o$ | 97.5 | 287.0 | 287.0 | 469.0 | 469.0 | 469.0 | 469.0 | 469.0 |
| Light | UV | UV | UV | UV | W | UV | UV | UV |
| T | 25 | 25 | 28 | 25 | 25 | 22 | 22 | 22 |
| P | 1 | 1 | 1 | 1 | 1 | 1 | 1 | 1 |
| RPM | 2600 | 2600 | 2280 | 2600 | 2450 | 2280 | 2280 | 2280 |
| $O_2$ | 0.082 | 0.082 | 0.008 | 0.082 | 0.082 | 0.041 | 0.041 | 0.041 |
| Solvent | decane | decane | decane | decane | decane | decane | hexane | toluene |

$(RCHO)_o$, initial benzaldehyde concentration, mol $L^{-1}$ x $10^3$

UV, ultraviolet at $\sim$ 85 $\mu$ watts/$cm^2$

W, white

T, temperature, °C

P, Pressure, atm.

RPM, stirring speed

$O_2$, oxygen flow rate, mol $min^{-1}$

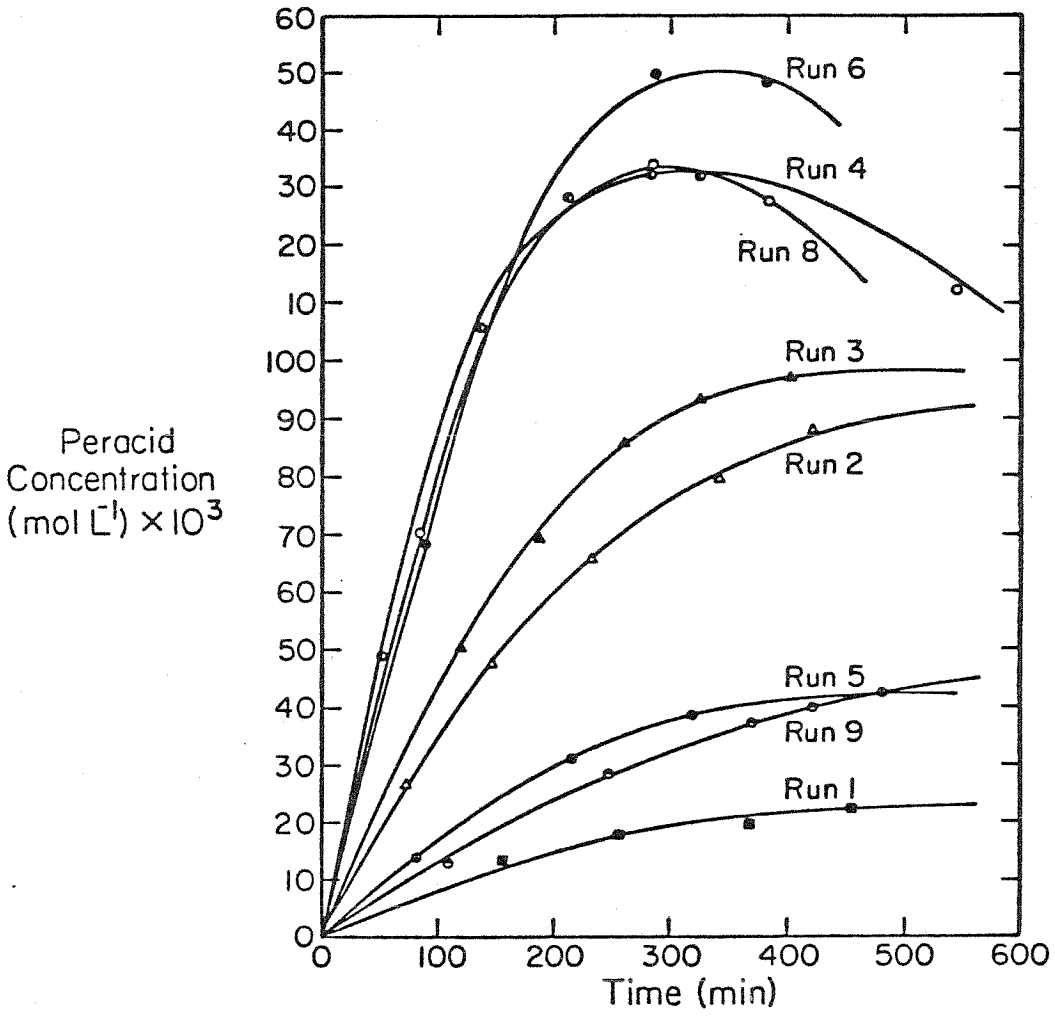


Figure A.3. Concentration profiles for perbenzoic acid.

Table A.2

Experimental Conditions for Runs G-N

| Run | G | H | J | K | L | M | N |
|---|---|---|---|---|---|---|---|
| $(RCHO)_o$ | 193.0 | 287.0 | 97.5 | 97.5 | 97.5 | 97.5 | 287.0 |
| $(DBT)_o$ | 11.1 | 0 | 5.4 | 5.5 | 8.1 | 5.4 | 2.64 |
| Light | UV | UV | UV | UV | UV | W | UV |
| T | 50 | 50 | 50 | 100 | 73 | 100 | 31 |
| P | 1 | 1 | 1 | 1 | 1 | 1 | 1 |
| RPM | 1470 | 1470 | 1470 | 1470 | 1470 | 1470 | 1470 |
| $O_2$ | 0.008 | 0.008 | 0.008 | 0.008 | 0.008 | 0.008 | 0.008 |
| Solvent | decane | decane | decane | decane | decane | decane | decane |

$(RCHO)_o$, initial benzaldehyde concentration, mol $L^{-1}x10^3$
$(DBT)_o$, initial dibenzothiophene concentration, mol $L^{-1}x10^3$
UV, ultraviolet at 85 μ watts/$cm^2$
T, temperature, °C
P, pressure, atm.
RPM, stirring speed
$O_2$, oxygen flow rate, mol $min^{-1}$

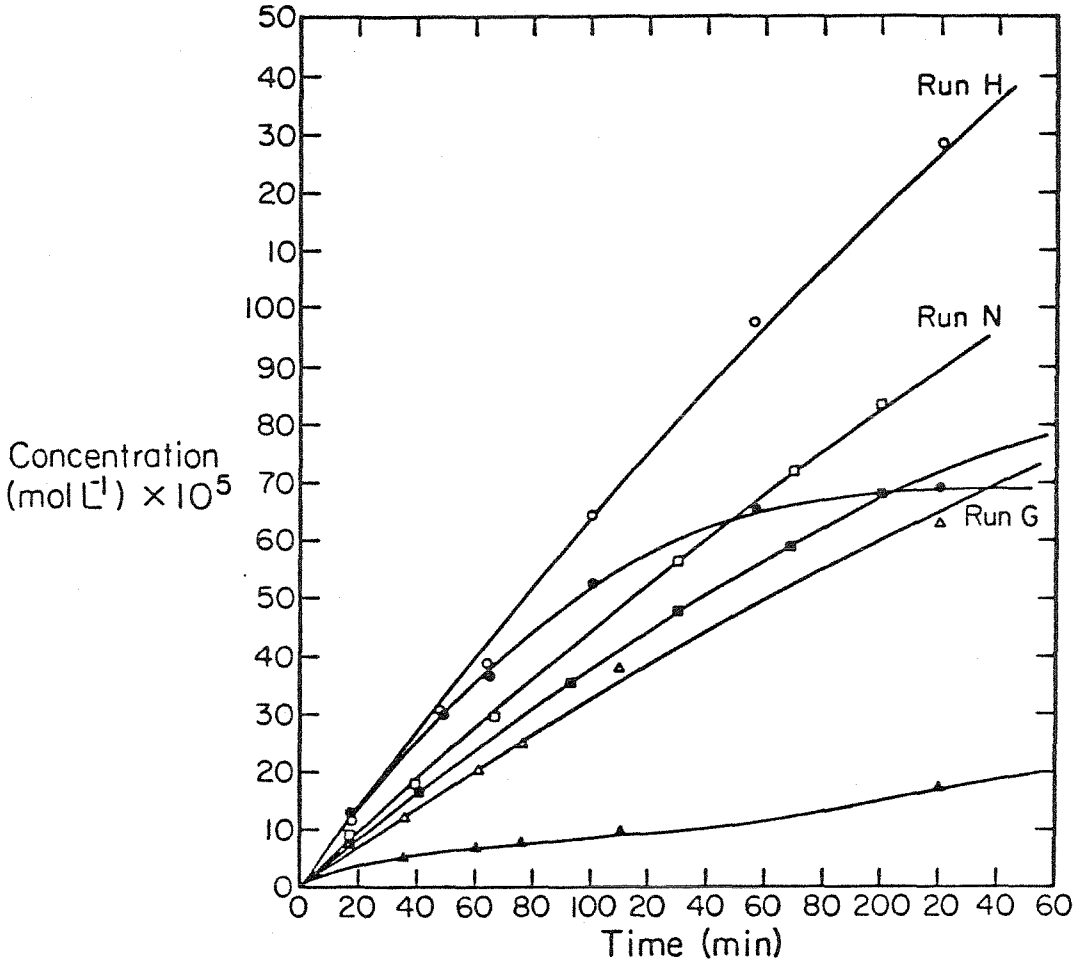


Figure A.4a. Reacted benzaldehyde and POB concentration profiles for runs G, H, and N. The similar open and closed indices represent the reacted benzaldehyde and POB profiles, respectively, for each run.

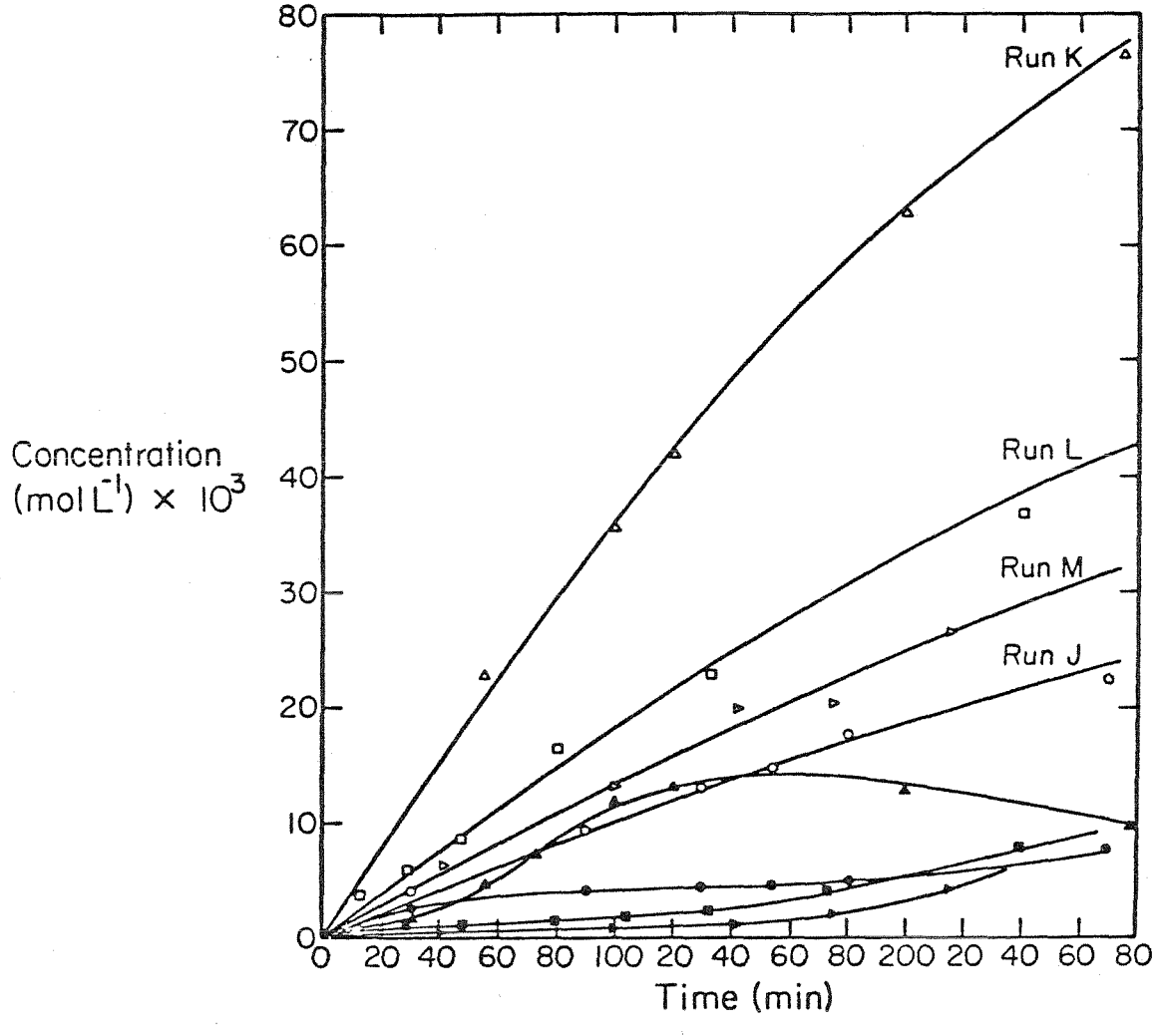


Figure A.4b. Reacted benzaldehyde and POB concentration profiles for runs J, K, L, and M. The similar open and closed indices represent the reacted benzaldehyde and POB profiles, respectively, for each run.

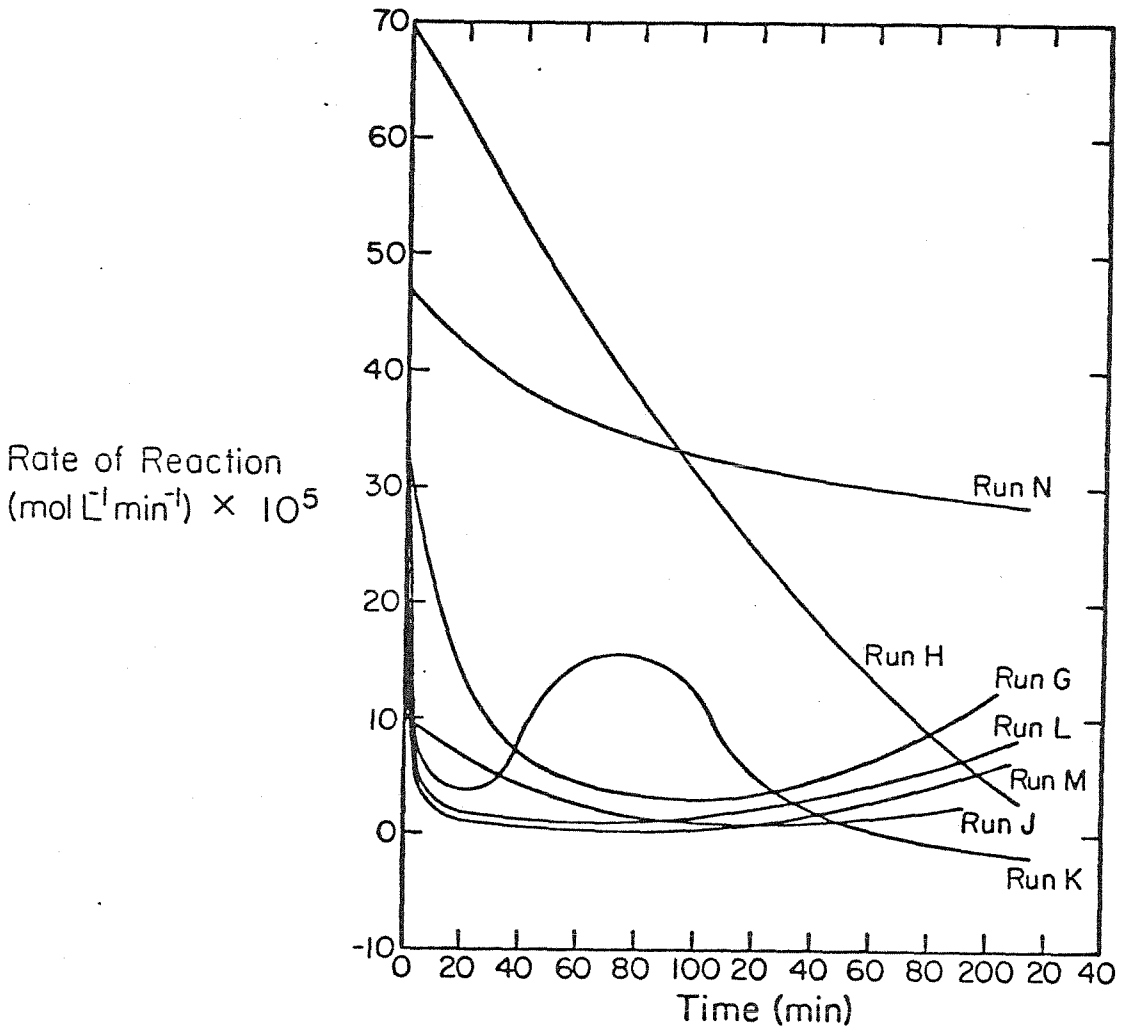


Figure A.5. Profiles for rate of formation of perbenzoic acid.

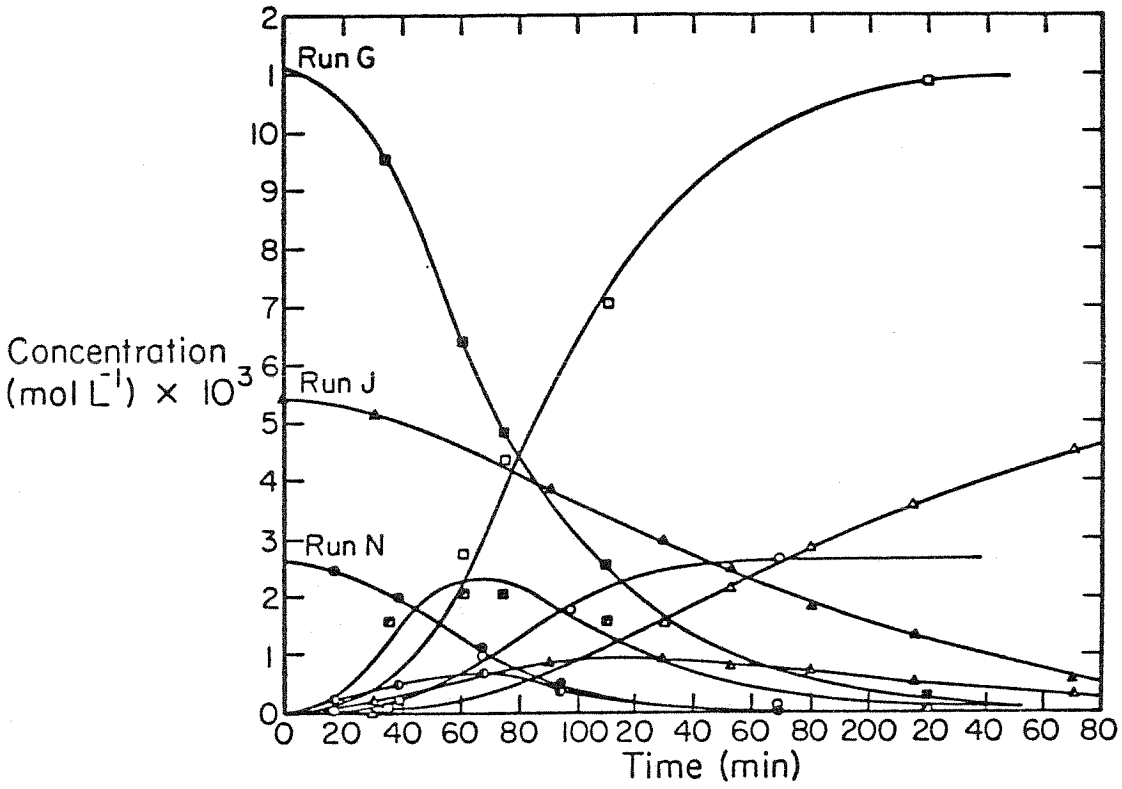


Figure A.6a. Concentration profiles for DBT, sulfoxide, and sulfone for runs G, J, and N. The similar closed, half open, and open indices represent the DBT, sulfoxide, and sulfone profiles, respectively, for each run.

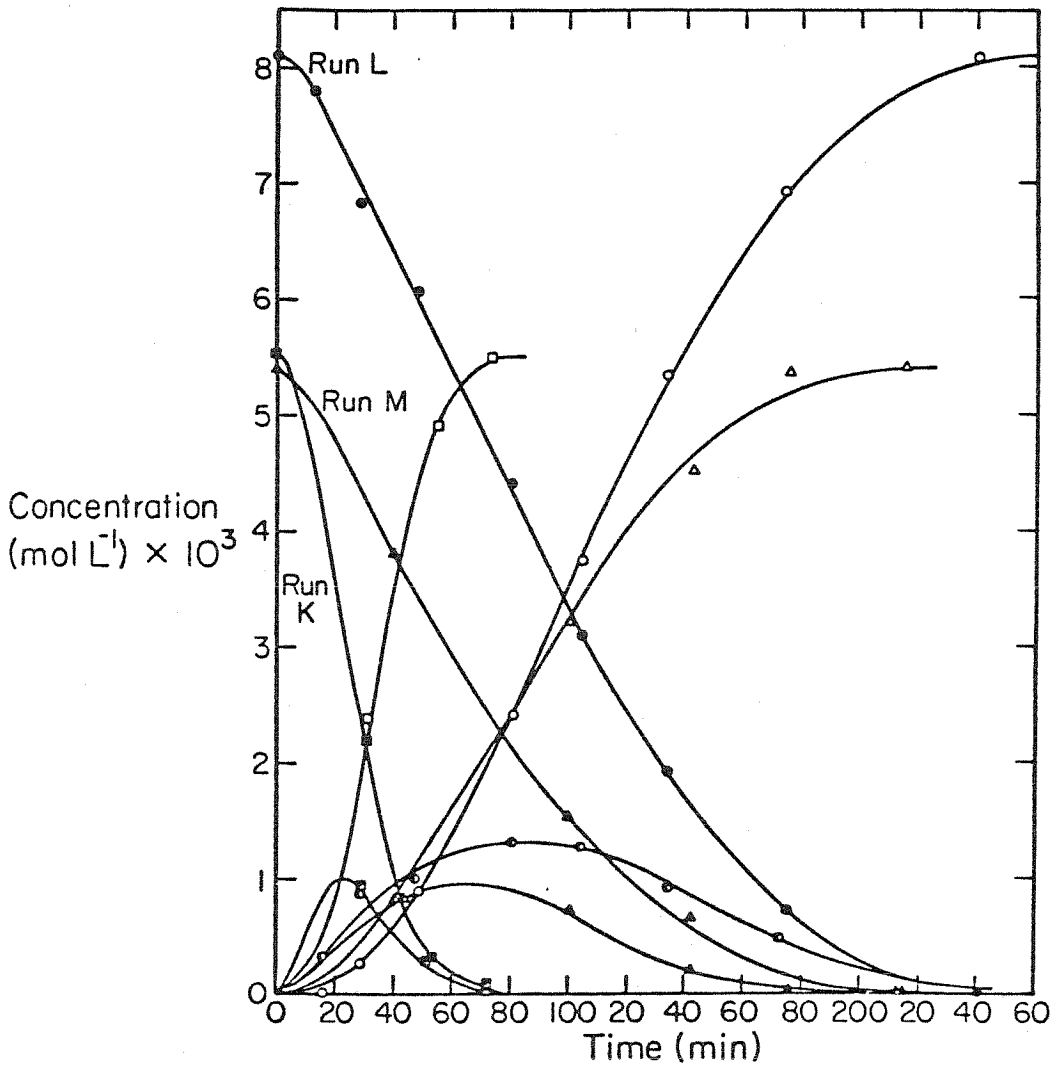


Figure A.6b. Concentration profiles for DBT, sulfoxide, and sulfone for runs K, L, and M. The similar closed, half open, and open indices represent the DBT, sulfoxide, and sulfone profiles, respectively, for each run.

oxidation of DBT, probably because of an inadequate concentration of POB. DBT sulfoxide gradually appears in the solution while sulfone is yet at a trace level. After some time, depending upon the system conditions, the sulfone concentration increases and exceeds the sulfoxide concentration. As might be expected, higher rates of oxidation occur at higher temperatures. Ultraviolet light increases the rate of DBT oxidation to sulfoxide and sulfone, but as will be shown later it does not affect the relevant rate constants. In all cases, with sufficient time, there is a total conversion of DBT to sulfone. A melting-point analysis of the crystalline product from run K confirmed the result of the LC. Values for $k_7$, $k_8$, $k_5$, and k' were calculated at several consecutive points for each run. Mean values are shown in Table A.3. The rates of decomposition of POB by combined thermal and photochemical effects for individual runs were calculated in accord with Equation 13, and the results are shown in Figure A.7. The rate constants for the oxidation of DBT and its sulfoxide, i.e. $k_7$ and $k_8$ in Equations 11 and 12, were calculated at several points for each run. Consistency of the rate-constant values supported the validity of the suggested reactions. The values of ln $k_7$ and ln $k_8$ vs. 1/RT for the individual runs are shown in Table A.3 and plotted in Figures A.8. The linearity in Figure A.8 suggests a consistent mechanism for the conditions considered. According to the rate constants in Table A.3, DBT sulfoxide is oxidized three times as rapidly as DBT. Comparisons of $k_7$ and $k_8$ show that POB reacts more rapidly with DBT

Table A.3

Dependence of the Rate Constants on Temperature and Evaluation of the Arrhenius Factors

| Run | T | $k_7$ $l\ mol^{-1}min^{-1}$ | $k_8$ $l\ mol^{-1}min^{-1}$ | $k_5$ $l\ mol^{-1}min^{-1}x10^3$ | $k'$ $min^{-1}x10^3$ |
|---|---|---|---|---|---|
| N | 31 | 0.84 | 1.98 | 1.0 | 1.64 |
| G | 50 | 2.0 | 6.0 | 4.7 | 1.74 |
| H | 50 | - | - | 4.4 | 2.44 |
| J | 50 | 2.0 | 6.3 | 5.1 | 1.08 |
| L | 73 | 7.6 | 24.6 | 34.1 | 2.06 |
| K | 100 | 29.0 | 101.3 | 156.8 | 3.95 |
| M | 100 | 29.6 | 106.1 | 41.1 | 1.45 |
| E, kcal $mol^{-1}$ | | 11.8 | 13.0 | 16.8 | |
| ln A | | 19.2 | 22.1 | 21.0 | |
| $-\Delta S$, cal $mol^{-1}{}^{\circ}C^{-1}$, 0°C | | 30.7 | 24.9 | 27.1 | |

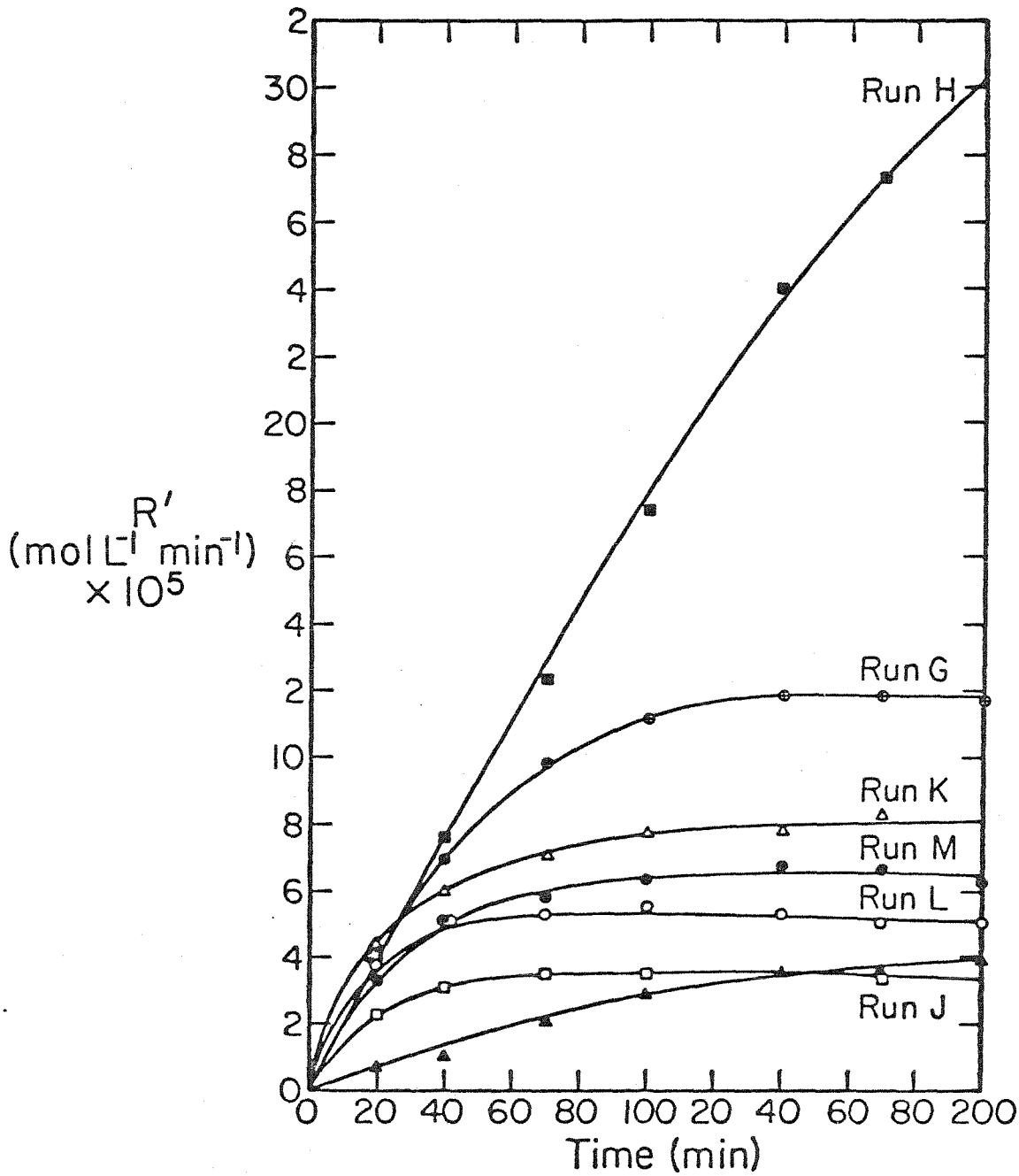


Figure A.7. Combined thermal and photodecomposition rates, R′, for perbenzoic acid.

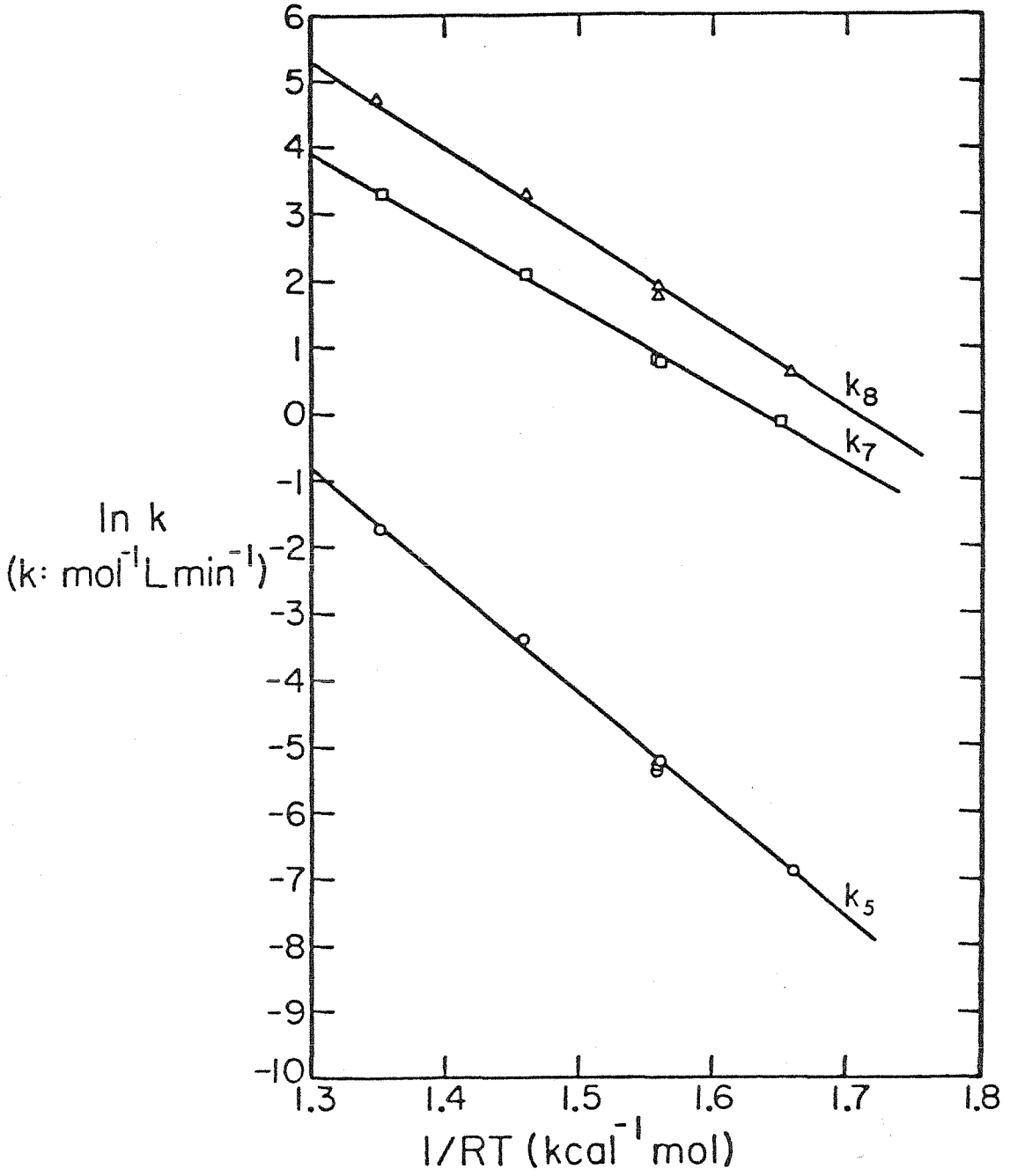


Figure A.8. Arrhenius plots for: o, reaction of POB with benzaldehyde; □, oxidation of DBT; Δ, oxidation of DBT sulfoxide.

than with benzaldehyde by two orders of magnitude. Comparison of the calculated values of $k_7$ and $k_8$ in runs K and M, that is with and without the effect of UV light, shows that oxidation of DBT and its sulfoxide are not photosensitive an indication of a non-free-radical mechanism for these steps.

A comparison of the rate quantities from this work with those obtained by other investigators is presented in Table A.4. This tabulation shows that the choice of the solvent may dramatically influence the course of reaction as shown in Cases (1) and (2) with n-decane and 50 per cent aqueous dioxane as the respective solvents and where $k_{7(1)}/k_{7(2)} \cong 1/7$ and $k_{8(1)}/k_{8(2)} \cong 5$.

Table A.4 shows that the results of oxidation of DBT by peracetic acid (POA) as obtained by Ford and Young (A5) in Case (4) are more or less similar to the oxidation by POB as in Case (1). A negligible oxidation of sulfoxide by POA, however, is reported by these authors, i.e., $k_8 \approx 0$.

$H_2O_2$ in conjunction with acetic acid oxidizes DBT as shown by Heimlich and Wallace (A.7) in Case (3), though it fails to perform such oxidation on its own. Even at its best, $H_2O_2$ gives rate constants below the values by POB by more than two orders of magnitude.

POB oxidizes p-p'dichlorobenzylsulfide at a far higher rate than it does DBT, i.e. $k_{7(5)}/k_{7(1)} > 1000$. A similar result was given by Ford and Young (A.5) for peracetic acid.

Table A.4

Comparison of Second-Order Kinetic Data for the Oxidation of DBT and DBT Sulfoxide* by Peracids (Evaluated by Different Authors)

| Case | Peroxyacid | Sulfur Compound | Solvent | k 50°C l $mol^{-1}min^{-1}$ | E kcal $mol^{-1}$ | ln A | -ΔS 0°C cal $mol^{-1}$ $°C^{-1}$ | Reference |
|---|---|---|---|---|---|---|---|---|
| 1 | POB | DBT | n-decane | 2.3 | 11.8 | 19.2 | 30.7 | this work |
| | | DBTO | | 6.3 | 13.0 | 22.1 | 24.9 | |
| 2 | POB | DBT | 50% aqueous dioxane | 14.2 | 13.7 | 24.0 | 20.8 | Greco et al. |
| | | DBTO | | 1.3 | 13.5 | 21.3 | 26.2 | |
| 3 | 30% $H_2O_2$ | DBT | white oil plus 64.5% Ac OH | 0.006 | 14.3 | 17.1 | 34.5 | Heimlich & Wallace |
| | | DBTO | | 0.13** | | | | |
| 4 | POA† | DBT | benzene | 2.1 | 14.7 | 23.7 | 21.4 | Ford & Young |
| 5 | POB | p-p´dichlorobenzyl-sulfide | toluene | 9450 | 5.1 | 17.1 | 34.5 | Overberger & Cummins |
| | | | iso-propanol | 3440 | 9.6 | 23.1 | 22.6 | |

*Case 5 is especially presented here to compare oxidation of an organic sulfide vs. thiophenic compounds.

**This value is at 100°C.

† Peracetic acid.

References

A1. Attar, A., "The Chemistry of Selective Oxidation of Sulfur Compounds and Its Relation to Fuel Desulfurization", Ph.D. Thesis, California Institute of Technology (1977).

A2. Brooks, W.N. and Haas, C.M., J. Phys. Chem. 71 (1967) 650.

A3. Cooper, H.R. and Melville, H.W., J. Chem. Soc. (1951) 1984 and 1994.

A4. Dankleff, M.A.D., Curci, R., Edwards, J.O. and Pyun, H.Y., J. Amer. Chem. Soc. 90 (1968) 3209.

A5. Ford, J.F. and Young, V.O., Prep. Div. Pet. Chem. ACS 10, 2 (1965) C111.

A6. Greco, A., Modena, G. and Todesca, P.E., Gaz. Chim. Italiana 90 (1960) 671.

A7. Heimlich, F.N. and Wallace, T.J., Tetrahedron 23 (1966) 3571.

A8. Ibne-Rasa, K.B., Edwards, J.O., Kost, M.T. and Gallopo, A.R., Chem. Ind. (London) (1974) 964.

A9. Ingles, T.A. and Melville, H.W., Proc. Roy. Soc. (London) A218 (1953) 175.

A10. Kokatnur, V.R. and Jelling, M., J. Amer. Chem. Soc. 63 (1941) 1432.

A11. Overberger, C.G. and Cummins, R.W., J. Amer. Chem. Soc. 75 (1953) 4250.

A12. Schomaker, V. and Pauling, L., J. Amer. Chem. Soc. 61 (1939) 1769.

A13. Senning, A., "Sulfur in Organic and Inorganic Chemistry",

Vol. 1, Marcel Dekker, Inc., New York (1971).

A14. Swern, D., Chem. Revs. 45 (1949) 1; "Organic Peroxy Acid", Chapter VI in Organic Peroxides, Vol I, Wiley-Interscience, New York (1956).

A15. Trahanovski, W.S. (ed.), "Oxidation in Organic Chemistry", Chapter III in Oxidations with Peroxy Acids and Other Peroxides by Bozo Plesnicar, Part C., Academic Press, New York (1978).

# APPENDIX B APPLICATION OF LIQUID CHROMATOGRAPHY

## Introduction

Liquid chromatography is an important analytical tool for the separation of nonvolatile compounds for which gas chromatography (GC) has limited applicability. The recent development of feedback-controlled high-pressure (5000 psig) pumps with very small flow rate fluctuations during the pumping cycle has overcome the previous major roadblock to the utilization of this method: the long time periods of elution required by gravity flow. A typical system consists of one or more of these pumps in combination with a small mixer which allows changes in the concentration of the liquid mobile phase, in contrast with the constant composition gaseous mobile phase used in gas chromatography. The mobile phase is pumped through a packed column analogous to a GC column and the effluent sent to a detector. The three most important detectors, in order of their present popularity, are ultraviolet (UV), refractive index, and flame ionization. If a nondestructive detector such as UV is used, the mobile phase can be collected in a fraction collector and the fractions corresponding to the separated peaks may be analyzed further. The sample is introduced at the head of the column, usually by an injection valve with a sample loop.

Depending on the sample to be analyzed (see Figure B.1) there are five LC modes which differ in the column packing and the associated mobile phase. The first and most commonly used are polar adsorption packings (silica and alumina) with non-

FIGURE B.1 GUIDE TO LIQUID CHROMATOGRAPHY MODE SELECTION (B1)

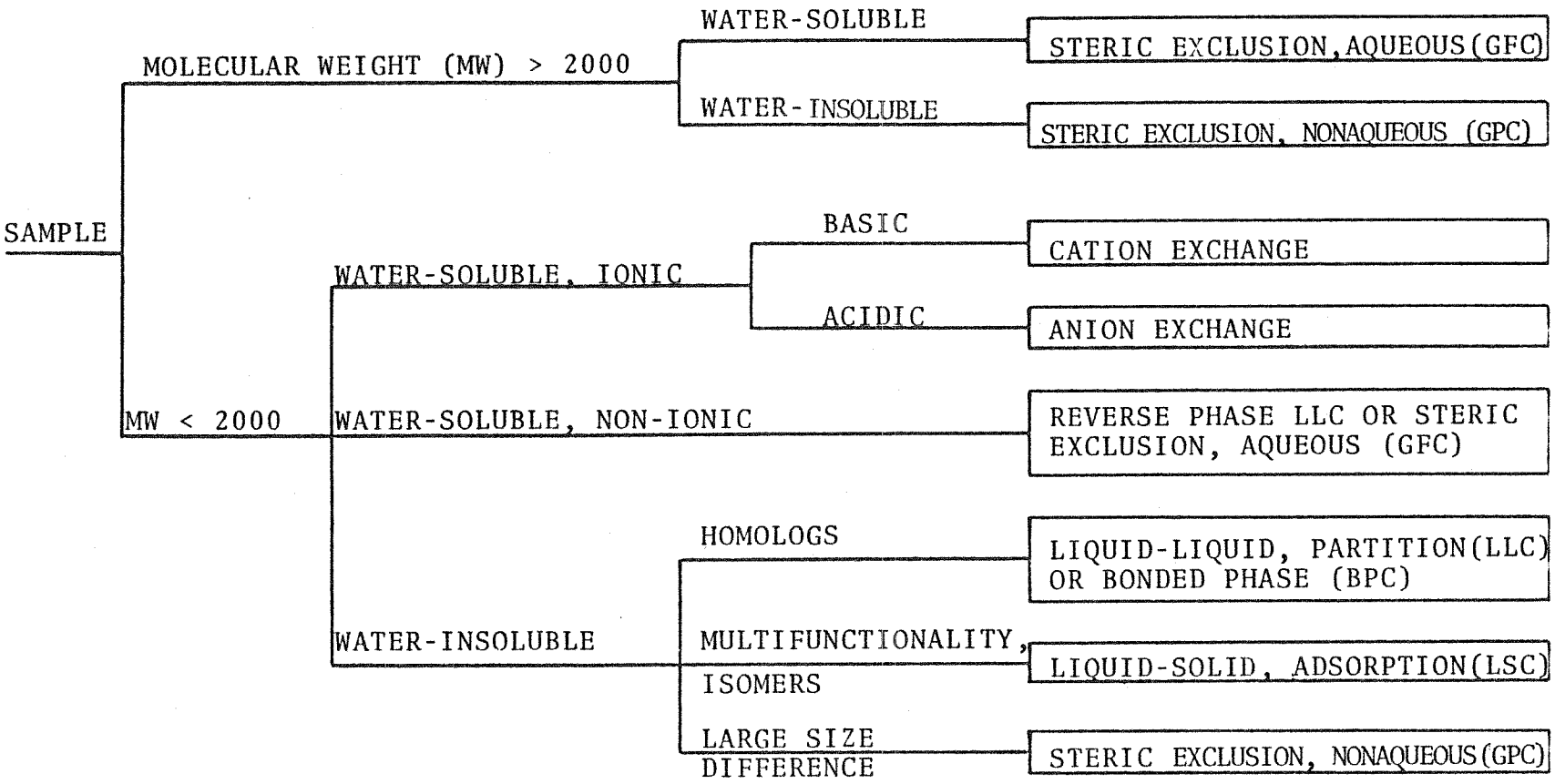

polar solvents. When these inorganic solids are coated physically or chemically with organic phases, it is known as the partition mode. Both of these modes are used for polar compounds; reverse phase packings are designed to extend the range of LC applicability to non-polar compounds. These are essentially non-polar partition packings used in conjunction with polar solvents. Ion exchange packings are used almost exclusively in water to separate ionic compounds. The fifth mode, steric exclusion, utilizes soft organic gels to separate molecules on the basis of size.

Two basic equations governing retention in chromatography are the focal point for column theory in liquid chromatography. The first relates the elution volume of a component to other parameters:

$$V_r = V_m + KV_s$$

where $V_r$ = retention volume = retention time x flow rate

$V_m$ = mobile phase interstitial volume or void volume

$V_s$ = stationary phase volume (partition), pore volume (exclusion), surface area (adsorption), or ion exchange capacity (ion exchange)

$K$ = distribution coefficient

Large values of K indicate high affinity for the stationary phase and strong retention of the solute. Separation is characterized by a ratio called the capacity factor k:

$$k = KV_s/V_m$$

Small values of k indicate that the components are retained very little by the column and thus are poorly separated, whereas large values of k lead to peak broadening. Optimum k values lie between 1.5 and 4; it is usually attained by changing to the appropriate mobile phase. In samples containing components with a wide variation in distribution coefficients, the composition of the mobile phase may be changed during the run to keep the value of k at the optimum. Current research in liquid chromatography is primarily directed toward predicting k values for given solutes using basic parameters such as activity coefficients and solubility parameters (B2,B3,B4,B5,B6,B7). To date, little progress has been made in developing a theory with predictive power.

Mode Selection

Based on the general guidelines for selection of liquid chromatography mode a column packed with 10μ particles of silica was orginally selected as appropriate for the separation of the dibenzothiophene, benzaldehyde, and their oxides. Silica is recommended for separating compounds which differ primarily in the polar part of the molecule and thus is considered useful in the analysis of oxidation products. Dibenzothiophene has a wide UV absorption band with a maximum at 235 nm, therefore this wavelength was utilized on the spectrophotometer detector in order to maximize sensitivity. All aromatics also absorb in this region. Numerous mobile-phase combinations were tried including

hexane, cyclohexane, dichloromethane, tetrahydrofuran, dioxane, and acetonitrile. The best results were obtained using a gradient involving hexane and dichloromethane. Several extraneous reproducible peaks were noticed along with those which could be attributed to sample components. They remained when the solvent-program gradient was run and no sample was introduced and were traced to impurities in the hexane which were adsorbed at the top of the column and eluted by the dichloromethane introduced later in the solvent program. This phenomenon is common to liquid chromatography separations which involve a change in mobile-phase composition (i.e., gradient) during the separation and points out the necessity of using high-purity solvents.

During some preliminary experiments, benzoic acid became increasingly difficult to elute from the silica column with the hexane/dichloromethane solvent system. The literature revealed that organic acids were easily separated by chloroform solvent on a low-pressure silica-gel column, the ancestor of modern high pressure liquid chromatography (B8). For chromatographic purposes, chloroform is essentially equivalent to dichloromethane. The ionization of the benzoic acid was also considered as a cause for its high retention, but Strain (B8) found that separability for organic acids was more closely related to solubility than polarity or ionization. Acids of lowest molecular weight were shown to be the least soluble in chloroform and thus, the most adsorbed. It was noted that in these studies great emphasis

was placed on the water content of the silica gel. Further investigation confirmed the suspicion that water content was an important factor affecting retention. The drier the silica gel, the more active it becomes, resulting in stronger retention of sample components. The continued use of solvents such as hexane and dichloromethane, although nominally insoluble in water, can eventually dry out the column enough to adversely affect performance if these solvents are not partially presaturated with water. The established procedure (B9) for presaturating the solvent involves percolating it through a column of 30 wt% water on silica and mixing it with an appropriate amount of dry solvent to attain equilibrium with the analytical column. The equilibrium water saturation level has been reached when the retention time of a standard component remains stable over a series of runs. In practice, this equilibrium was very difficult to achieve and the separation based on the silica column was abandoned in favor of a more stable system.

The reverse-phase mode of liquid chromatography is recommended for mixtures with highly aromatic character. Therefore, a column containing 10μ particles of octadecyl silica (ODS) was also considered an appropriate option for separating the reaction products of benzaldehyde and dibenzothiophene co-oxidation. A mobile-phase gradient of water and acetonitrile was found to perform the desired separation satisfactorily with much greater reproducibility in retention

time. This method was also found to be applicable to other oxidation systems (see Appendix C).

Fraction Collection

In order for the fraction collector to be useful, the delay time between the detector and the fraction collector must be known so that a particular peak may be correlated with a specific fraction. This delay time is usually calculated from the mobile-phase flow rate and the tubing dimensions. A method was devised to check this result utilizing a sample containing indicator. This technique was specifically demonstrated with a silica column, an isocratic mobile-phase of acetonitrile, and a sample containing phenolpthalein. NaOH was added to the fractions and the resulting red color of the phenolpthalein indicated its presence in a particular timed fraction. The delay time can be calculated by subtracting the retention time as given by the detector/integrator. The delay time may be obtained as accurately as desired by varying the rate of fraction collection. This method may also be used to ascertain the amount of peak broadening between the detector and the fraction collector, which should be kept to a minimum for best results.

Preparation of Solvents

Only the highest quality, spectrophotometric grade, particulate-free solvents should be utilized as mobile phases in high-pressure liquid chromatography. For this study, 99+ %, spectrophotometric grade acetonitrile was obtained

from Aldrich, and HPLC grade water from Baker. Before HPLC water was available, water of equivalent quality was purified by distilling demineralized water over $KMnO_4$, followed by a second distillation. All solvents were vacuum filtered through a fine (4 - 5.5 μ) or ultrafine (0.9 - 1.4 μ) Pyrex millipore filter before use. As a part of the daily start-up procedure, all solvents were degassed by being subjected to a partial vacuum during slow magnetic stirring.

Column Slurry-Packing Technique

The liquid chromatograph (LC) columns were slurry-packed with a lab-built apparatus consisting of 1) a Haskell Engineering DST-150C liquid pump driven with laboratory compressed air, 2) a 2 ℓ stainless-steel beaker serving as a solvent reservoir, 3) a 30,000 psig pressure gauge, 4) a slurry reservoir fabricated from a 3 ft section of 1 in OD stainless steel bar drilled to ¼ in ID, and machined at both ends to accept the appropriate high pressure fittings, 5) a drilled out ¼ in Swagelok union for attaching the column to the slurry reservoir, and 6) ½ in high pressure stainless steel tubing and fittings, including some shop-built high-pressure valves. A schematic of the apparatus is given in Figure B.2. The following procedure was developed as a composite of established methods in the literature (B10,B11,B12) for slurry packing reverse-phase LC columns:

1. 500 ml of heptane/chloroform (1.2 vol) solvent were degassed and filtered and all but 20 ml were loaded into the pump solvent reservoir. The pump was primed.

FIGURE B.2 DIAGRAM OF SLURRY-PACKING APPARATUS

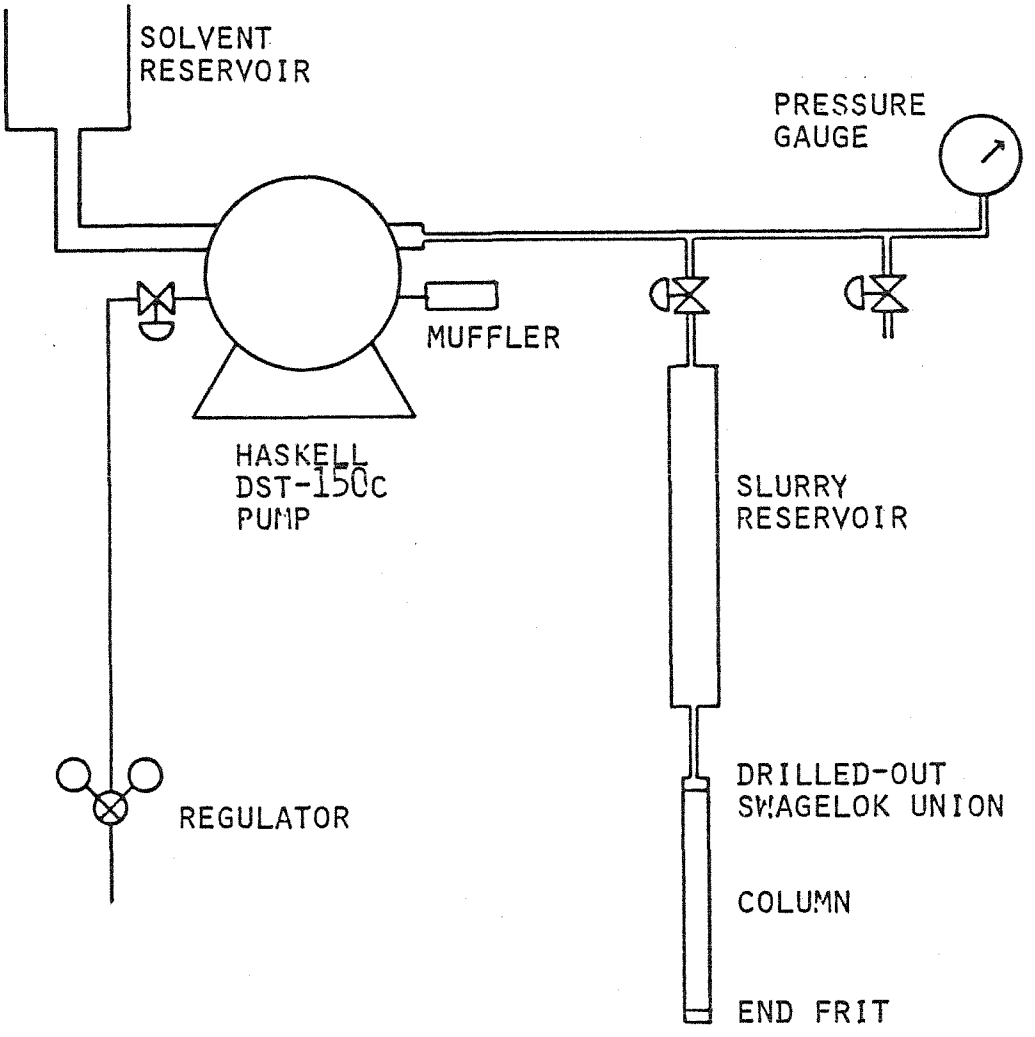

2. Approximately 1.4 g of 10μ packing material (for a 3 x 250 mm column) were weighed into a small bottle with an inert cap.

3. The column with end fitting was attached to the slurry reservoir.

4. 6 ml of butanol were added to the packing material, the cap was sealed, the bottle shaken thoroughly and placed in an ultrasonic bath for 5 minutes.

5. 6 ml of tetrabromethane were added and mixed as in previous step.

6. All valves were closed on the packing apparatus, and the slurry reservoir was removed with column and end-fittings attached.

7. The slurry of packing material was placed in the ultrasonic bath for an additional 10 minutes immediately before packing.

8. The column was filled with the heptane/chloroform solvent. Approximately 2 ml were used for a 3 x 250 mm column.

9. The slurry was rapidly added to the slurry reservoir.

10. The slurry reservoir was filled to the top with degassed heptane/chloroform (1:2 vol).

11. The reservoir and column were rapidly attached to the pumping apparatus.

12. The appropriate valves were opened and the pump started immediately.

13. The heptane/chloroform was initially pumped at approximately 5000 psig; this rate was increased to produce

8000 psig and held at this pressure for 5 minuts.

14. The pump was turned off and the system drained to atmospheric pressure.

15. The column was carefully removed, the excess packing material scraped off with a razor blade, and the other end fitting attached.

16. The column was washed with methanol on the liquid chromatograph for 30 minutes before aqueous mobile phases were used.

Parameters Used in Analysis

The following operational parameters for liquid chromatography were used in the analysis of the samples from the oxidation reaction studies:

| | |
|---|---|
| Sample Loop Size | 10 µl |
| Nominal Flow Rate | 0.8 ml/min |
| Solvent Program | |
| Initial Concentration | 0% (100% $H_2O$) |
| Final Concentration | 99% (100% $CH_3CN$) |
| Sweep Time | 15 minutes |
| Gradient | Linear |
| UV Wavelength | 235 nm |
| Integrator Attenuation | x 64 |
| Chart Speed | 0.2 in/min |
| Integrator Parameters | All at default values except slope sensitivity = 100 |

The procedures for operation of the liquid chromatograph as outlined in the "Liquid Chromatograph Instruction Manual,

3500B" by Spectraphysics were followed with only slight modification.

References

B1. Bauman, F. and Hadden, N., et al., "Basic Liquid Chromatography", Varian Aerograph (1971).

B2. Snyder, L.R., J. Chromatogr. 92 (1974) 223.

B3. Sleight, R.B., J. Chromatogr. 83 (1973) 31.

B4. Mikes, O. and Vespalec, R., J. Chromatogr. Lib. 3 (1975) 233.

B5. Bakalyar, S.R., Am. Lab. 10 (1978) 43.

B6. Tijssen, R., et al., J. Chromatogr. 122 (1976) 185.

B7. Paanakker, J.E., et al., J. Chromatogr. 149 (1978) 111.

B8. Strain, H.H., Anal. Chem. 23 (1951) 25.

B9. Kirkland, J.J.,'Modern Practice of Liquid Chromatography", Wiley: New York (1971).

B10. McIlwrick, R., Spectraphysics Chromatogr. Rev. 3 (1977) 5.

B11. Bakalyar, S., Jackson, Y., et. al., Spectraphysics Chromatogr. Tech. Bull. (1976).

B12. Krull, I.S., Wolf, M.H., et. al., Am. Lab. 10, 5 (1978) 45.

# APPENDIX C OXIDATIVE CHLORINATION OF DIBENZOTHIOPHENE*


## Abstract

The conversion of dibenzothiophene to the corresponding sulfoxide and sulfone by the action of chlorine and water was studied. The effects of temperature, reaction time and solvent on the yield of these products and on the concurrent ring chlorination of dibenzothiophene were examined. Slurry-phase chlorination of dibenzothiophene in water at 70°C was found to be an excellent method for the preparation of the sulfone.


## Introduction

Dibenzothiophene is an organic sulfur compound whose structure is present in fuel oil and coal. It then can be considered as a model compound that can be examined in potential desulfurization reactions. Any knowledge so developed can be applied to the desulfurization of fossil fuels, an area of major import in environmental control. Therefore the oxidation of dibenzothiophene by $Cl_2$ was examined as part of a study of oxidative desulfurization at moderate conditions, namely, at atmospheric pressure and at temperatures less than 100°C.

Though the $Cl_2$-$H_2O$ system is widely used as an oxidizing agent, very few references exist in the literature on the use of this system for the oxidation of dibenzothiophene (DBT).

*Appendix C is essentially an article by N.P. Vasilakos, R.L. Bone, and W.H. Corcoran which has been accepted for publication.

Most of these references are concerned with the first step of oxidation, i.e., the formation of the sulfoxide.

In a method which was first proposed by Fries and Vogt (C6), Brown et al. (C3) treated a solution of 15 g of dibenzothiophene in 150 ml of $CCl_4$ at $0^{\circ}$-$5^{\circ}C$ with chlorine until 6 g had been added. The addition compound which was produced was hydrolyzed by vigorously shaking the reaction mixture with ice and water in accord with the reaction:

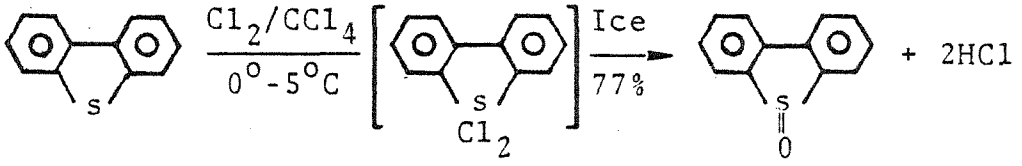


The intermediate dichloride was not isolated. The yield of dibenzothiophene sulfoxide (DBTO) melting at 174-180°C was 15.8 g (97%). It was crystallized from benzene and the yield of pure compound was 12.5 g (77%). It has a melting point of 185°-187°C.

Using the same method, Attar and Corcoran (C1) employed chlorine to oxidize dibenzothiophene in a solution of $CCl_4$ at -10°C and then hydrolyzed the product at 15°C. They observed that substantial chlorination of the phenyl groups occurred.

Baciocchi and Mandolini (C2) investigated the kinetics of the reaction of dibenzothiophene with chlorine in 99.1% acetic acid at 20°C to give dibenzothiophene sulfoxide. The reaction was found to follow second-order kinetics. It was first order in chlorine and first order in dibenzothiophene.

The production of HCl did not affect the rate constants which were also insensitive to the presence of LiCl. NaOAc showed a very strong accelerating effect. In the presence of sodium acetate, chlorine and dibenzothiophene gave dibenzothiophene sulfoxide even when the reaction was carried out in anhydrous acetic acid. The results were consistent with a reaction scheme in which the formation of the dibenzothiophene-chlorine adduct occurs in a fast pre-equilibrium step which is nearly completely shifted toward the reactants. The formation of dibenzothiophene sulfoxide was rapid and practically quantitative when dibenzothiophene was treated with chlorine in 99.1% acetic acid, but a slow ring chlorination of dibenzothiophene was observed when the reaction mixture was allowed to stand for some time.

Finally, Dronov et al. (C4,C5) reported that passing chlorine through 5 g of dibenzothiophene in 50 ml of 90% by volume methanol or in aqueous acetic acid at $0^{o}$-$14^{o}C$ gave the dibenzothiophene sulfone ($DBTO_2$) in very high yields (>90%).

Experimental Section

Oxidative chlorination was conducted by passing chlorine at a feed rate of 0.3 g/min through 15 g of dibenzothiophene (Aldrich grade > 95% purity) in 350 ml of a reagent grade solvent ($CCl_4$, $MeOH/H_2O$, $H_2O$) for an appropriate period of time and at a chosen temperature. Dibenzothiophene was completely dissolved in $CCl_4$. It was mostly in slurry form with $H_2O$ or $MeOH$-$H_2O$ because of its low solubility in

water.

With an anhydrous solvent such as $CCl_4$ the reaction mixture after chlorination was hydrolyzed by vigorous shaking with ice and water for three minutes. No hydrolysis was necessary after chlorination when aqueous solvents were used. The time for the hydrolysis period was chosen to be small enough to prevent further reaction between the unreacted dibenzothiophene and the chlorine dissolved in the water. After chlorination and hydrolysis of the reaction mixture and filtering of the solid product, the $CCl_4$ phase was evaporated. Only small amounts (less than 0.5 g) of solid residue were obtained after evaporation in the low temperature ($0^{o}C$) runs. However, a significant amount of residue was obtained in the high temperature ($60^{o}C$) run and therefore its analysis was included in Table C.1.

In all cases the solid product (or residue) was washed with water and dried under vacuum for 48 hours at $50^{o}C$. It was analyzed with a Spectraphysics Model 3500B liquid chromatograph using a reverse-phase column of 10μ Spherisorb ODS and a solvent program of water and acetonitrile. Identification of the main compounds present in the solid sample and determination of its composition were made by comparison of retention times and peak areas of the sample with standard solutions of dibenzothiophene, dibenzothiophene sulfoxide, and dibenzothiophene sulfone.

Under the conditions of the analysis the relative retention times were 1 (DBTO) to 1.12 ($DBTO_2$) to 1.44 (DBT), and

the relative $\frac{\text{mole}}{\text{peak area}}$ ratios were 1 (DBTO) to 0.235 ($DBTO_2$) to 0.325 (DBT).

Further identification of the solid products included melting-point determinations, infrared spectra of the solid phase and elemental analyses for sulfur and chlorine.

Results and Discussion

Chlorination of dibenzothiophene in carbon tetrachloride. The experimental conditions and the analyses of the products obtained by chlorination of dibenzothiophene in $CCl_4$ followed by hydrolysis of the chlorinated solution are summarized in Table C.1. Chlorination of dibenzothiophene in $CCl_4$ at $0^{\circ}C$ beyond the stoichiometric requirement for the formation of the sulfoxide, a reaction time of 20 minutes for the given conditions, leads in the subsequent hydrolysis step to the formation of dibenzothiophene sulfone. Continuous addition of chlorine in excess of the amount required for complete conversion of dibenzothiophene to the corresponding sulfoxide yields a solid in the hydrolysis step which is progressively richer in sulfone.

Whether the sulfone is produced by direct hydrolysis of a tetrachloride:

$$\left.\begin{array}{l} DBT + Cl_2 \longrightarrow DBT\text{-}Cl_2 \xrightarrow{H_2O} DBTO + 2HCl \\ DBT\text{-}Cl_2 + Cl_2 \longrightarrow DBT\text{-}Cl_4 \xrightarrow{2H_2O} DBTO_2 + 4HCl \end{array}\right| \quad \text{I}$$

or by chlorination and subsequent hydrolysis of the sulfoxide:

Table C.1 Experimental Conditions and Analysis of Products of Chlorination of Dibenzothiophene in $CCl_4$

| Experimental Conditions | | Analysis of the Solid Product | | | |
|---|---|---|---|---|---|
| Temperature ($^oC$) | Reaction time (min) | Weight[a] (g) | DBT/DBTO/$DBTO_2$ (mole ratio) | Relative retention times of byproducts[c] | Chlorine (% wt.) |
| 0 | 30 | 14.9 | 1/20.3/2.0 | None detected | 0 |
| 0-2 | 120 | 14.3 | 1/2.6/23.1 | 1.23 | 1.4 |
| 60 | 30 | 2.5 | 1/7.5/27.2 | 1.23, 1.50, 1.57 | 8.8 |
| 60 | 30 | 11.4[b] | 1/2.9/4.3[b] | 1.23, 1.50, 1.57, 1.63[b] | 14.5[b] |

a For an initial amount of dibenzothiophene of 15 grams.

b This line presents the analysis of the solid residue obtained by evaporation of the $CCl_4$ phase after chlorination and hydrolysis of the reaction mixture and filtering of the solid product. The analysis for the solid product of the hydrolysis is given on line 3.

c Relative retention times with respect to dibenzothiophene sulfoxide (retention time = 1).

$$\text{DBT} + Cl_2 \longrightarrow \text{DBT-}Cl_2 \xrightarrow{H_2O} \text{DBTO} + 2HCl$$

$$\text{DBTO} + Cl_2 \longrightarrow \text{DBT} \overset{\overset{O}{\|}}{-} Cl_2 \xrightarrow{H_2O} \text{DBTO}_2 + 2HCl \qquad \text{II}$$

is not yet clear. The feasibility of route II was demonstrated in a separate experiment, where 10 grams of the solid product of the 0°C-30 min run, noted on the first line of Table C.1, were suspended in 350 ml of $CCl_4$ and chlorinated for 20 minutes at 0°C and at a feed rate of chlorine of 0.3 g/min. The reaction mixture was hydrolyzed the usual way, and the solid product was filtered, water-washed and dried as before. The analysis for this solid is given as follows:

Weight: 9.5 grams

DBT/DBTO/$DBTO_2$ mole ratio: 1/12.9/25.5

No other compounds detected.

Chlorine: 0 wt. %

The results show that chlorination of dibenzothiophene sulfoxide in $CCl_4$ followed by hydrolysis of the new addition compound, presumably DBTO-$Cl_2$, leads to a significant (~60%) conversion of the sulfoxide to the corresponding sulfone. This conversion is considerably slower than the dibenzothiophene ⟶ dibenzothiophene sulfoxide conversion under similar reaction conditions.

Higher chlorination temperatures result in drastically reduced yields of oxidized dibenzothiophene. The amount of solid product was 14.9 g for the 0°C-30 min experiment and

only 2.5 g for the one at 60°C-30 min. This result is consistent with the equilibrium:

$$DBT + Cl_2 \rightleftharpoons DBT\text{-}Cl_2$$

which at low temperatures (0°C) is shifted towards the DBT-chlorine adduct. These addition compounds are generally unstable and can liberate chlorine (C7). Thus, at higher temperatures the equilibrium is shifted more towards the reactants so that the yield of $DBT\text{-}Cl_2$ and of DBTO or $DBTO_2$ in a subsequent hydrolysis step is substantially decreased.

Finally, chlorination of the phenyl groups is very slow at 0°C but becomes the main reaction path at higher temperatures such as 60°C, as indicated by the appearance of a series of new compounds in the solid product and the very high chlorine content of both the product and the residue after evaporation. It should be noted that 100% conversion of dibenzothiophene to chlorodibenzothiophene

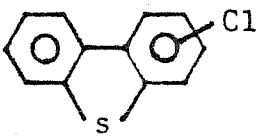


would yield a product with a chlorine content of 16.2 wt %. These new compounds are most probably mono- or di-chloro derivatives of dibenzothiophene, dibenzothiophene sulfoxide and dibenzothiophene sulfone.

Aqueous Chlorination of Dibenzothiophene

No hydrolysis step was employed here. The results are summarized in Table C.2.

Table C.2 Experimental Conditions and Analysis of Products of Chlorination of Dibenzothiophene in Aqueous Phase

| Experimental Conditions | | | Analysis of the Solid Product | | |
|---|---|---|---|---|---|
| Temperature ($^{o}C$) | Reaction time (min) | Solvent | Weight[a] (g) | DBT/DBTO/$DBTO_2$ (mole ratio) | Sulfone yield (% of theoretical) |
| 10 | 60 | $H_2O$ | 14.8 | 1/0.79/5.05 | 64.0 |
| 10 | 60 | MeOH[b]-$H_2O$ | 16.6 | 0/1/16.15 | 89.2 |
| 70 | 60 | $H_2O$ | 16.4 | 0/0/1 | 93.2 |

a For an initial amount of dibenzothiophene of 15 grams

b 90% by volume of MeOH

In all cases the only compounds present in the reaction products were DBT, DBTO and $DBTO_2$. No chlorine was detected in any of the solid samples. Ring chlorination of dibenzothiophene during the DBT $\xrightarrow{Cl_2/H_2O}$ $DBTO_2$ conversion did not occur under the experimental conditions employed, even at the highest temperature examined (70°C).

The overall rate of oxidation of dibenzothiophene in water is higher at higher temperatures despite the lower chlorine concentration at these temperatures.

The unfavorable equilibrium at high temperatures of the reaction:

$$DBT + Cl_2 \rightleftharpoons DBT\text{-}Cl_2$$

did not appear to affect the overall rate as it did in the case of $CCl_4$, probably because in the presence of water the DBT-chlorine adduct is readily hydrolyzed, and so the equilibrium is shifted continuously towards the products.

Use of methanol in the DBT-chlorine/$H_2O$ system significantly improves the yield of oxidized products, even at a low reaction temperature such as 10°C.

Finally, slurry-phase chlorination of dibenzothiophene in water at 70°C proved to be an excellent method for the preparation of the dibenzothiophene sulfone. The sulfone was obtained in very high yields (>93%) and was 100% pure as proved by the melting-point determination (231°-233°C), the liquid-chromatograph analysis (only a single $DBTO_2$ peak), the elemental analysis for sulfur (calcd. for $DBTO_2$: S, 14.8

found: S, 14.8), and the solid-phase IR spectrum. Under the experimental conditions of the 70°C run conversion of DBT to $DBTO_2$ was complete after 40 minutes of reaction as indicated by the appearance of a stable yellow-green color (excess chlorine).

To determine whether the chloride ion ($Cl^-$) was an active species in the aqueous oxidation of dibenzothiophene by chlorine, a separate experiment was conducted. Fifteen grams of dibenzothiophene were suspended in 350 ml of a concentrated HCl solution for 120 minutes at room temperature and under intense stirring. The treated solid was filtered, water-washed, and dried by the usual method. Analysis of this solid showed no other compound present except for the original dibenzothiophene. No chlorine was detected in the product. Thus, the chloride ion was not active in the conversion of DBT to $DBTO_2$.

Conclusion

Because the dibenzothiophene in an aqueous system can be quantitatively oxidized by chlorine to the sulfone, it is expected that the dibenzothiophene structure in fuel oil and coal can be similarly oxidized with a minimum of attack of other atoms by the chlorine. That result suggests that the oxidation of the sulfur then would be accompanied by relatively minor losses of heating value. Even though the sulfur is quantitatively oxidized, desulfurization requires an additional step to split out the sulfone structure.

References

C1. Attar, A., Corcoran, W.H., Ind. Eng. Chem. Proc. Res. Dev. 17 (1978) 102.

C2. Baciocchi, E., Mandolini, L., Ric. Sci. 37 (1967) 863.

C3. Brown, R.K., Christiansen, R.G., Sandin, R.B., J. Am. Chem. Soc. 70 (1948) 1748.

C4. Dronov, V.I., Lebedeva, M.N., Enikeev, R.S., Kreis, E.A., "Chemistry of Organic Sulfur Compounds in Petroleum and Petroleum Products", Akademiya Nauk SSSR, Vol. VI (1964). (Translated from Russian, Jerusalem, 1967, p. 316).

C5. Dronov, V.I., Kundryutskaya, N.N., Prokhorov, G.M., Anikeey, R.S. and Valitova, G.Z., Khim. Seraorg. Soedin., Soderzh. Neftyakj Nefteprod 9 (1972) 158.; Chem. Abstracts 79 (1973) 115388f.

C6. Fries, K. and Vogt, W., Ann. Chem. 381 (1911) 341.

C7. Reid, E.E., "Organic Chemistry of Bivalent Sulfur", Vol. II, Chemical Publishing Co.: New York (1967) 48.